Mechanically-Induced Chemical Changes in Polymeric Materials

Mary M. Caruso,[†] Douglas A. Davis,[†] Qilong Shen,[†] Susan A. Odom,[†] Nancy R. Sottos,[‡] Scott R. White,[§] and Jeffrey S. Moore*[,†,‡]

Departments of Chemistry, Materials Science and Engineering, and Aerospace Engineering and Beckman Institute, University of Illinois at Urbana−Champaign, Urbana, Illinois 61801

Received April 3, 2009

Contents

1. Introduction 5755
   1.1. Polymer Mechanical Behavior 5756
   1.2. Historical Perspective 5757
   1.3. Methods of Study 5758
   1.4. Coverage 5761
2. Responses at the Atomic Level 5762
   2.1. Flow-Induced Mechanochemistry of Polymers in Solution 5762
      2.1.1. Turbulent Field 5762
      2.1.2. Elongational Field 5762
   2.2. Mechanisms of Mechanochemical Activation 5763
      2.2.1. Homolytic Bond Cleavage 5764
      2.2.2. Heterolytic Bond Cleavage 5765
   2.3. General Features of Ultrasound-Induced Polymer Chain Scission: Chain-Length Dependence and M_{lim} 5765
   2.4. Factors Influencing Ultrasound Mechanochemistry 5766
      2.4.1. Ultrasound Intensity 5766
      2.4.2. Solvent 5766
      2.4.3. Temperature 5767
      2.4.4. Concentration 5768
      2.4.5. Initial Molecular Weight 5768
      2.4.6. Bond-Specific Activation 5768
   2.5. Alternative Methods To Induce Polymer Chain Scission 5771
      2.5.1. Repeated Freeze−Thaw Chain Scission 5771
      2.5.2. Adsorption-Induced Chain Scission 5771
      2.5.3. Mechanochemical Reactions in Bulk Polymers 5771
3. Responses at the Molecular and Supramolecular Levels 5773
   3.1. Disruption of Interactions 5773
      3.1.1. Dispersion of Aggregates 5773
      3.1.2. Fluorescence Resonance Energy Transfer (FRET) 5776
      3.1.3. Diacetylenes 5777
      3.1.4. Hydrogen Bonding 5780
   3.2. Induced Interactions 5782
      3.2.1. Strain-Induced Crystallization (SIC) 5782
      3.2.2. Excimer Formation 5782
      3.2.3. Mechanically-Induced Optical Changes Due to Increased Conjugation 5783
      3.2.4. Mechanically-Induced Dichroism 5785
      3.2.5. Ionic 5785
4. Responses at the Microscopic and Macroscopic Levels 5786
   4.1. Self-Healing Materials 5786
      4.1.1. Microcapsule-Based Systems 5787
      4.1.2. Fatigue Responses 5788
      4.1.3. Other Microencapsulated Self-Healing Chemistries 5789
      4.1.4. Microvascular Systems 5790
      4.1.5. Alternative Damage Repair Systems 5791
   4.2. Self-Healing Coatings 5791
      4.2.1. PDMS-Based Systems 5791
5. Conclusions and Outlook 5792
6. Abbreviations 5793
7. Acknowledgments 5793
8. References 5793

1. Introduction

Engineering applications of synthetic polymers are widespread due to their availability, processability, low density, and diversity of mechanical properties (Figure 1a). Despite their ubiquitous nature, modern polymers are evolving into multifunctional systems with highly sophisticated behavior. These emergent functions are commonly described as "smart" characteristics whereby "intelligence" is rooted in a specific response elicited from a particular stimulus. Materials that exhibit stimuli-responsive functions thus achieve a desired output (O, the response) upon being subjected to a specific input (I, the stimulus). Given that mechanical loading is inevitable, coupled with the wide range of mechanical properties for synthetic polymers, it is not surprising that mechanoresponsive polymers are an especially attractive class of smart materials.

To design materials with stimuli-responsive functions, it is helpful to consider the I−O relationship as an energy transduction process. Achieving the desired I−O linkage thus becomes a problem in finding how to transform energy from the stimulus into energy that executes the desired response. The underlying mechanism that forms this I−O coupling need not be a direct, one-step transduction event; rather, the overall process may proceed through a sequence of energy transduction steps. In this regard, the network of energy transduction pathways is a useful roadmap for designing stimuli-responsive materials (Figure 1b). It is the purpose of this review to broadly survey the mechanical to chemical

* To whom correspondence should be addressed. Phone: 217-244-4024. Fax: 217-244-8024. E-mail: jsmoore@illinois.edu.
[†] Department of Chemistry and Beckman Institute.
[‡] Department of Materials Science and Engineering and Beckman Institute.
[§] Department of Aerospace Engineering and Beckman Institute.

10.1021/cr9001353 CCC: $71.50
Published on Web 10/14/2009

Mary M. Caruso (center) was born and raised in Tampa, FL. She received a B.S. degree in Chemistry from Elon University (Elon, NC) in 2006, where she worked under the direction of Prof. Karl D. Sienerth. Her research included the synthesis and electrochemical characterization of a novel palladium complex. She is currently pursuing her Ph.D. in Organic Chemistry at the University of Illinois at Urbana−Champaign under the guidance of Prof. Jeffrey S. Moore and Prof. Scott R. White. Her research interests include the development of new catalyst-free self-healing polymers, microencapsulation, and mechanical testing of bulk polymers.

Douglas A. Davis (second from left) was born in Martin, TN. In 2004, he received his B.S. degree in Chemistry from the University of Tennessee, Knoxville, where he worked on surface enhanced Raman spectroscopy (SERS) in an electrospray plume with Professors Charles Feigerle and Kelsey Cook. He joined Prof. Jeffrey Moore's group at the University of Illinois, Urbana−Champaign in 2005 to pursue his Ph.D. in Organic Chemistry. His current research interests include designing and synthesizing mechanophores, which can be induced to undergo chemical reactions with mechanical force.

Qilong Shen (third from left) was born in 1974 in Zhejiang Province, China. He received his B.S. degree in Chemistry (1996) from Nanjing University, China, and his M.S. in Chemistry (1999) from Shanghai Institute of Organic Chemistry, the Chinese Science Academy, China, under the supervision of Prof. Long Lu. After a two-year stay at the University of Massachusetts at Dartmouth with Prof. Gerald B. Hammond, he moved to Yale University, where he received his Ph.D. under the guidance of Prof. John F. Hartwig in 2007. He is currently a postdoctoral researcher with Prof. Jeffrey S. Moore at University of Illinois at Urbana−Champaign. His research interests include the discovery, development, and understanding of new transition metal-catalyzed reactions, and the mechanochemistry of polymers.

Susan A. Odom (far right) was born and raised in western Kentucky. She attended the University of Kentucky (Lexington, KY), where she received a B.S. in Chemistry in 2003, working under the guidance of Prof. John E. Anthony on the synthesis of tetracene and anthradithiophene derivatives. She obtained a Ph.D. in 2008 from Georgia Institute of Technology (Atlanta, GA) under the guidance of Prof. Seth R. Marder and Dr. Stephen Barlow. She is currently a postdoctoral researcher in Prof. Jeffrey S. Moore's group at the University of Illinois at Urbana–Champaign, where her research interests include the development of new mechanochemically active chromophores and microencapsulated organic semiconductors.

energy transduction process in polymeric materials. The mechanochemical transduction event enables a variety of other functional responses through the secondary pathways seen in Figure 1b.

Nancy R. Sottos (second from right) received her B.S. degree in Mechanical Engineering (1986) and her Ph.D. (1991) in Mechanical Engineering from the University of Delaware. She is currently the Willett Professor of Engineering in the Department of Materials Science and Engineering at the University of Illinois at Urbana−Champaign. She is also the co-chair of the Molecular and Electronic Nanostructures Research Theme at the Beckman Institute for Advanced Science and Technology. Her research group studies the mechanics of complex, heterogeneous materials, such as self-healing polymers, advanced composites, thin film devices, and microelectronic packaging.

Scott R. White (third from right) received his B.S. degree in Mechanical Engineering (1985) from the University of Missouri—Rolla, an M.S. in Mechanical Engineering (1987) from Washington University (St. Louis, MO), and a Ph.D. in Engineering Science and Mechanics (1990) from Pennsylvania State University. He is currently the Willett Professor of Engineering in the Department of Aerospace Engineering at the University of Illinois at Urbana−Champaign and is the Group Leader for the Autonomous Materials Systems Group at the Beckman Institute for Advanced Science and Technology. His research is focused on self-healing materials and microvascular materials systems.

Jeffrey S. Moore (far left) received his B.S. degree in Chemistry in 1984 and his Ph.D. in Materials Science in 1989, both from the University of Illinois at Urbana−Champaign. After postdoctoral studies at Cal Tech, he began his independent career at the University of Michigan. In 1993 he returned to the University of Illinois, and he is currently appointed as the Murchison-Mallory Chair in Chemistry. His research focuses on molecular self-assembly, macromolecular architecture, and self-healing polymers.

1.1. Polymer Mechanical Behavior

Polymeric materials exhibit an extraordinary range of mechanical responses (Figure 1a), which depend on the chemical and physical structure of the polymer chains.[3] Polymers are broadly categorized as thermoplastic, thermoset, or elastomer. Thermoplastic polymers consist of linear or branched chains and can be amorphous or semicrystalline. The mechanical response of thermoplastic polymers is highly influenced by the molecular mass, chain entanglements, chain alignment, and degree of crystallinity. Thermosetting polymers consist of highly cross-linked three-dimensional networks. The mechanical properties of these amorphous polymers depend on the molecular mass and the cross-link density. Elastomers (e.g., rubber) are highly deformable elastic networks that are lightly cross-linked by chemical or physical junctions.

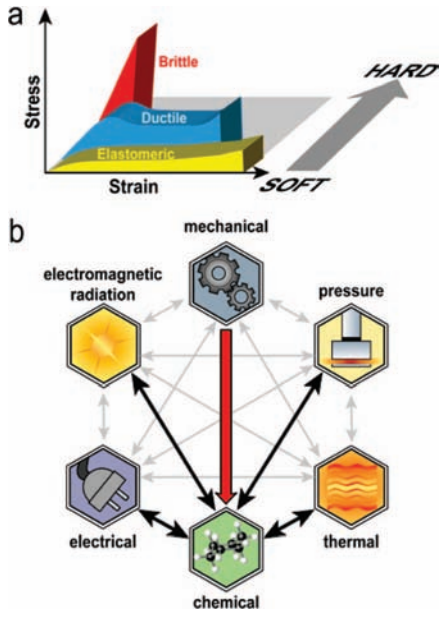

Figure 1. (a) The macroscopic response of polymeric materials subjected to mechanical load is generally described by a stress−strain curve. Polymeric materials exhibit a range of mechanical behavior from elastomeric to brittle. The area under these curves is proportional to the total mechanical work that is available for conversion into other forms of energy.[1] (b) The network of energy transduction pathways is the basis for the rational design of stimuli responsive polymers.[2] This review covers the mechanochemical transduction pathway.

The deformation response of most polymers is viscoelastic, displaying characteristics of both an elastic solid (reversible mechanical response) and a viscous liquid (irreversible mechanical response).[4] Hence, the reaction to stress depends not only on the structure of the polymer but also on time and temperature. A critical property for understanding viscoelastic behavior is the glass transition temperature (T_g) of the polymer. At temperatures above T_g, the polymer chains display increased mobility, enabling the bulk material to flow. At temperatures below T_g, mobility is restricted and the polymer behaves like a glassy, elastic solid. The T_g of a polymer is determined by chemical structure, molecular weight, and degree of chemical or physical cross-linking.[1,5] Lower temperatures and faster loading rates favor a more glassy, elastic response due to insufficient time or mobility for viscous or dissipative deformation mechanisms to take place. Similarly, higher temperatures and slower loading rates lead to a more viscous or rubber-like elastic response.

The macroscopic response of polymers to mechanical force is characterized by a variety of measures, including tensile strength, failure strain, fracture toughness (resistance to crack growth), and elastic modulus (initial slope of the stress−strain curve). These and other terms associated with mechanical testing of polymers have been reviewed in detail in a recent publication.[6] However, translating macroscopic response to micro- and molecular deformation is challenging and highly dependent on the proximity of T_g and polymer structure.

At the microscopic level, the mobility of polymer chains in the presence of an external stimulus is dependent on the degree of cross-linking and entanglements present in the network.[7,8] A competition exists within a polymeric network between chain deformation as a response to external stress and chain contraction as an entropic response. Strain energy is stored in the polymer until the chains deform to become laterally displaced or bent, or bond rotation occurs to relieve the tension (energy dissipation).[9] Curro and co-workers have conducted molecular dynamics simulations to study the mechanical response of strained polymer networks in terms of shear modulus changes.[10] They found that entanglements become more permanent under cross-linking conditions (heat, UV irradiation), forming a rigid network. Upon deformation, the localization of stress on particular polymer chains is caused by entanglements or cross-links in the material (Figure 2). The deformed polymer networks undergo further cross-linking reactions or bond-breaking, also known as chemical aging. These phenomena were observed in the resulting network after deformation because they were either directly or indirectly confined via cross-links or entanglements by neighboring chains.

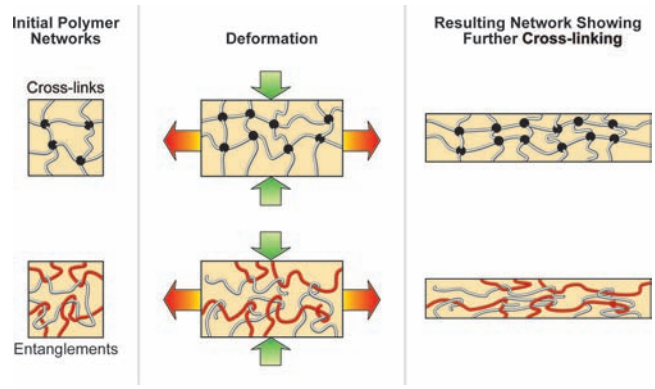

Figure 2. Stress-induced polymer networks (above T_g) as a result of additional covalent cross-links or a permanent set of physical chain entanglements.[10]

1.2. Historical Perspective

In designing stimuli-responsive materials, researchers have turned to biology for inspiration. Many biological systems are mechanoresponsive to their environment in which a mechanical stimulus is transduced into an electrical signal.[11] Most eukaryotic cells have the capability to detect mechanical stress, which allows for touch sensitivity, hearing, and detecting the flow of blood and urine.[12] Proteins catalyze various cellular processes and reactions, some of which involve mechanical manipulation. For example, in some specialized sensory cells, transmembrane ion channels are forced open when a complex arrangement of proteins is subjected to mechanical stress.[13,14] The coupling of molecules to the active sites of enzymes results in mechanical deformation of the bound molecule, causing distortions as it coordinates to the active site geometry defined by the tertiary protein structure, and thus leading to a variety of efficient chemical reactions.[15,16] Some enzyme-catalyzed reactions have reportedly been accelerated by stretching fibers or compressing gels containing covalently-bound enzymes.[17]

Early work in understanding the response of polymeric materials to mechanical stress was published by Staudinger, who observed a decrease in the molecular weight of polymers in response to mastication.[18−20] It was suggested that the molecular weight reduction resulted from homolytic carbon–carbon bond cleavage due to mechanical force.[21] This suggestion was supported by electron spin resonance (ESR) experiments of polymers cleaved by ball-milling, drilling, slicing, or sawing, as described in a review by Sohma.[22] Some of these polymer chains were cleaved in the presence of radical acceptors, giving more distinct ESR spectra.[23] Solution-based experiments have also been used to cleave

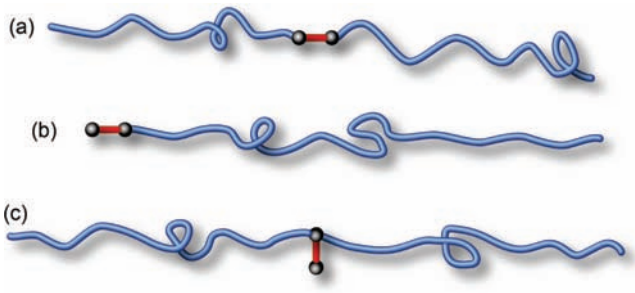

Figure 3. Schematics of a bifunctional mechanophore (a) and control molecules containing a mechanophore linkage at the polymer chain end (b) or in the center of the chain (c). The mechanophore is colored in red for emphasis.

polymers, which has allowed for kinetic analysis of polymer bond scission. This analysis examined molecular weight dependence, minimum molecular weight required for cleavage, and forces required for chain cleavage.[24]

In the 1930s and 1940s, classical physical chemistry such as Eyring's activated-rate theory began to establish the molecular-scale link between mechanical force and chemical change.[21] For example, statistical mechanical methods were used to ascertain the mechanism of the flow of large molecules.[21] Already at this time, the concept that an external force could be used to modify molecular potential energy surfaces was clearly established. Following the pioneering work of Porter et al.,[25] Odell and Keller's elegant extensional flow experiments[26,27] ushered the field into the modern era with quantitative physicochemical studies.

More recent work has demonstrated that cleavage occurs more easily for certain chemical bonds than for others. Earlier work by Encina and co-workers reported that ultrasonic chain scission of poly(vinylpyrrolidone) with randomly incorporated peroxide linkages occurred ten times faster than that of neat poly(vinylpyrrolidone).[28] More recently, targeted cleavage or rearrangement of bonds has been demonstrated in polymer-bound small molecules called mechanophores,[29] which attempt to mimic biological mechanochemical transduction. Mechanophores (indicated in red in Figure 3) possess strategically weakened bonds that undergo useful reactions when force is transferred to the mechanophore from the polymer chain segments. The importance of this configuration (polymer chains linked on either side of the mechanophore) for force transfer has also been demonstrated using control polymers in which the mechanophore is located at the chain ends or in the center without spanning the force-activated portion of the mechanophore.[30] Examples include the rearrangement[31] and cleavage[32] of azo-linkages, the electrocyclic opening of benzocyclobutene derivatives,[29] and the conversion of a spiropyran to its merocyanine form.[30,33] Other reports have focused on the effect of mechanical stress on interactions between polymer chains, specifically focusing on the disruption of hydrogen bonding[34] or aggregation,[35] causing interactions such as excimer formation,[36−38] orientation of polymer chain segments,[39] breaking of metal−ligand coordination bonds,[40] and changing the pH of an environment.[41]

The ability to predict the behavior and limitations of polymers in response to mechanical stress is important for determining their performance in a variety of applications. For example, it is necessary to know how much force can be applied to a glassy plastic such as polycarbonate (used in windows and eyeglasses) before yield occurs. In elastic polymers such as natural rubbers, where mastication is used to reach the desired rheological properties,[42−44] it is necessary to know the limits of elasticity before the material stretches to failure. Automobile tires are thought to have increased lifetimes because of the stress-induced reactions in cross-linked and filled rubber components.[45] The carbon–carbon bonds and thioether and polysulfide cross-links can reversibly cleave, leading to self-healing of damaged tires. Mastication is also used to reduce nonuniformity in chain length polydispersities.[46,47] Several medical applications also depend on the mechanical stability of polymers and composites such as biopolymers in the synoidal fluid for joint lubrication[48] and dental resin composites.[49] Mechanical degradation of biopolymers such as starches and proteins is also relevant to the food processing industry.[50−52] Controlled degradation of other natural polymers such as chitosan (deacylated chitin) is important in biomedical applications such as drug delivery and bioadhesives.[53]

On a bulk scale, various polymer responses indicate that structural damage has occurred, thus signaling that repair is necessary to prevent complete failure of the material. Changes in a polymer's color upon application of mechanical force can be useful as a damage sensor for the visual indication of stress. When the chemical identity, intermolecular interactions, or orientation of chromophores are altered using mechanical stress, the appearance or change of color can be used to identify a strained or damaged polymer.[30,33,54−56] This indication is relevant for any polymer-based material subjected to mechanical damage. Mechanical stress might also lead to the initiation of self-repair by the formation of new interchain interactions or new covalent bonds.[22,57−59] These responses can increase the lifetime of plastics and composites and can repair polymer coatings.

1.3. Methods of Study

While mechanical force has been demonstrated to promote several chemical reactions, a thorough fundamental understanding of the nature of mechanochemical transduction does not exist and would be beneficial for the design of new mechanochemically responsive materials. The products of mechanically-induced reactions may be different[32] than products resulting from activation by thermal or electromagnetic radiation.[29,60,61] Thus, chemical analysis is essential to advancing the field. The problem is especially acute in bulk polymers, where the application of force displaces atoms from their equilibrium positions, creating large local strains.[62] Coupled to these large strains are large localized forces that can lower or raise the activation energies of the various reaction pathways. More studies—both experimental and computational—are needed to better understand the fundamentals of mechanochemical transduction. Figure 4 summarizes a number of experimental methods that have been exploited to characterize mechanochemical changes over a range of strain rates and size scales.

Given the experimental challenges of the analytical chemistry, much effort has been given to theory and simulations. Forced bond separation has been discussed in numerous articles, including the change in reaction coordinate in an energy landscape upon adding an external force.[63] Kramer's theory has been used to derive analytical solutions for the rate at which bonds rupture when subjected to constant external force and force−rupture distributions under constant loading rates, as described by Hummer, Szabo, and Dudko.[64−67] In addition to the constant forces, these studies claimed that the survival probability of bonds was assumed

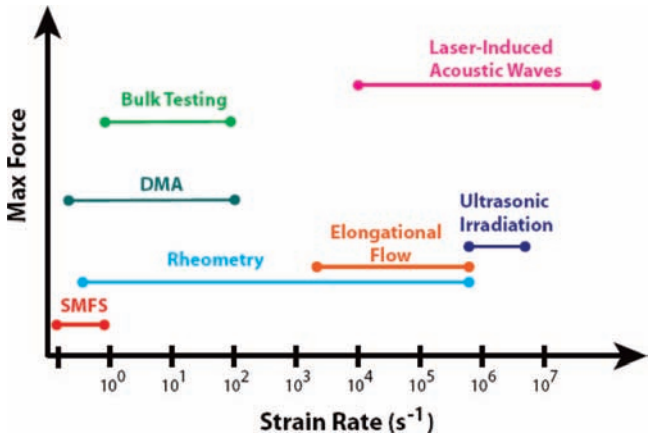

Figure 4. Summary of experimental methods for characterization of mechanochemical activity at the single molecule level, in solution, and in a solid polymer.

to be a first order differential equation. More recently, Freund used the concept of the Gibbs external coordinate to provide a versatile analysis for force-induced bond rupture.[68] Freund concluded that two aspects of a generic one-dimensional energy landscape are relevant to bond separation: (1) the external deterministic constraint that tends to induce bond separation and (2) an energy landscape that allows for a calculation of force transmitted by the bond (Figure 5a).[68] Freund analyzed parameters thought to characterize the resistance of a molecular bond under external mechanical force, which yielded an expression for the probability of bond survival (i.e., Figure 5b) as well as an expression for the time-dependent rate of bond cleavage under constant force. As Freund and Dudko have both addressed, while their results are quite useful, these calculations simplify the bond potential surface into a one-dimensional description of force-induced rupture and are far from a molecular bond interaction potential that includes depth, width, and rate coefficient.[64,68] Continued refinement should enable a more refined reconstruction of energy landscapes.

Quantum mechanical calculations and simulations have been used to predict the energy required to break bonds in small molecules and polymers and to predict which bonds are most likely to be cleaved. In general, small molecule models are stretched away from their relaxed state, and computational routines such as density functional theory (DFT) are used to obtain the energy and new molecular geometry. For example, a simulated force is applied to two chosen points on the molecule's minimized structure by elongating the distance between the two points in small steps. The molecular geometry is minimized at each step. This technique, termed COGEF (COnstrained Geometries simulate External Force), yields the energy change per unit length extension of the molecule, which allows for the calculation of the bond rupture rate constant as a function of applied force.[69] COGEF calculations have mainly been used to model homolytic bond cleavage,[30,69−71] with a few examples discussed in a recent review by Beyer.[72] Some studies have analyzed the effect of the position of substituents on a mechanically active chromophore. Moore and co-workers used COGEF calculations to analyze the effect of substituent placement on the effectiveness of the mechanically induced Bergman cyclization on enediyne substrates.[73] In a similar manner, COGEF was used to model the effects of mechanical force on the electrocyclic ring-opening of functionalized spiropyrans (SP).[30] COGEF has also been used in combination with another DFT-based technique—"External Force is Explicitly Included" (EFEI)—to model the mechanically induced ring-opening reaction of benzocyclobutene reactions,[74] which predicted the previously experimentally observed products,[29,33] including those that were symmetry forbidden by the Woodword−Hoffman rules for electrocyclic reactions.

First principles calculations have also been used to model heterolytic bond cleavage. Frank and co-workers simulated the extension of a small PEG chain in the presence of several water molecules.[70] Using various methods for energy minimization with molecular dynamics simulations, the authors reported comparisons for the energies required for homolytic and heterolytic bond cleavage. They found that upon C−O bond stretching in the presence of water, when the bond length reached 3.2 Å, a water molecule attacks the chain, resulting in proton transfer, three-membered ring formation, and chain fragmentation.[70] More details of this work are given in section 2.2.2. The issue of molecular architecture poses many interesting questions that are best answered by computational means. For example, *ab initio* methods have been used to investigate the effect of the presence of a knot on the breaking strength of a polymer strand.[75] Using classic molecular dynamics (MD), a loosely knotted polyethylene chain was subjected to increasing end-to-end distances. This

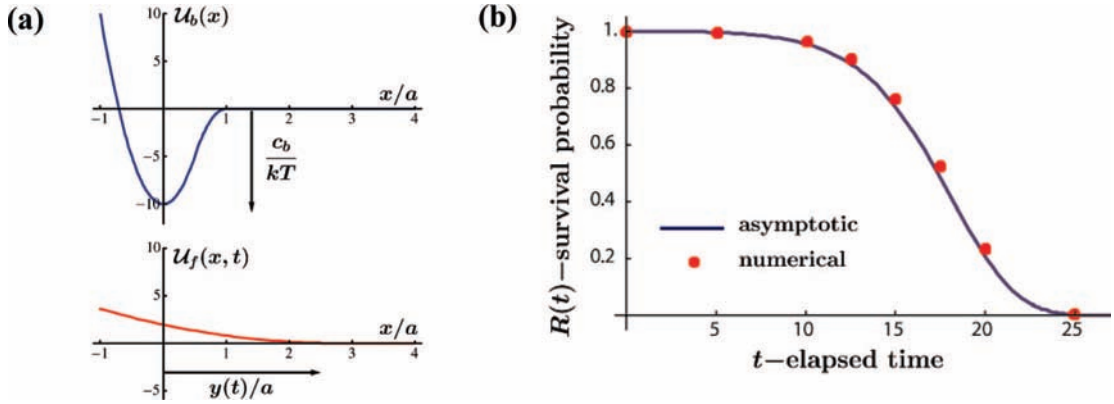

Figure 5. (a) Interaction energy landscape (top) with a typical time-independent bond energy profile with well depth c_b with dimensions of energy and a width a with dimension of length and force potential profile (bottom) that is fixed in shape and translates in the x direction in a way prescribed by $y(t)$. (b) Bond survival probability versus time as from the analytical result for bond $R(t)$ (found by applying approximate methods of analysis) with numerical simulation results for a fixed loading rate and loading stiffness.[68] Reprinted with permission from ref 68. Copyright 2009 National Academy of Sciences.

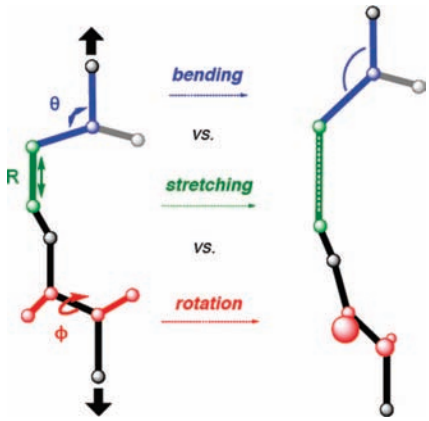

Figure 6. Examples of the deformation of a portion of a polypropylene chain: valence angle bending ($\Delta\theta$, blue), bond stretching (ΔR, green), and torsional angle rotation ($\Delta\phi$, red).[78]

knot weakened the chain, causing breakage at the knot entrance at lower energies than those for the unknotted chain.

Mechanical energy can also alter the reactivity profile of polymers. Mechanical forces can modify the rate of chemical reactions and the outcome of a reaction, yielding products that are not typically observed by thermo- or photochemistry.[29,33] Some molecular modes are more deformable under mechanical stress than others, as observed by infrared (IR) spectroscopy of polymers under stress.[76−79] In one case, the molecular deformation of polypropylene (PP) was studied using a grating dispersion double-beam IR spectrometer to obtain difference spectra.[78] Difference spectra were measured in addition to first-order peak shift measurements, and a polarizer was used to examine parallel and perpendicular dichroic bands. Deformation of helical PP resulted in considerable bond stretching (ΔR), valence angle bending ($\Delta\theta$), and torsional angle changes ($\Delta\phi$) (types of changes are represented in Figure 6), with an average ratio of $\Delta R/\Delta\theta/\Delta\phi = 1:2.4:9$. Deformation was nonuniform; the axial C−C bonds were stretched twice as much as the equatorial C−C bonds. The authors noted that while PP can serve as a model for polyethylene (PE), the chain extension of PP may not be as significant as the changes in PE, where chain extension involves considerable C−C stretching in addition to angle bending.

Due to numerous advances in analytical techniques, it is now possible to measure the force required to break bonds in single molecules and polymers.[72,80] Atomic force microscopy (AFM) techniques, optical and magnetic tweezers, biomembrane force probes, and glass needles are among the tools used in single molecule force spectroscopy (SMFS) measurements.[72,80] This variety of tools allows for the measurement of forces ranging from 0.01−1000 pN, depending on the technique. Of these techniques, AFM[81] and glass-microneedles[82] are the most precise techniques for nanonewton forces, which are on the order of the force required for the investigation of chemical-binding forces.[72] Polymers with appropriate functional groups can be covalently attached both to a functionalized substrate and to an AFM tip.[83−86] The force to retract the AFM tip is measured and gradually increases as the polymer chain is lifted from the surface and elongated, sometimes reaching local maxima as different conformations are minimized, and it gradually reaches a maximum value as covalent bond rupture occurs.[72,80] Craig and co-workers recently reported a simple treatment for extracting single molecule kinetic data from variable loading-rate force spectroscopy data.[87] This technique was recently used to break sulfur−sulfur bonds in a single molecule of a protein bound to a surface, and the AFM SMFS[88] have been reviewed in more detail by Liang and Fernández.[89] A limitation of SMFS experiments is the lack of direct structural information to elucidate the detailed chemical changes brought about by the force. Various experimental methods are available to apply force to polymer molecules in solution, whereby it is then possible to isolate and characterize chemical changes with modern separation techniques and spectroscopic methods.

Ultrasound can be used to apply force to dilute polymer solutions. Since its initial use to degrade starch and agar,[90] this technique has also been employed to degrade cellulose,[91] polypeptides, polysaccharides,[92,93] proteins,[94] DNA,[95] transition metal-coordinated polymers,[40,96,97] and various organic polymers.[98,99] Polymer chain scission results from solvodynamic shear caused by cavitation: the nucleation, growth, and collapse of bubbles in solution. A polymer molecule near the vicinity of a collapsing bubble is pulled toward the cavity of the bubble, and the solvodynamic shear elongates the polymer backbone, leading to scission.[24] Scission generally occurs near the midpoint of a polymer chain (approximately within the middle 15% of the chain, in the case of homopolymers), where solvodynamic forces are the greatest.[24,99] The rate of cleavage from ultrasonic irradiation of polymer solutions depends on several experimental factors, including temperature, solvent, and sonication intensity,[98] which are discussed in detail in section 2.4 of this review. The kinetics are also affected by the initial polymer molecular weight,[100−103] polymer structure,[104−109] and chemical composition.[28]

The sonication experiments benefit from controls (i.e., small molecules and chain-end functionalization of mechanophores onto polymers), isotopic labeling,[29,32] and systematic chain-length dependence[100−102] investigations to ensure that the observed change is due to mechanical forces and not other factors. For example, because chain scission is a nonrandom process (with cleavage at the chain center), it follows that chain scission is not a thermal process.[110,111] Also, changes in maximum cavitation temperature have no effect, as determined by varying the cavitation temperature using different dissolved gases.[98] Although ultrasound is known to produce a vast amount of radicals in solution, a radical degradation mechanism is also excluded because of the chain-centered scission; polymers degraded by benzoyl peroxide radicals produced random chain scission.[112] Even stronger support comes from chain-length dependent studies in which it has been shown that the rate coefficient for cleavage increases with increasing molecular weight of the polymer[32,100−102] (see section 2.4.5). Moore and co-workers have reported examples of ^{13}C labeling at specific sites within the polymer backbone. By ^{13}C NMR analysis of polymers before and after sonication, they were able to demonstrate that changes in the NMR spectrum were only significant in the mechanically active portion of the polymer.[29,32] Moore has also reported examples of control studies in which chain-centered mechanophores were mechanically sensitive and the chain-end functionalized controls and small molecule controls did not undergo the same reactions under sonication.[33]

Elongational flow at high strain rates can also be used to stretch and break polymers in dilute solutions.[113] In one approach, a flow cell with opposing jets provides a stagnation point between opposing orifices surrounded by rapidly flowing solution.[114−118] When a coiled polymer chain be-

comes trapped in the stagnation point, each end of the chain is pulled in opposite directions, resulting in polymer elongation. When the rate of flow is high enough, polymer cleavage occurs after elongation. Elongational flow in well-defined flow cells generally results in narrow size distributions of the fractured polymers, consistent with midchain scission.[26,115−117] An alternative setup employs the use of faster, transient flows across abrupt contractions.[119−123] This method for polymer cleavage does not allow for the full elongation of polymer chains and results in broad size distributions of polymer fragments, suggesting more random chain scission, which may be due to the lack of full extension of the coiled polymer.[119−123]

Other methods have been used to accomplish and observe covalent bond cleavage. Matyjaszewski and co-workers synthesized bottlebrush polymers and used absorption-induced tension to cleave covalent bonds. By depositing the polymer brushes either onto substrates[124] or onto Langmuir–Blodgett films,[125] they observed scission of carbon−carbon bonds[124,126] or sulfur−sulfur[125] bonds within the polymer backbone. Repeated cycles of freezing and thawing of dilute solutions of polymers have been shown to cleave polymer chains, possibly resulting from polymer chain adhesion to solvent crystallites formed upon freezing.[127] Analysis of polymer chain length by gel-permeation chromatography (GPC) showed a correlation between decreasing polymer molecular weight and increasing number of freeze−thaw cycles. Rockhill and co-workers sliced atactic polystyrene rods by microtoming; the effect of microtoming on average molecular weight was determined by monitoring the viscosity of solutions of the crazed samples.[128] The polystyrene rods underwent significant reduction in molecular weight upon slicing, which was strongly dependent on the initial molecular weight.

At the macroscopic level, rheology, the study of deformation and flow, is used to characterize the response of a polymer when stress is applied.[3] Most linear polymer molecules generally assume the shape of a coil, a state of maximum entropy in the absence of load, which can be distorted upon application of mechanical stress.[129] The factors affecting response to mechanical stresses include molecular weight, chain composition and flexibility, degree of interchain attraction, degree of cross-linking and entanglement, presence of plasticizers, and temperature at which the measurements are recorded.[5] These measurements can be performed using static, transient, impact, and cyclic forces.[130] Stress can also be induced to cross-linked polymers by soaking them in solvents to induce swelling and increase the mobility of polymer chains.[8,131,132] For swelling experiments, the polymer network absorbs the solvent and dilates to the point of reaching equilibrium without damaging the material.[131] Qualitative calculations suggest that the forces typically found in swollen polymers may not be sufficient to cause significant covalent bond activation.[73]

When monitoring the mechanical response of polymeric materials on a specific time scale, dynamic mechanical analysis measurements are useful. In these experiments, a polymer is loaded or strained at a set frequency and the response of the polymer is reported.[4] Another category of testing is studying a material's response to long-term cyclic motions, also known as fatigue testing. This test serves to predict the lifetime of a material under periodic stress.[130,131]

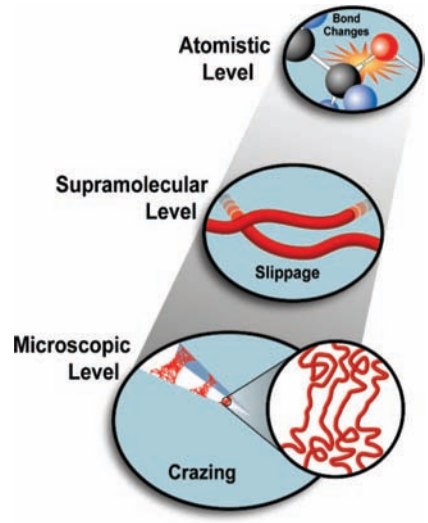

Figure 7. Diagram depicting the hierarchical levels of mechanochemical change that will be covered in this review. At the atomistic level, chemical bond changes and conformational changes occur. On a supramolecular level, chain slippage occurs as a response to force and deformation. At the microscopic level, voids, cavitation, yield or crazing, and crack formation take place along with large scale viscoelastic deformation.[9]

1.4. Coverage

This review focuses on the chemical changes that accompany polymeric materials subjected to mechanical stimuli (Figure 7). We have organized the review by the length scale over which the chemical change takes place. The first section describes responses on the scale of the covalent bond. Ultrasound-induced and flow-induced chain scission of polymers in solution are covered in depth. A few examples of other solution-based chain scission techniques are included such as turbulent flow, repeated freeze−thawing, and stress induced by surface adsorption. Next we discuss the effects of mechanical force at the molecular and supramolecular levels. This section includes the disruption of noncovalent interactions upon mechanical loading as well as the formation of new supramolecular interactions that result from force. The last section considers the responses of bulk polymers at the microscopic level, including systems in which self-repairing mechanisms have been incorporated. The effects of various self-healing techniques are compared, including polymer composites containing microcapsules and microvascular networks with embedded healing agents. Advanced polymeric coatings containing self-healing components are discussed as materials that respond to stress by providing anticorrosion functionality.

This review covers the chemical response of polymers to mechanical stimuli. It does not cover polymers that exhibit mechanical changes (changes in volume, length, etc.) in response to other external stimuli by energy transduction pathways shown in Figure 1b. For example, photodeformable materials, which convert light energy into mechanical energy,[133−136] are outside the scope of this review. Photochromic mechanical actuators, which convert rotary motion into linear displacement, are also beyond the scope of this review. The mechanical deformation of biomolecules has been recently reviewed[137−140] and is not discussed here. Single molecule force spectroscopy experiments, which have begun to provide useful mechanochemical molecular level detail,[141] are not included and have been described in great detail in several review articles.[72,80,142]

2. Responses at the Atomic Level

2.1. Flow-Induced Mechanochemistry of Polymers in Solution

The experimental and theoretical study of the chain scission of polymers in flow fields has been an active area of research for more than 70 years,[143,144] beginning with the work of Staudinger when he reported the shearing of polystyrene across platinum jets in efforts to show the existence of macromolecules.[113] Two classes of flow fields are of interest for chain scission studies and will be discussed in this section: (1) turbulent fields and (2) elongational fields.

2.1.1. Turbulent Field

Experimental studies of polymer chain scission in turbulent flow can be dated back to 1948, when Toms reported that very dilute solutions of poly(methyl methacrylate) (PMMA) in chlorobenzene underwent larger reductions in the turbulent flow pressure than those of pure solvent at the same flow rate.[145] Since then, numerous investigators have observed this drag reduction behavior in turbulent fields.[146] It is generally accepted that drag reduction is caused by polymer chain scission due to the shearing forces in the turbulent flow field. Horn and Merrill studied the chain scission of narrow polydisperse polystyrene in a turbulent flow device that was carefully constructed to minimize all sources of extensional flow. Their studies provided convincing evidence that full chain extension does indeed occur in turbulent flow before chain scission and that chain scission took place at the chain midpoint.[120]

2.1.2. Elongational Field

The shear field in turbulent flow is nonuniform and not well-defined. It is thus difficult to study the kinetics of mechanochemical processes and understand the fundamental mechanisms of mechanical activation. This limitation prompted researchers to study polymer solutions in laminar and uniform, well-defined shear fields. Early studies by Porter and Johnson clearly demonstrated that the chain scission of polyisobutene in cetane at high shear rates under laminar flow conditions was attributed to the extending forces.[25] Since then, substantial efforts have been aimed at understanding the mechanisms and nature of flow-induced conformation and covalent changes in the scission of macromolecules.[147]

In general, in an elongational flow field, an isolated flexible-chain molecule is expected to undergo a coil−stretch transition at a critical strain rate, $\dot{\varepsilon}_c$. A coiled polymer passing through an elongational flow field experiences a strong hydrodynamic force. The polymer chain begins to elongate when the force exceeds the entropic elasticity that tends to result in coiling. As the extension rate is further increased, chain scission occurs.[143] Ryskin, motivated by Frenkel's description of the terminal equilibrium configuration of a polymer stretched by a strong flow, proposed a "yo-yo" model to explain the dynamics of chain stretching.[148] The "yo-yo" model considers that the stretching force along the length of the chain is not uniform. The stretching force is zero at the ends and maximum in the middle with a roughly parabolic distribution. If the strain rate $\dot{\varepsilon}$, is greater than $\dot{\varepsilon}_c$, the central portion of the polymer is elongated first and then remains taut and grows in length at the expense of the two coiled end portions. The end portions move apart in a symmetric fashion under the influence of the flow, simultaneously diminishing in size. If the flow becomes weak, the chain will curl back into a coil; hence, each half of the chain behaves as a "yo-yo." Rabin calculated the dependence of the critical strain rate on the molecular weight of the polymer for the scission of a polymer in transient extensional flow ($\dot{\varepsilon}_f \propto M^{-1.1}$).[149] This model of scission was roughly in agreement with some observed results in transient capillary flows but in contrast to the scaling law ($\dot{\varepsilon}_f \propto M^{-2}$) observed for stagnation points in extensional flow fields.

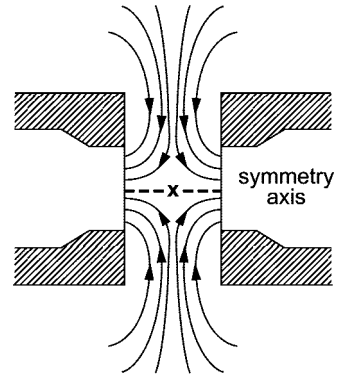

Figure 8. Opposite-jet flow cell. A schematic illustration of the flow pattern where the lines represent solvent velocity contours and the **x** represents the stagnation point.[143]

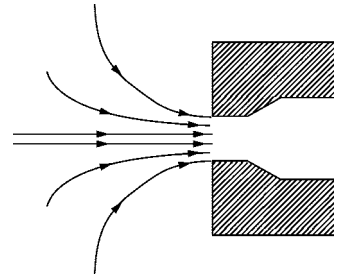

Figure 9. Constriction flow cell for transient elongational flow.[143]

Two different types of elongational flow, opposed jets elongational flow[114] and transient elongational flow,[120,121] have been used to study flow-induced polymer chain scission in solution (Figure 8). Keller and Odell used a cross-slot device to generate an opposite-jet flow.[26,27,115,150−152] The flow field created by the opposing orifices has a region of zero velocity—a stagnation point (**x** in Figure 8)—where a rapidly flowing polymer solution experiences a high velocity gradient. Polymer chains trapped in the center of the flow field remain there long enough to uncoil and fully elongate. Experimentally, birefringence measurements were used to determine the extent of chain elongation. As the strain rate is increased, it eventually reaches the fracture strain rate ($\dot{\varepsilon}_f$), at which point polymer scission occurs. The critical strain rate for chain fracture ($\dot{\varepsilon}_f$) was found to decrease with increasing molar mass of the polymer ($\dot{\varepsilon}_f \propto M^{-2}$).[118]

Merrill and Leopairat designed an apparatus in which constrictions in the direction of flow generated a transient elongational effect (Figure 9), localized to the region of the constriction.[120,121] Flow through this kind of device has no stagnation point, and it is believed that full elongation of the polymer chain does not occur. Nonetheless, midpoint scission does occur. This suggests that chain scission occurs before full chain elongation and midpoint scission occurs in the partially uncoiled polymer.[120,121] The $\dot{\varepsilon}_f$ still decreases with increasing molar mass of the polymer but scales with

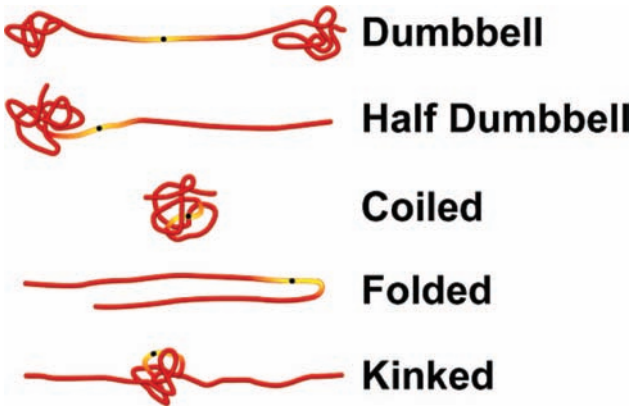

Figure 10. Schematics of different possible polymer conformations during the act of stretching.[118] The midpoint of each polymer chain has been indicated in black with a gradient to include the central 15% of the chain where bond scission has been shown to occur.[24,99]

M^{-1} ($\dot{\varepsilon}_f \propto M^{-1}$). Nguyen and Kausch have performed extensive studies of polystyrene chain scission in transient elongational flow.[123,143,153−155] They observed that the critical strain rate for chain fracture in transient elongational flow was only weakly dependent on solvent viscosity and temperature. It was proposed that internal viscosity forces resulting from intramolecular friction between monomer units provide the predominant mechanism for bond scission. This mechanism should be negligible in the opposite-jet flow field, since the polymer chains are highly elongated with a lower probability of collision between polymer segments.

Recently, Smith and Chu directly observed the stretching of individual polymers in a spatially homogeneous velocity gradient through use of fluorescent labeled DNA molecules. Even at the highest strain rates, distinct conformational shapes (dumbbell, kinked, half dumbbell, or folded) were observed (Figure 10).[118] They concluded that the rate of stretching of individual DNA molecules in an elongational flow field is highly variable and depends on the molecular conformation that develops during stretching. The variability is due to a dependence of the dynamics on the initial, random equilibrium conformation of the polymer coil. If a coiled chain starts out at equilibrium with both of its ends on the same side of the center of mass with respect to a plane perpendicular to the stretching axis, a large fold is likely to develop. If the same initial shape is rotated by 90°, it is likely to develop a dumbbell, a half dumbbell, or a kinked shape. Given the variety of conformations that have been observed in the extensional flow studies (Figure 10), it remains poorly understood in what polymer conformation selective midpoint scission occurs.

It should be noted that experiments for polymer chain scission in an elongational flow field require specialized devices and are relatively difficult to perform. Perhaps an even greater limitation in these experiments is the need for very high molecular weight polymers (10^6 Da) of low polydispersities, which is relatively difficult to achieve in general (Figure 11).[156] Even with more recent advances in living polymerization (post-1993),[157−162] the combination of ultrahigh molecular weight, single mechanophore incorporation, and low polydispersity (to ensure that the mechanophore is at the chain's midpoint) remains a synthetic challenge. Finally, the fact that only a single mechanophore is present in such a large macromolecule makes analytical characterization of the mechanochemical reaction a daunting challenge.

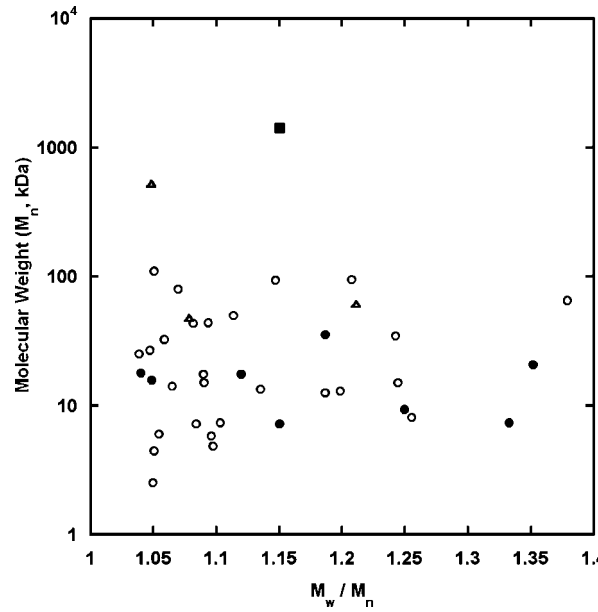

Figure 11. Molecular weight (M_n) vs PDI (M_w/M_n) for various living polymerizations: cationic (●), anionic (○), and coordination catalysts (△).[156] SET-LRP (■) is shown for comparison.[160]

These practical aspects are the major limitations of using extensional flow studies for exploration of new mechanophores.

A significant breakthrough in polymer synthesis that shows promise for meeting the previously mentioned synthetic challenge is Percec's single-electron-transfer living radical polymerization (SET-LRP).[160] When compared to previous polymerization reactions, SET-LRP can be used to produce polymers with molecular weights an order of magnitude higher than the rest of the techniques shown in Figure 11 and with lower polydispersities. More recently, Percec and co-workers demonstrated that even copper wire can catalyze the SET-LRP efficiently for the synthesis of tailored polyacrylates.[163] Moore and co-workers use this polymerization technique to synthesize mechanophore-linked polymers with low polydispersity and high molar mass (see section 2.4.3). However, extensional flow studies with these systems have yet to be reported.

More recently, acoustic field has emerged as a tool for more elegant flow field studies. In addition to the simplicity of the devices used for the acoustic studies, bulk phase chemical characterization methods such as conventional separation and spectroscopy techniques can also be used to study the mechanisms and nature of flow-induced conformation and covalent changes in the scission of macromolecules. Moreover, when combined with isotopic labeling, acoustic field polymer chain scission becomes a powerful technique for surveying new mechanochemical reactions.

2.2. Mechanisms of Mechanochemical Activation

The chemical effects of acoustic fields on the chain scission of polymers in solution have been extensively studied over the past several decades.[72,98,99,164] Although there is still some debate about the precise mechanism of mechanical activation,[104,165,166] it is generally accepted that the chain scission of polymers is the result of solvodynamic shear created by cavitation, which involves the nucleation, growth, and collapse of microbubbles in solution (Figure 12). Polymer segments in the high-gradient shear field near the collapsing bubble move at a higher velocity than those

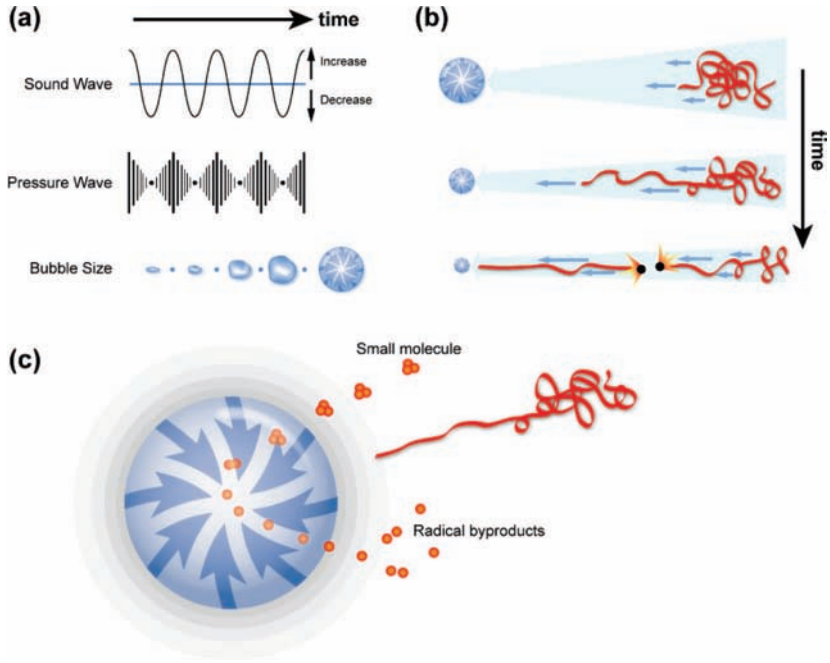

Figure 12. Mechanism for ultrasound-induced polymer chain scission: (a) gradual bubble formation results from pressure variations induced by the acoustic field; (b) rapid bubble collapse generates solvodynamic shear; (c) small molecules undergo pyrolytic cleavage to form radical byproducts upon bubble collapse, while polymer chains do not undergo pyrolytic cleavage because they do not penetrate the bubble interface.[171]

segments further away from the collapsing cavity. This velocity gradient causes the polymer chain to become elongated, and tension develops along the backbone of the polymer, which finally leads to chain scission.

Similar to the chain scission of the polymer in an elongational flow field, an isolated flexible-chain molecule in an acoustic flow field is expected to undergo a coil−stretch transition. A coiled polymer experiences a strong hydrodynamic force generated by the collapse of the bubble (as discussed in section 2.1.2). However, the polymer chain does not have to be fully elongated; a coiled polymer with various conformational shapes (dumbbell, kinked, half dumbbell) experiences chain scission.[167−170]

In general, polymer mechanochemistry induced by an acoustic field is a nonrandom process; for example, the scission of polymer chains in solution occurs at a preferential position near the midpoint. Several models have been proposed based on the studies of the kinetics of chain scission and mathematical simulations.[99,104,165,166,172] The best model to date comes from the work of van der Hoff and Gall.[173−175] They found that the chain scission of polystyrene in THF could be modeled well when it was assumed that the probability of chain cleavage was distributed in a Gaussian manner within the middle 15% of the chain. This center cleavage model is also consistent with the "stretching and breakage" mechanism, since the solvodynamic forces are predicted to be the greatest in the center of the polymer chain.

2.2.1. Homolytic Bond Cleavage

It has been generally accepted that ultrasound-induced cleavage of the covalent bonds of homopolymers occurs homolytically.[99,165,176,177] The radical pair that forms subsequently recombines, disproportionates, reacts with atmospheric oxygen, or attacks another polymer chain. The evidence for the existence of these macromolecular radicals was first supported by radical trap experiments. Henglein and co-workers reported experiments on the sonication of a benzene solution of PMMA in the presence of 2,2-diphenyl-1-picrylhydrazyl (DPPH), a well-known, stable free radical with an absorption band in ethanol solution centered at ca. 520 nm.[109,177] The violet color of DPPH disappeared with sonication time due to reaction with radicals formed in solution under sonication conditions. The loss of the color of DPPH was much slower when it was sonicated in a solution that lacked polymers. Spectroscopic analysis of the loss of DPPH can be used for the determination of the polymer chain scission rate.

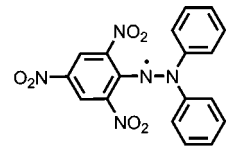

Diphenylpicrylhydrazyl (DPPH)

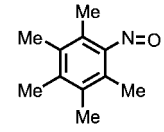

Pentamethyl nitrosobenzene (PMNB)

Direct evidence for the formation of radicals in ultrasound-induced polymer chain scission in solution has also been supported by studies using ESR techniques.[22,178] Sohma et al. reported that an ESR signal was observed for the sonication of PMMA in benzene in the presence of pentamethyl nitrosobenzene (PMNB), a spin-trap reagent (Figure 13).[178] No ESR signal was observed for the control experiment without polymer under the same conditions.

The macromolecular radicals generated by chain scission of the polymer upon sonication can initiate the polymerization of a second unsaturated monomer. The formation of copolymers was first used by Melville and Murray as proof of the presence of a radical, and it has been used by a number of other groups in the production of a variety of copolymers.[179,180]

These experimental results correlate well with predictions based on the thermally activated barrier to scission (TABS) model (Figure 14).[181−183] The TABS theory[152] is based on the assumption that the backbone scission of a linear polymer is a thermally activated process and the rate is determined

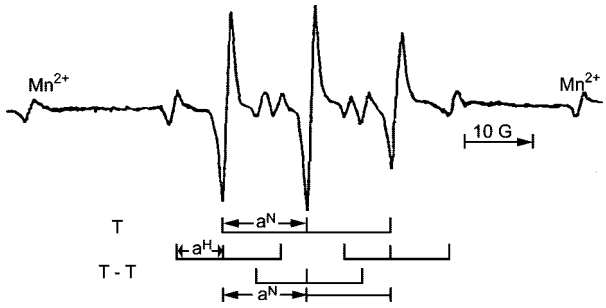

Figure 13. ESR spectrum observed at room temperature for a PMMA−benzene solution with added PMNB after 2 h of ultrasonic irradiation at 40 °C. Stick diagrams are also shown in which a^H and a^N (the hyperfine coupling constants) stand for separations due to coupling of the radical to a hydrogen and nitrogen nucleus.[178]

by an Arrhenius type equation. The force can be derived from the Morse potential energy function,

$$U(r) = D_e(1 - e^{-a(r-r_e)})^2 \quad (1)$$

where U is the potential energy, r is the distance between the two atoms, r_e is the distance corresponding to the minimum in the potential energy, D_e is the well depth of the minimum, and a is the parameter defining the width of the minimum.

During mechanoactivation, the polymer chain is stretched, and when thermal fluctuations overcome the required energy barrier, bond scission occurs. Thus, strain energy is converted into chemical energy simply by increasing the bond distance between two atoms. This action decreases the activation energy barrier by increasing the energy of reactants in the ground state. Mechanical rupture can only occur if the mechanical stress exceeds the tensile strength of the bond and if it is applied in a time frame ($<10^{-10}$ s) that is less than the vibration period of the bond.

The relation between the rate of scission k_0 and the temperature T according to this model is given by

$$k_0 \propto \exp[-U_0/(kT) + (\alpha/l)\beta N^2/8] \quad (2)$$

where β is proportional to strain rate, N is the number of monomers, α is the stretched bond length, and l is the monomer length. The TABS model successfully explains the precision of chain halving and the temperature dependence of scission-rate in extensional and acoustic flow fields. This finding is significant because it means that new mechanophores can be designed from considerations of known reaction pathways. As shown in section 2.4.6, the combination of force plus thermal activation may bias the pathway away from that favored under pure thermal conditions.[184] The directional nature of force overcomes the isotropic thermal path of Brownian motion.

2.2.2. Heterolytic Bond Cleavage

In all of the cases of ultrasound-induced chain scission of organic polymers studied to date, experiments have supported the homolytic bond cleavage mechanism for polymer cleavage. In striking contrast to the vast amount of work on homolytic scission, mechanically-induced heterolytic cleavage has been little studied. Recently, however, Aktah and Frank proposed that heterolytic bond cleavage is also a feasible mechanism for mechanically-induced polymer chain scission.[70] Using first principles molecular dynamics simulations, the stretching of a PEG chain was modeled in the presence of water molecules (Figure 15). The results indicated that the heterolytic cleavage of a stretched bond in solution is strongly influenced by solvation. In this case, the positive partial charge carried by the solvent proton stabilizes the localization of the both electrons at one side of the stretched bond. Electron transfer is then accompanied by the transfer of a proton from the solvent. The cation is then neutralized through rapid proton exchange.

2.3. General Features of Ultrasound-Induced Polymer Chain Scission: Chain-Length Dependence and M_{lim}

Polymer chain scission occurs more rapidly for polymers with higher molecular weights. Chain scission ceases as the polymer chain length approaches a lower limiting value, M_{lim}. Below the M_{lim}, the polymer chain is too short to experience the forces required for bond cleavage. The molecular-weight dependence on the rate of bond cleavage is strong evidence that the cleavage process is mechanochemical in nature (Figure 16) and not a result of ultrasound-induced temperature and pressure fluctuations. As will be discussed in detail in later sections, recent sonication studies have shown that the chain scission rate of polymers is greatly affected if a weak bond is incorporated into a polymer chain (bond-specific activation, section 2.4.6).[28,29,32,33]

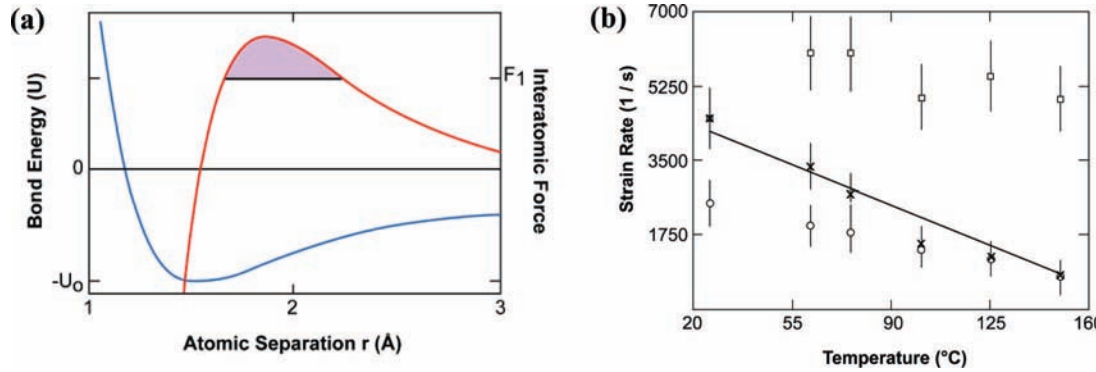

Figure 14. (a) Morse function for a C−C covalent bond (blue) and its derived interatomic force (red). The shaded region (purple) indicates the activation energy required to break a C−C bond under an applied force (F_1).[182] (b) Critical strain rate for chain scission ($\dot{\varepsilon}_f$) as a function of temperature, uncorrected (□) and corrected (**x**) for solvent viscosity. Also shown is the variation of critical strain rate for the coil−stretch transition ($\dot{\varepsilon}_0$) as a function of temperature (○). The continuous line is the "best fit" for the TABS model. The molecular weight of this polymer is 8100 kDa with a PDI of 1.07.[182]

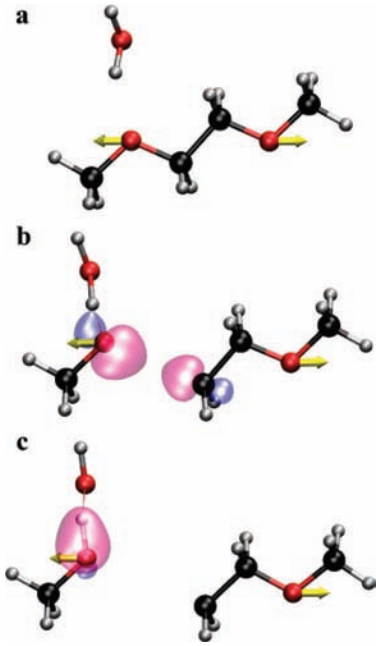

Figure 15. Schematic demonstrating bond cleavage of PEG chains before and after the electron transfer. (a) PEG molecule before stretching, with yellow arrows denoting the stretching direction. (b) PEG molecule during bond cleavage, a process that is greatly facilitated by solvation. (c) PEG molecule after bond cleavage where the electron moves from the carbon to the oxygen, as denoted by a change in orbital location.[70]

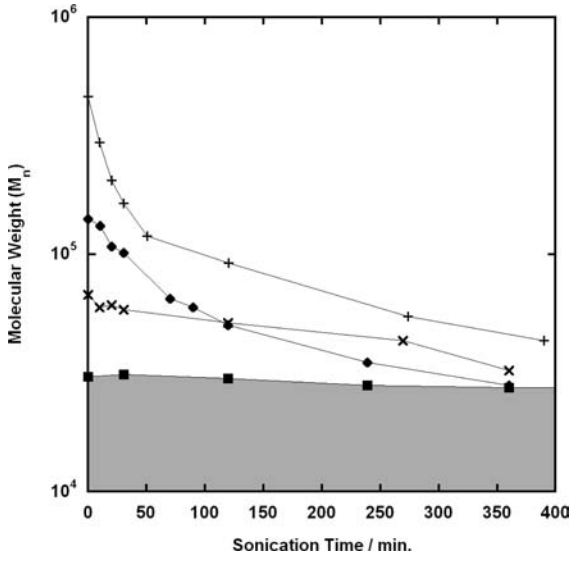

Figure 16. Ultrasonic chain scission of narrow polydispersity polystyrene in toluene: (■) 30,000; (×) 68,000; (◆) 140,000; (+) 460,000.[185] The limiting molecular weight, M_{lim}, is represented by the shaded region. (Experimental conditions: 50 cm^3 of 0.5 wt % solution irradiated at $I = 17.4$ W cm^{-2} at 25 °C).

2.4. Factors Influencing Ultrasound Mechanochemistry

The rate of chain scission during ultrasonic irradiation in solution is dependent on many factors including ultrasound intensity, solvent vapor pressure and viscosity, temperature, solution concentration, initial polymer molecular weight, and the chemical structure of the polymer. The following sections will discuss each of these factors in more detail.

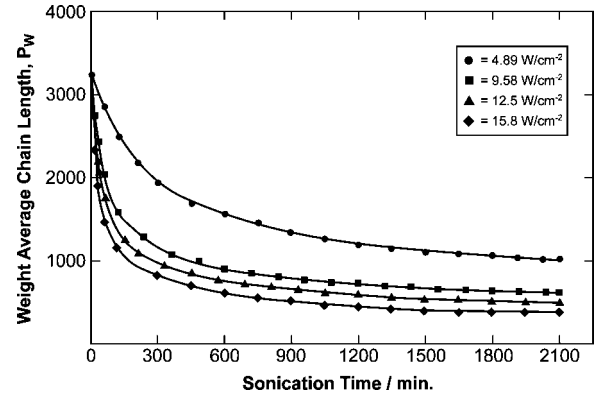

Figure 17. Effect of ultrasonic intensity on the chain scission of 25 mL samples of polystyrene in benzene (1 wt/vol %). Plot of chain length vs time in minutes for various ultrasonic intensities: (●) 4.89 W cm^{-2}; (■) 9.58 W cm^{-2}; (▲) 12.5 W cm^{-2}; (◆) 15.8 W cm^{-2}.[186]

2.4.1. Ultrasound Intensity

Higher ultrasound intensities lead to a faster rate of chain scission, and M_{lim} for chain scission is lowered.[98,103,166,168,185−188] For example, Mostafa reported that the weight average chain length (P_w) of a polystyrene solution in benzene (1 wt/vol %) decreased from 3240 to 1004 after sonication for 35 min if the ultrasound intensity was 4.89 W cm^{-2}, while P_w decreased to 380 if a stronger ultrasound intensity (15.8 W cm^{-2}) was used for the equivalent polymer solution and same sonication time (Figure 17).[186] Analysis of numerous systems has shown that the rate coefficient, k, for polymer cleavage does not increase linearly with an increase in ultrasound intensity. Below a threshold of ultrasonic intensity, chain scission does not proceed because cavitation does not occur. Furthermore, an upper threshold also exists, above which cavitation is suppressed.

Noltingk and Neppiras stated that the maximum radius of the bubble R_m is proportional to the square root of the ultrasound intensity. Therefore, higher ultrasound intensities result in both larger sizes of cavitation bubbles and an increase in the density of bubbles in solution, as well as higher shear forces.[187,189] However, when the ultrasound intensity is too high, the increased number of bubbles indicates that the ultrasound field does not pass through the solution as efficiently, thus reducing cavitation and decreasing the rate of chain scission.

2.4.2. Solvent

Solvent plays a crucial role for ultrasound-induced polymer mechanochemistry.[175,190−198] Vapor pressure is the most influential solvent factor affecting the process. Other solvent properties, such as viscosity, surface tension, and the nature of the polymer−solvent interactions, can also influence the rate of ultrasound activation. The nature of the polymer−solvent interactions modulates the chain's equilibrium "coil size" prior to activation, with more miscible solvents facilitating the coil−stretch transition (refer to Figure 10).[118,150,167−170]

A large number of studies have demonstrated that the chain scission rate of polymers is insensitive to the chemical composition of the polymer when sonicated under the same conditions. Polymers with the same backbone, such as poly(methyl acrylate) (PMA) and PMMA, degraded with similar rates under the same sonication conditions. Instead,

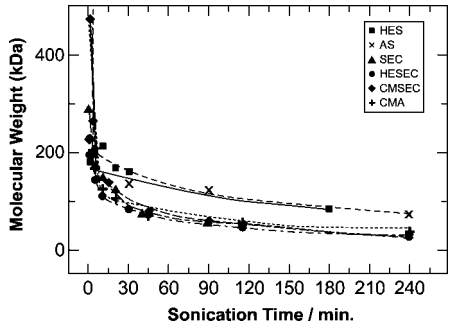

Figure 18. Comparison of starch and cellulose derivatives in their chain scission behavior demonstrated by the molar mass as a function of the sonication time. (HES: hydroxylethyl starch; AS: acetyl starch; SEC: sulfethyl cellulose; HESEC: hydroxyethylsulfethyl cellulose; CMSEC: carboxymethylsulfethyl cellulose; CMA: carboxymethyl amylose).[199]

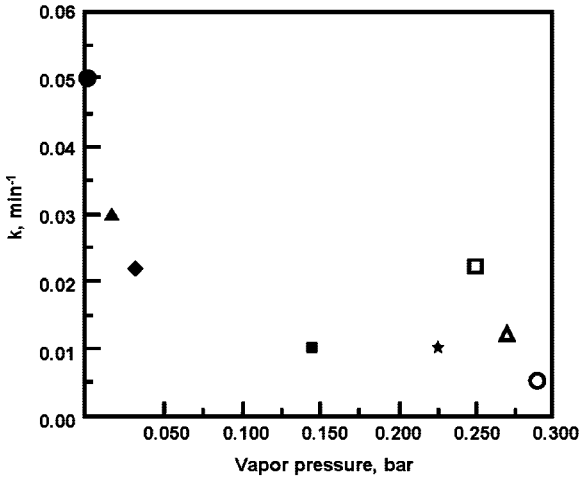

Figure 19. Effect of vapor pressure on the chain scission rate coefficient, k (min^{-1}), of poly(vinyl acetate) at a concentration of 2 g/L: ●, *o*-dichlorobenzene; ▲, chlorobenzene; ■, benzene; ◆, toluene; ★, chloroform. Model predictions: ○, acetone; △, 9:1 acetone/water; □, 4:1 acetone/water (ratios by volume).[194]

the scission rate depends on the polymer chain dimensions in solution.[104−109] For instance, Kulicke and co-workers investigated the chain scission of cellulose derivatives and observed that the molar degree of substitution and the introduction of a second substituent have no observable influence on the degradation process (Figure 18).[199] However, strongly coiled starch is degraded much more slowly than linear cellulose derivatives. In solution, strongly coiled starch needs higher forces to stretch the polymer backbone. With the same available energy, the strain generated along the polymer backbone was smaller and chain scission was slower.

The rate for the ultrasound-induced chain scission typically decreases in solvents with higher vapor pressures.[191,194,197,200,201] For example, Madras and co-workers systematically studied the ultrasonic chain scission of poly(vinyl acetate) in six different individual solvents and two solvent mixtures (Figure 19).[194] The chain scission rate constants decreased with increasing solvent vapor pressure in this order: *o*-dichlorobenzene, chlorobenzene, toluene, and benzene. Similar trends have been observed for the chain scission of polystyrene,[196] poly(butyl methacrylate),[200] polypropylene,[202] and dextran[191] in different solvents.

The effect of solvent vapor pressure is believed to influence the magnitude of shear forces generated upon the collapse of bubbles. Solvents with higher vapor pressures are more volatile, and as a result, more solvent vapor will enter the bubbles. This difference provides a cushioning effect on the collapse of the bubbles. The solvent movement is thus slower, and the shear stress exerted on the polymer chain segments is lowered, thereby leading to lower chain scission rates.

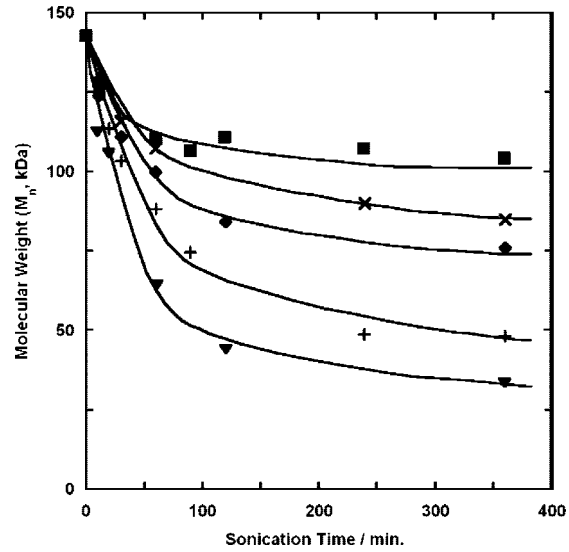

Figure 20. Ultrasonic chain scission of polystyrene in toluene at different temperatures: ■, 61 °C; ×, 50 °C; ◆, 40 °C; +, 5 °C; ▼, −10 °C (Experimental conditions: 50 cm^3 of 0.5 wt % solution irradiated at $I = 17.4$ W cm^{-2} at 25 °C).[185]

Compared to the effect of solvent vapor pressure on the rate of chain scission, the effect of the solvent viscosity is not as significant.[193,196,202,203] Increasing the solution viscosity typically leads to a decrease in the rates of chain scission. In more viscous solutions, an increase in viscosity raises the cavitation threshold. The hydrodynamic shear forces resulting from the bubble collapse are decreased. Furthermore, a polymer chain in a more viscous solvent is less flexible and moves more slowly toward the collapsing bubbles.

2.4.3. Temperature

The majority of chemical processes are accelerated by an increase in temperature. However, the opposite effect is typically observed for the ultrasonic chain scission of polymers in solution. The chain scission rate decreases with increasing temperature (Figure 20).[185,195,204−207] This negative temperature coefficient has been observed for the ultrasonic chain scission of polystyrene,[185] poly(alkyl methacrylate),[195] poly(vinyl chloride), and poly(vinyl acetate).[208] In contrast, Yen and Yang reported that an increase in temperature increases the chain scission rate coefficient for the ultrasonic chain scission of polyacrylamide in water.[209] The negative temperature coefficient has often been cited as evidence that ultrasound-induced polymer chain scission is mechanical in origin.

The effect of temperature is attributed to changes in the physical state of the system, such as the vapor pressure and the viscosity of the solvent. At increased temperatures, the solvent pressure is higher, and a larger quantity of the solvent vapor enters the cavitation bubbles during expansion. As mentioned previously, this change exerts a "cushioning" effect during the bubble collapse. The intensity of the shear forces is lessened, and the solvent velocity is reduced. Consequently, the chain scission rate is decreased.

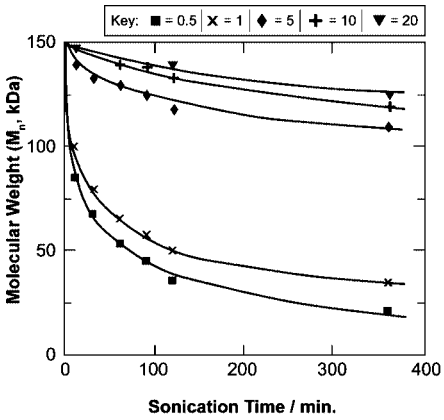

Figure 21. Chain scission of polystyrene in toluene at 25 °C at various concentrations (wt/vol %); the critical overlap concentration, C^*, was estimated to be 2.4 wt/vol %.[196]

2.4.4. Concentration

The rate of polymer chain scission in solution is also influenced by the polymer concentration. The higher the concentration of the polymer, the slower the chain scission rate.[196,198,202,210−216] For example, Price and Smith studied the chain scission of polystyrene at different concentrations in toluene (Figure 21) or methyl butyrate.[196] The chain scission in both solvents is much faster, and the M_{lim} is lower in less concentrated solutions. In both solvents, chain scission is suppressed when the concentration reaches 20 wt/vol %. Presumably, this effect is a result of cavitation suppression due to more viscous solutions at higher concentrations. Other groups have also investigated the effect of solution concentration on polymer chain scission. In each case, the effect of polymer concentration is consistent with the aforementioned results.

These observations are explained in terms of viscosity changes for different polymer concentrations. At higher concentrations, the solution viscosity increases. An increase in viscosity raises the cavitation threshold. This increased threshold makes it more difficult for cavitation bubbles to form. More importantly, the velocity gradients around collapsing bubbles become smaller, and the elongation of the polymer backbone is reduced.

Price noticed a large jump in the scission rate of polystyrene from polymer concentrations of 1% and 5% solution in toluene. The significant differences are attributed to the critical overlap concentration, C^*, the concentration at which chains begin to entangle. When chains begin to overlap, their movement and cleavage are more restricted, and chain recombination is more likely. Hence, the extent of chain scission is reduced. The critical overlap concentration in good solvents is estimated as 2.4 wt/vol % for polystyrene with molecular weight 448 kDa. This value matched the large difference observed for the chain scission rate between 1% and 5% polystyrene solutions (Figure 21).[196]

2.4.5. Initial Molecular Weight

Investigations of the initial molecular weight on the ultrasonic-induced chain scission of polymers in solution provide insight into the degradation mechanism. The effect of the initial molecular weight on the rate coefficient for the chain scission is well-established; ultrasonic chain scission proceeds more rapidly at higher molecular weights.[98,217,218] In some cases, the rate coefficient increases with increasing initial molecular weight of the polymer (Figure 22).[100,101] This dependence follows an empirical relation of the form

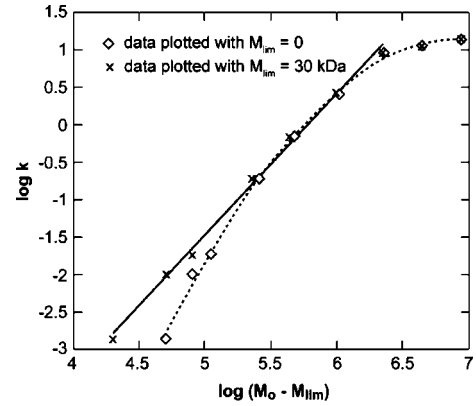

Figure 22. Double-logarithmic plot of the dependence of the scission rate coefficient on the initial molecular weight (M_n, dotted line) and on ($M_0 - M_{lim}$) (solid line). The empirical value for M_{lim} is 30 kDa.[100]

$$k \propto (M - M_{lim})^x \quad (3)$$

where k is the rate coefficient, M is the molecular weight of the polymer, M_{lim} is the limiting molecular weight, and the exponent (x) is a value from 0 to 3, depending on the experimental conditions. For example, Nguyen reported that the best fit was obtained with $M_{lim} = 30$ kDa, giving $x = 1.9$ over the molecular range 50−2200 kDa for the chain scission of polystyrene in decalin.[100] For polymers with extremely high molecular weights (>2200 kDa), the rate constant becomes independent of molecular weight. Taghizadeh et al. also reported that a nonlinear dependence of ln k on the molecular weight of the polymer was observed for the ultrasonic chain scission of poly(vinyl pyrrole) in water.[219]

In contrast, Madras recently reported that the chain scission rate coefficient k is linearly dependent on the initial molecular weight of polymers.[103] This claim is based on a mathematical fitting of the model with experimental data for ultrasonic chain scission of a number of polymers, including poly(ethylene oxide) (PEO), polyacrylamide (PAa), poly(butyl acrylate) (PBA), and PMA. The chain scission rate k is assumed to be of the form $k = k_d(M - M_{lim})^\lambda$, where k is the chain scission rate, k_d is the degradation coefficient, M is the initial molecular weight of the polymer, M_{lim} is the limiting molecular weight, and the exponent λ is a value between 0 and 3. When $\lambda = 1$, expressions were derived analytically and the experimental data was fitted to the theory by linear regression. Representative data for PEO is given in Figure 23.

2.4.6. Bond-Specific Activation

The rate of chain scission for polymers is greatly affected if a specific weak bond is incorporated into a polymer chain. Encina found that the rate of chain scission of poly(vinylpyrrolidone) increased 10-fold when peroxide linkages were randomly incorporated into the polymer backbone (Figure 24).[28] The peroxide bond with a homolytic bond dissociation energy (the standard enthalpy change when a bond is cleaved) of 51 kcal/mol is much weaker than the C−C (88 kcal/mol) and the C−O (91 kcal/mol) bonds. Through this experiment, Encina demonstrated that a polymer can be degraded at specific locations in its backbone if those bonds

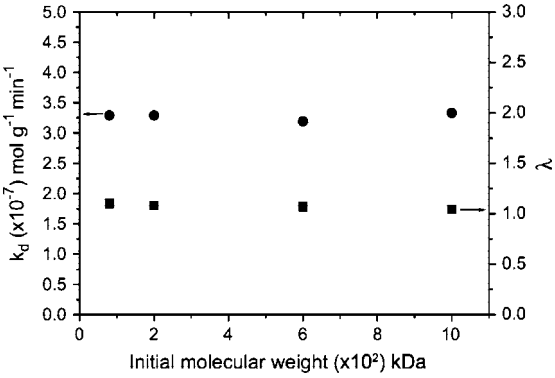

Figure 23. Variation of rate coefficient, k_d, and exponent, λ, with the initial molecular weight of PEO.[103]

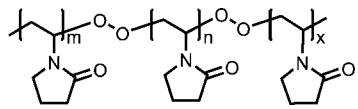

Figure 24. Poly(vinylpyrrolidone) with random peroxide linkages.[28]

are considerably weaker than the rest of the bonds in the polymer backbone.

Moore and co-workers demonstrated that when a single weak azo link was positioned at the center of a linear PEG chain (Figure 25), mechanically-induced cleavage was localized almost exclusively to the single weak site. The energy of activation for the homolytic extrusion of nitrogen from the azo group is 24−30 kcal/mol, about two to three times lower than that of the C−C and C−O bonds in the PEG backbone. Considering that only one bond in 1000 C−C/C−O bonds that make up the polymer backbone was cleaved, the selectivity is remarkable.[32]

The azo-centered link-functionalized polymer was subjected to pulsed ultrasound at 20 kHz and 8.7 W cm^{-2} in acetonitrile, and the chain scission was analyzed by GPC, using refractive index (RI) as the mode of detection. GPC traces showed that the concentration of a 40 kDa polymer decreased with sonication time, while the concentration of a new 20 kDa molecular weight species increased (Figure 26). The formation of and the sharpness of the new 20 kDa peak indicated that the 40 kDa polymer cleaved at its midpoint into two 20 kDa fragments upon exposure to an acoustic field. As a control, the chain scission of a 40 kDa sebacic acid link-functionalized PEG chain (Figure 27) was much slower, and the new peak with an average molecular weight of 20 kDa was much broader (not shown).

More importantly, ^{13}C isotope labeling experiments provided direct evidence that the azo linkage was reacting by homolytic extrusion of nitrogen, and not by some other mechanical degradation process (Figure 28). The major product that resulted from ultrasonic-induced chain scission, cyanohydrin, was different from the major products that resulted from thermolysis, which result from radical recombination. Two mechanisms were proposed for the formation of cyanohydrin. In the first mechanism, radical intermediates formed after homolytic C−N bond cleavage of the polymer under sonication reacted with molecular oxygen, and the peroxide radical then further degraded to form cyanohydrin. In the second mechanism, each macroradical reacted with a hydroxide radical to directly form cyanohydrin.[32]

More recently, Moore and co-workers showed that incorporation of mechanically sensitive chemical groups made it possible to harness the mechanical forces generated by an acoustic field to open otherwise forbidden orbital symmetry pathways.[171,220] Thus, mechanical deformation can be used to activate specific reaction pathways to yield products not obtainable from purely thermal or light-induced reactions. In this study, benzocyclobutene (BCB) mechanophores positioned near the midpoint of PEG or PMA chains underwent stress-induced 4-π electrocyclic ring-opening prior to, or competitively with, chain scission. The electrocyclic ring-opening was demonstrated by the incorporation of UV-active *N*-(1-pyrene)maleimide, as evidenced by GPC analysis using RI and UV detection and ^{13}C labeling experiments (Figure 29).[29,33] The same reaction was not observed for a polymer with the BCB unit incorporated at the chain end.

More specifically, when placed within long polymer strands, the *trans* and *cis* isomers of a 1,2-disubstituted BCB underwent an ultrasound-induced electrocyclic ring-opening in a formally conrotatory and disrotatory process, respectively, that yielded identical products, as confirmed by ^{13}C labeling experiments. These results run counter to conventional theory, which states that when the electrocyclic ring-opening of *cis* and *trans* cyclobutene isomers is initiated by heat, different double-bond configurations of products are expected. According to the principle of conservation of orbital symmetry, when the molecule is thermally activated, conrotatory motion is expected, so a *trans* isomer should undergo a conrotatory motion to yield the *E,E* diene, whereas the *cis*-cyclobutene should produce the *E,Z* product (Figure 30). Photochemically, disrotatory motion is expected (*trans* yields the *E,Z* product while *cis* yields the *E,E* product). However, when mechanical force is used as the stimulus, both isomers yield the *E,E* product (shown in Figure 30a, in red). Force has thus biased the *cis* isomer along the less favorable disrotatory pathway.

Martinez and co-workers simulated the response of cyclobutene and BCB under applied forces using steered molecular dynamics combined with *ab initio* quantum chemistry.[221] When the external force is applied to *cis* H atoms, the ring does open in a disrotatory fashion, in agreement with the experiment results. In contrast, ring-opening proceeds with stereochemistry when the external force is applied to the *trans* H atom. Minimal energy pathways are shown in Figure 30b for each case at a variety of applied forces. Similar force-biased reaction pathways were also observed by Craig and co-workers during the mechanoactivation of *cis*- or *trans-gem*-dichlorocyclopropane-incorporated polymers (Figure 31).[222] The reaction probabilities for these polymers were nearly equivalent, despite the fact that the *cis* isomer reacts ~20× faster than the *trans* isomers under stress-free conditions. This nonstereoselective process allows for a high percentage of mechanoactivation along the polymer chain.

Studies on cyclobutene were recently accomplished using a molecular device in which mechanochemical activation followed a photoinduced geometry change. In this study, a cyclobutene ring was connected to a "stiff" stilbene derivative at both ends of each unit (Figure 32).[223,224] Upon photoisomerization of the stilbene from *Z*- to *E*-isomer, mechanical stress converted the cyclobutene ring to the open *trans*-2,4-hexadiene form. This unique, small molecule approach to analyzing chromophores and functional groups for mechanically-induced chemical reactions is important when analyzing new systems in a controlled manner. This method does not suffer from the variable molecular weights of polymeric

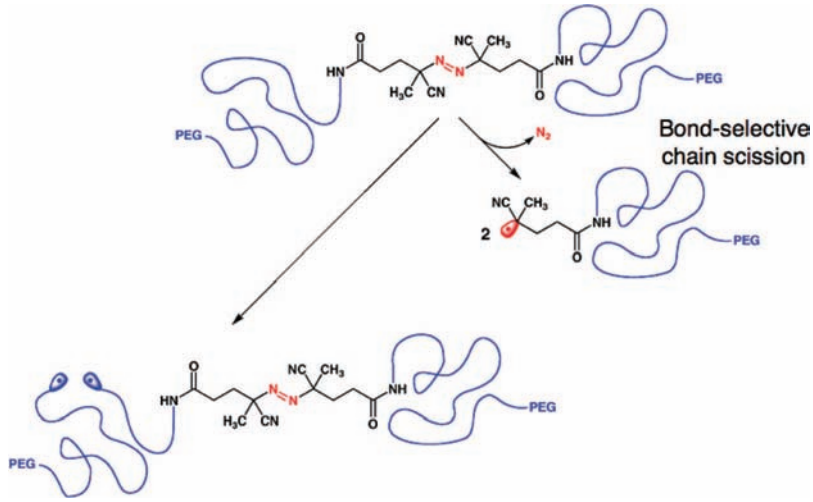

Figure 25. Highly selective bond cleavage for the ultrasound-induced azo-centered PEG chains. For a 30 kDa polymer, selectivity is 1 bond in ca. 1000.[32] Bond-selective chain scission is the predominant pathway.

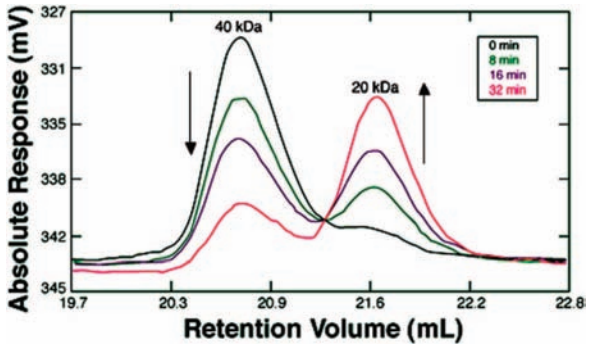

Figure 26. GPC traces showing the chain scission of the 40 kDa PEG azo-linked polymer **1**.

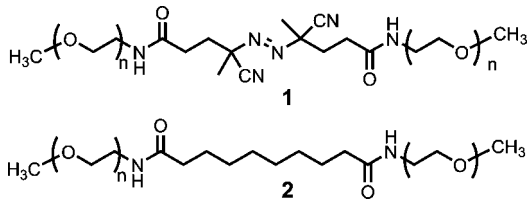

Figure 27. Chemical structures of azo link-functionalized PEG chain (**1**, top) and sebacic acid (**2**, bottom) link-functionalized PEG chain.

systems and allows for simple control of linking chains for kinetic analysis. There is great opportunity to use stilbene-functionalized chemical moieties for investigation as mechanically active units and then incorporate the successful groups into polymeric systems.

Moore and co-workers have also used sonication experiments to cause the stress-induced 6π-electron electrocyclic ring-opening of a spiropyran (SP) mechanophore.[33] In this study, a bisfunctionalized SP molecule with α-bromo-α-methylpropionyloxy groups was incorporated into the center of a PMA polymer (Scheme 1). When subjected to pulsed ultrasound, the originally colorless center-linked mechanophore PMA-SP-PMA solution became pink. The absorption spectrum of the sonicated solution showed a band characteristic of the open merocyanine form (Figure 33). Upon visible light irradiation, the sonicated solution again became colorless. This reaction was not observed in a control experiment in which the solution consisted of a terminally linked spiropyran (PMA-SP), indicating that the reaction was indeed mechanically induced.

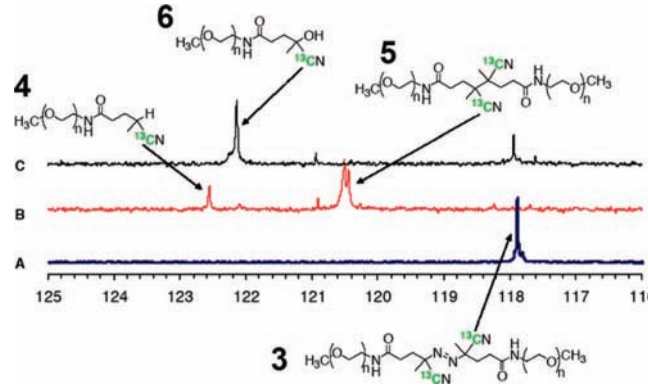

Figure 28. Comparison of portions of the ^{13}C NMR spectra of polymer **3** (a) thermalized polymer **3** (b) yielding polymers **4** and **5**, and sonicated polymer **3**, yielding polymer **6** (c), including assignments. All spectra were recorded at 125 MHz in $CDCl_3$ solution (ca. 20 mg/mL).[32]

Sijbesma has reported on the sonication of palladium, platinum, and silver coordination polymers, examples of which are shown in Schemes 2 and 3. Such metal coordination polymers could yield interesting reactive catalysts for subsequent reactions in a system subjected to mechanical stress. Upon sonication, the authors observed a decrease in polymer molecular weight for all examples, in some cases determined by GPC and ^{31}P NMR, others with ^{1}H NMR. While the authors conclude that the resultant chain scission was mechanically induced, their results are not definitive and lack adequate controls. In the cases of platinum-[97] and palladium-coordinated[40,97] polymers (Scheme 2), a small molecule was not sonicated for comparison, so it is unknown if the same reaction would have occurred in the small molecule case. In the silver-carbene-based polymer (Scheme 3), when small molecule versions of the polymers were studied, they dissociated significantly under sonication, and analysis of molecular weight was only obtained by ^{1}H NMR, as GPC analysis was unsuccessful.[96] One possible explanation for this observation is that the small molecules could be cleaved inside of the cavitation bubble during ultrasonic irradiation (see Figure 12). Although the reported reactions may indeed be mechanochemical in nature, more control reactions and a thorough investigation of the small molecule side reaction are needed for definitive answers.

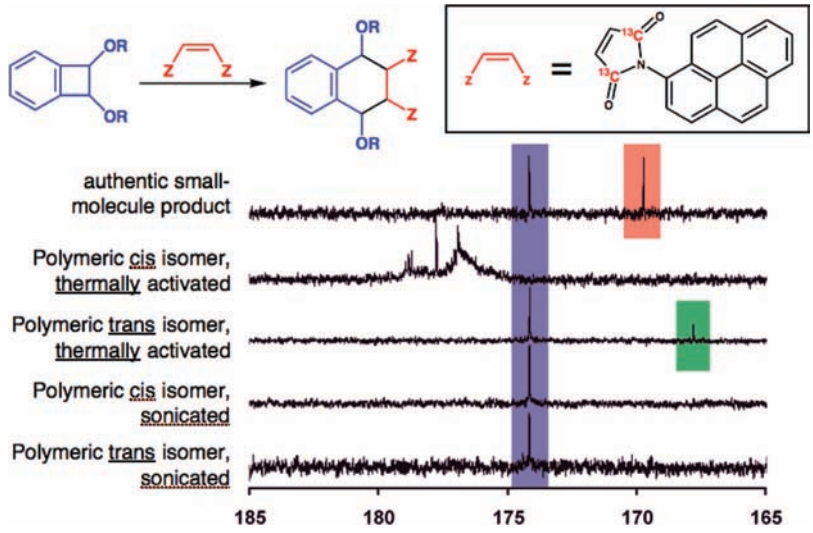

Figure 29. Comparison of reaction products and pathways for *trans*- and *cis*-benzocyclobutenes induced by ultrasound and by heating through ^{13}C NMR spectra.[29] The ^{13}C label of the maleimide is the peak at 174.2 ppm (blue), the red peak is the ester carbonyl at natural abundance (C═O of the OR group), and the green peak is an acid elimination product *N*-pyrene-2,3-naphthimide.

Based on these earlier observations, Sijbesma and coworkers recently reported that mechanically activated N-heterocyclic carbene (NHCs) coordinated silver- and ruthenium-based catalysts could be used to catalyze transesterification, ring-closing metathesis (RCM), and ring-opening metathesis polymerization (ROMP) reactions (reactions shown in Scheme 4).[225,226] Upon sonication, the shear force generated from the collapsing bubbles in solution cleaved the metal−ligand bond to generate the active catalyst center. The rate of metal−carbene bond cleavage was dependent on the length of the polymer chain. The longer polymer chains experienced faster catalytic reactions and higher turnover numbers (Figure 34). Interestingly, when the ultrasound was turned off, the conversion of the starting material did not increase. Fast catalyst degradation may account for the diminished conversion of reactant into product. Therefore, these mechanochemically activated catalysts were limited in the number of times they could be activated.[225] Overall, these studies demonstrated that mechanochemical activation can offer new opportunities for homogeneous catalysis—a field that will be vital for the development of greener methods of synthesizing and processing chemicals.

2.5. Alternative Methods To Induce Polymer Chain Scission

2.5.1. Repeated Freeze−Thaw Chain Scission

Repeated freezing and thawing of dilute polymer solutions has also been shown to induce polymer chain scission.[127,227−234] Zysman, Nguyen, and Kausch reported that chain scission occurred during the crystallization of dilute polystyrene in *p*-xylene solutions.[127] The chain scission rate was independent of the initial polymer concentration, but the rate increased with higher initial polymer molecular weight. The extent of chain scission also increased with the number of freeze−thaw cycles. One model based on interfacial cohesion between the polymer coils and the growing solvent crystallites fits best with the observed experimental data. Rather remarkably, chain scission during freeze−thawing is nonrandom and occurred with some preference for bond cleavage near the middle of the chain. However, the polydispersities of the degraded fragments were much higher in comparison to the results obtained in transient elongational flow.

2.5.2. Adsorption-Induced Chain Scission

Adhesion of complex macromolecular architectures to a surface can trigger the rupture of covalent bonds in that molecule.[61] Sheiko et al. reported that the deposition of brushlike macromolecules with long side chains onto a substrate can induce not only conformational deformations but also the spontaneous rupture of covalent bonds in the macromolecular backbone (Figure 35).[124−126] Backbone scission is highly sensitive to the substrate surface energy and the side chain length. If the surface energy is decreased to below 60 $mN\cdot m^{-1}$, molecules with long side chains (n = 140) that readily break on the water/propanol surface (γ = 69 $mN\cdot m^{-1}$) remain intact. Bond scission is much slower with shorter side chains. For example, brushlike molecules with a poly(2-hydroxyethyl methacrylate) backbone and PBA side chain with n = 130 instead of n = 140 on the water/propanol surface (γ = 69 $mN\cdot m^{-1}$) did not lead to any noticeable cleavage of the backbone. These observations were attributed to the fact that the attractive interaction between the side chains and the substrate enhances the steric repulsion between the side chains. This results in extension of the polymer backbone and a subsequent increase in the tension along the polymer backbone. When the side chain is long enough, the tension generated along the polymer backbone is strong enough to rupture covalent C−C bonds.

More recently, the same group reported that when a brushlike macromolecule was installed with a disulfide (S−S) bond in the middle of the all-carbon PMA backbone, bond scission was much faster than for those with an all-carbon backbone without the disulfide bond or with C−S in the middle of the backbone. The significant difference in rate constants suggests that midchain scission of the S−S bond containing linkers occurs due to scission of S−S bonds rather than the surrounding C−C, C−S, and C−O bonds.[125]

2.5.3. Mechanochemical Reactions in Bulk Polymers

Force-induced chemical reactions have also been achieved in bulk polymers. In this emerging area of mechanochemistry, macroscopic loads applied to the bulk polymer cause selective chemical transformations at the atomic level. The examples given in this section focus on mechanophores designed to react by mechanical activation. The analytical

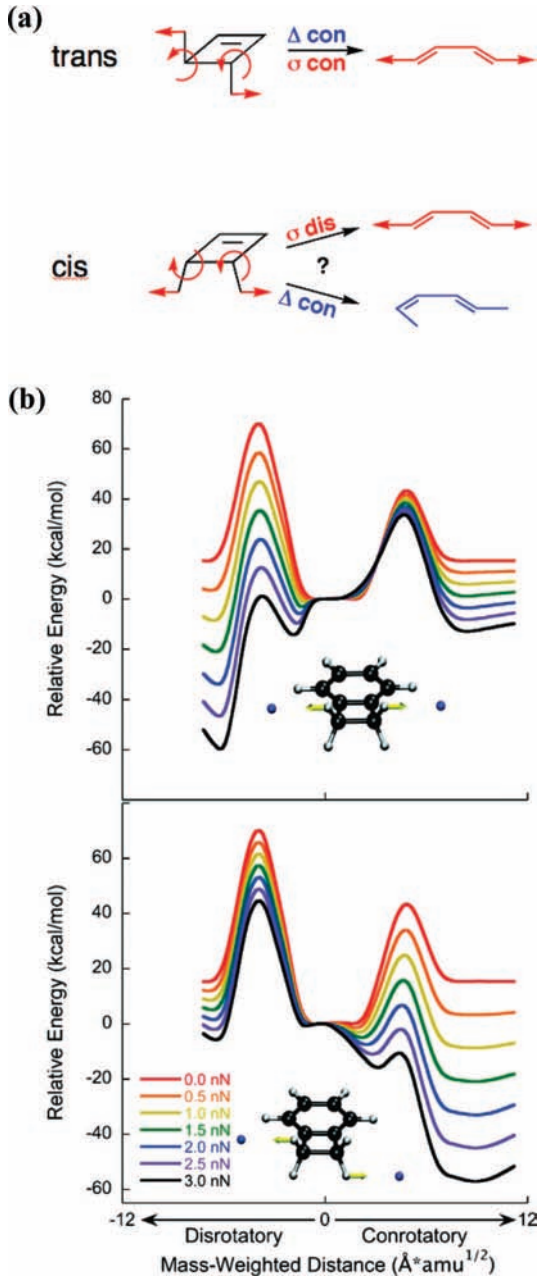

Figure 30. (a) Mechanical activation (σ) of *trans*- or *cis*-cyclobutene leads to the same isomeric diene shown in red, while thermal activation (Δ) yields two different diene products (in blue).[29] (b) Minimal energy pathways for the ring-opening of BCB. The *cis*-pulling case is shown in the top panel, and the *trans*-pulling case is given in the bottom panel.[221] Reprinted with permission from ref 221. Copyright 2009 American Chemical Society.

chemistry to create and characterize these polymers is a significant challenge. The mechanochemical change is often highly localized to regions of high stress concentration in the bulk polymer. Rigorous demonstration of the inferred chemical change requires carefully designed controls. However, the necessary controls have not been performed for all of the examples cited below, leaving open questions about the mechanochemical activation.

Chung et al. inferred a retrocycloaddition reaction upon mechanical damage to a polymer film. A tricinnamate monomer, 1,1,1-tris(cinnamoyloxymethyl)ethane (TCE), was cross-linked using photoirradiation to create a hard, transparent polymer film.[235,236] The cross-linking of TCE resulted from the [2 + 2] cycloaddition, which is a well-known

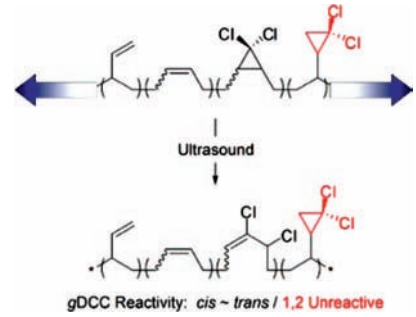

Figure 31. Electrocyclic ring-opening of *gem*-dichlorocyclopropane-incorporated polymers under mechanical stress.[222] Reprinted with permission from ref 222. Copyright 2009 American Chemical Society.

reaction of cinnamoyl groups when exposed to light. After grinding the polymer films, a fluorescent signal was generated, presumably via a cycloreversion, as evidenced by the change in emission spectra, the appearance of cinnamoyl C=C bands in the infrared spectrum, and the appearance of C=C proton peaks in the ^{1}H NMR spectrum.[236] Additionally, the authors were able to detect damage using fluorescence microscopy of cracked polymer films (Figure 36).

Another chemical approach to developing mechanically responsive polymers relies on the reversible Diels−Alder reaction. These polymer systems have been shown to heal crack damage by relying on external stimuli (heat, light, pressure, etc.) to trigger the healing event. Rather than the healing process being diffusion-controlled, these systems demonstrate healing kinetics on a time scale that correlates with the reversible chemical reaction promoted. Monomers with furan and maleimide functionality were shown to undergo a Diels−Alder reaction and retro-Diels−Alder reactions during cooling−heating cycles, creating a thermally reversible polymer.[57,237] Initial studies reported 57% healing efficiencies for compact tension samples subjected to healing conditions of 120−150 °C for 2 h under minimal pressure, followed by cooling to room temperature.[57] The next generation of highly cross-linked remendable polymers consisting of 1,8-bis(maleimido)-1-ethylpropane (2MEP) and a tetrafuran monomer (4F) to make 2MEP4F (shown in Scheme 5) reported higher healing efficiencies of ca. 80% attributed to an improved synthetic design.[237] A recent quantitative study of this furan-maleimide polymer 2MEP4F using a double cleavage drilled compression (DCDC) specimen reported full recovery of fracture toughness at lower temperatures (85−95 °C) and shorter times than what had been previously observed.[238]

Subsequent work in this area shows that furan-maleimide monomers can be synthesized from epoxy-containing starting materials, making them more compatible with epoxy thermosets.[239] These materials also possess good solubility in low boiling point solvents and improved processability. The more recent advancements in synthesis of furan-maleimide dendrimers have shown that thermal reversibility of Diels−Alder reactions occurs within a smaller, milder temperature range (60−95 °C).[240]

Sottos and co-workers recently studied the stress-induced 6π-electron electrocyclic ring-opening of a SP mechanophore[33] in the solid state.[30] Two different types of polymers have been studied thus far, and these include elastomeric PMA and glassy PMMA (Figure 37). For the PMA, a bis-functional SP with bromo-α-methylpropionyloxy groups was incorporated into linear PMA to make an elastomeric

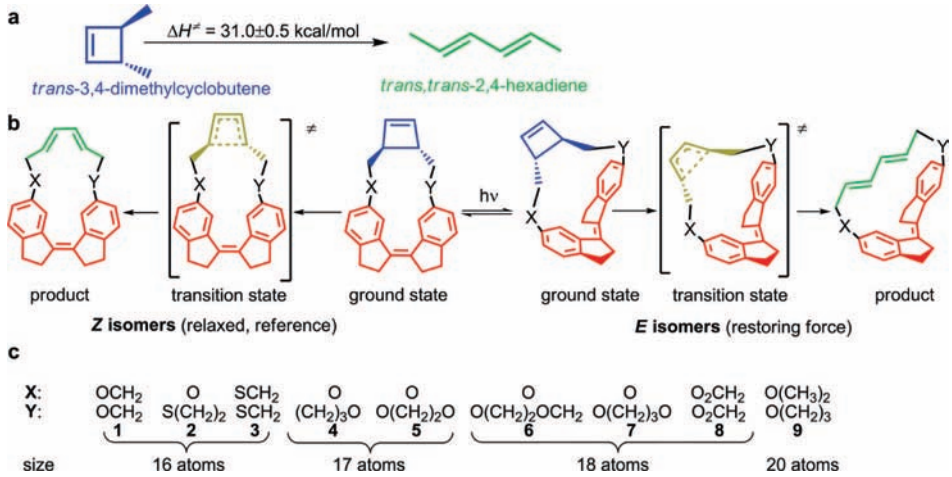

Figure 32. Experimental system used to illustrate the use of the molecular force probe stilbene (red), for studies of the chemomechanical kinetics of localized reactions: (a) substrate reaction, (b) general structure of the studied *Z* and *E* isomers showing the transition states and final product conformations, (c) chemical composition of the linkers. The macrocycles are numbered in order of decreasing $\Delta\Delta H^{\ddagger}_{exp}$—the difference in activation enthalpy of the substrate reaction in the *Z* and *E* isomers of the same macrocycle. Reprinted with permission from ref 224. Copyright 2009 Nature Publishing Group.[223,224]

Scheme 1. Ultrasound-Induced[a] Electrocyclic Ring-Opening of PMA-SP-PMA[33]

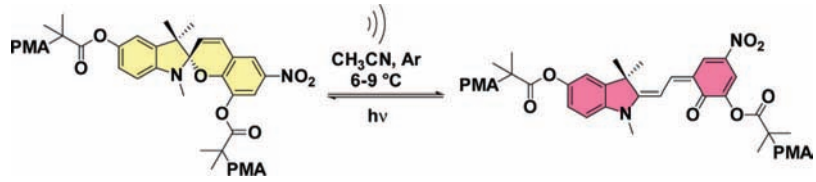

[a] Sonication studies were carried out in acetonitrile with excess BHT under Ar; 8.7 W cm^{-2} at 6−9 °C.[33]

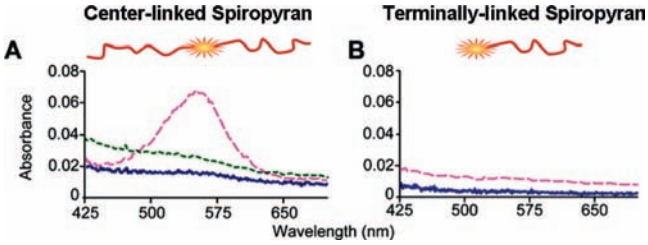

Figure 33. UV−Visible absorption spectrum of the center-linked spiropyran, PMA-SP-PMA (A), and the terminally linked spiropyran, PMA-SP (B), before sonication (blue), after sonication (dashed red), and after subsequent visible photoirradiation (dotted green).[33] Reprinted with permission from ref 33. Copyright 2007 American Chemical Society.

polymer. In a second sample, a bis-functionalized SP bearing methacryloyl esters was used as a cross-linker for PMMA to make glassy beads. Both stretching of the elastomeric PMA samples and compressing the glassy cross-linked PMMA samples resulted in color changes consistent with the merocyanine form of the SP. The compression of the spherical beads induces large tensile forces in the center of the sphere transverse to the compression axis. The color appearance was highly localized to regions of high deformation and high tensile stresses. In both samples, the mechanically induced reactions reversed upon exposure to light. Additionally, mechanical stress did not induce ring-opening reactions in chain-end functionalized polymers. A second control SP (Figure 37) was synthesized in which both PMA units were attached to the indolene portion of the SP. Consistent with COGEF calculations, no mechanically-induced reactions occurred for this control SP. Given that color generation is localized to regions of high stress concentration, and that the control samples show no color change, this is convincing evidence for the mechanically induced reaction.

3. Responses at the Molecular and Supramolecular Levels

The previous section discussed the response of polymers to mechanical force at the atomic level wherein covalent bonds of a polymer chain are cleaved. At larger size scales involving more atoms, noncovalent forces begin to shape the characteristics of a polymer at both the local and global level. Such responses include chain slippage and the disruption of noncovalent interstrand interactions (e.g., H-bonding), chain segment alignment, and conformational changes. Some of these interactions are inherent to the structure of the material while others have been designed to impart specific mechanical responses or enhance properties already present in the material. When discussing these effects, both the cessation of interactions and the inducement of interactions must be considered. We have used this distinction to organize the content in this section.

3.1. Disruption of Interactions

3.1.1. Dispersion of Aggregates

Inspired by their work showing the molecular dispersion of a phase-separated polymer by mechanical deformation,[241] Weder et al. have pioneered the use of mechanical force to dissociate dye aggregates leading to a change in photoluminescent (PL) character.[242] The initial report involved the use of cyano oligo(*p*-phenylene vinylenes) (OPVs) dispersed in linear low-density polyethylene (LLDPE).[242] These OPVs experienced large, bathochromic shifts of up

Scheme 2. Reaction of a Scavenger Complex (Bottom Left) with Sonicated Heteronuclear Coordination Polymer (Top Left) Resulted in the Formation of Palladium and Platinum Heterocomplexes[97]

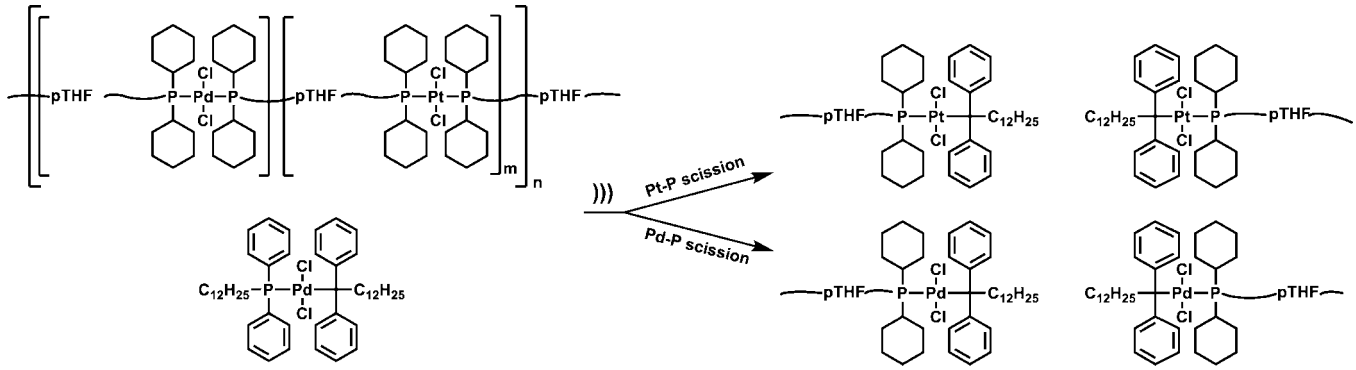

Scheme 3. Chain Scission of Silver-Carbene-Based Polymer upon Sonication and Subsequent Trapping of the Carbene with Water[96]

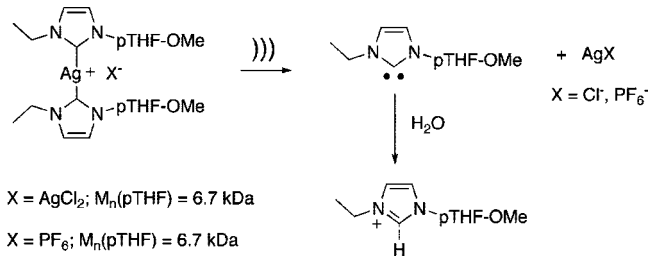

Scheme 4. Mechanochemical Activation of a Catalytic Transesterification, Ring-Closing Metathesis (RCM), and Ring-Opening Metathesis Polymerization (ROMP)[224]

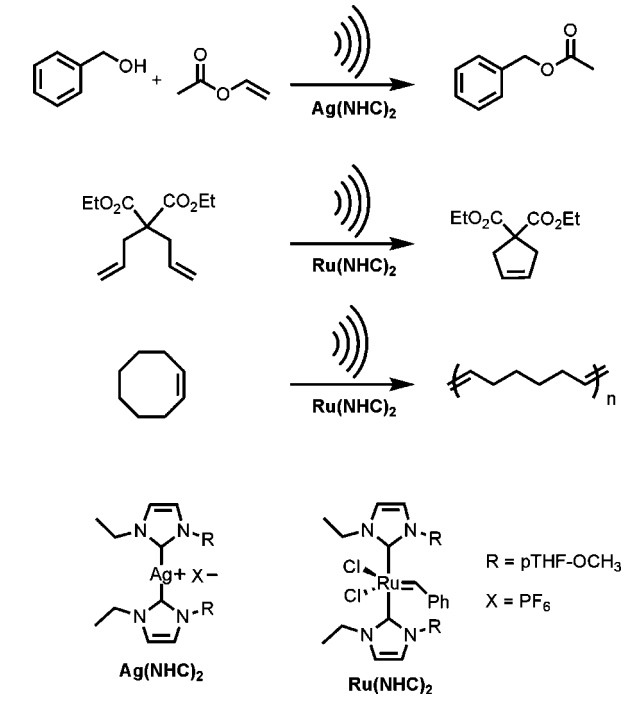

to 138 nm upon aggregation to form the excimer (excited dimer whose emission is generally red-shifted compared to the unassociated molecules). This aggregation behavior was exploited by swelling the LLDPE films in chloroform or toluene OPV solutions at various concentrations and elevated temperatures in order to dye the LLDPE. The resulting films showed PL spectra that indicated the presence of varying concentrations of dye aggregate excimers. Upon tensile deformation, the photoluminescence shifted back to that of the dispersed molecules, indicating breakup of the excimers. This concept was extended in later studies by incorporating the OPVs into the LLDPE by melt processing and examining the effect of aggregate size on the mechanically induced PL response (Figure 38). Small aggregates were needed because deformation was unable to break up large scale aggregates.[243]

More recently, the concept was extended to other chromophore-polymer blends including polyethylene terephthalate (PET) and polyethylene terephthalate glycol (PETG). These polymers required a modification of the OPVs used.[244] The original OPVs[242,243] were too soluble in these new polymers and failed to form excimers. Long alkyl chains consisting of 12 or 18 carbons were attached to the ends of the OPV to decrease their solubility. These modifications allowed for the incorporation of the OPVs into the PET-based polymers. These long-chain OPVs were also used to impart a visible color change in a LLDPE polymer.[245]

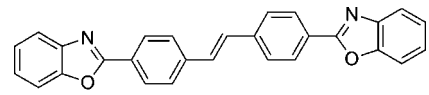

BBS

Pucci et al. utilized commercially available 4,4′-bis(2-benzoxazolyl)stilbene (BBS), which also exhibits large changes in photoluminescence upon aggregation. BBS was melt processed into both polypropylene[39,246] and biodegradable poly(1,4-butylene succinate).[246] BBS has an advantage over some of the OPV systems in that it is low in cost and showed higher thermal stability as compared to the OPV-LLDPE system.[39] These deformed films also exhibited significant PL emission dichroism due to the alignment of the BBS molecules with the drawing axis.

In the course of making mechanoresponsive thermoplastic polyurethanes (TPU),[247] a surprising effect was observed for one of the OPVs. The blended TPU and 1,4-bis-(*R*-cyano-4-methoxystyryl)-2,5-dimethoxybenzene (BC-MDB, Figure 38) that had been rapidly quenched initially had a PL spectra indicating a large proportion of molecularly dispersed dye. After stretching and releasing the polymer to five times its original length, the PL spectrum initially showed little change. However, when the polymer was allowed to rest for 1 day at room temperature, a new band appeared in the fluorescence spectrum at 625 nm, indicating the formation of excimers. The authors speculated that this result was due to kinetic trapping of the OPVs in a thermodynamically unstable state when the polymer was quenched. A similar effect was observed when grafting OPVs into natural rubber at lower concentrations (≤2%), in which

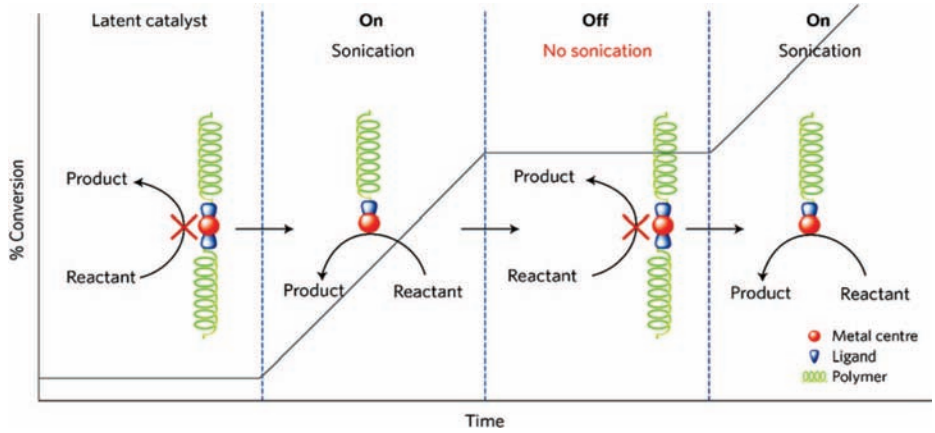

Figure 34. Schematic representation emphasing the ease of "on" and "off" switching of a mechanically activated catalyst that is generated via ultrasound waves, and the corresponding effect of metal−carbene bond scission on the rate of the catalysis.[226] Reprinted with permission from ref 226. Copyright 2009 Nature Publishing Group.

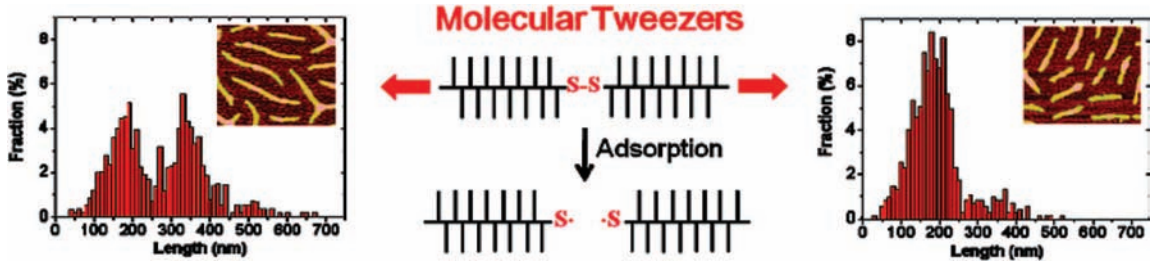

Figure 35. Adsorption-induced chain scission of macromolecules with a disulfide link at the center of the backbone.[125] On the left is the bimodal distribution and AFM for the as-synthesized material, while the right shows the brush molecules on a surface with a higher surface tension after bond scission. Reprinted with permission from ref 125. Copyright 2009 American Chemical Society.

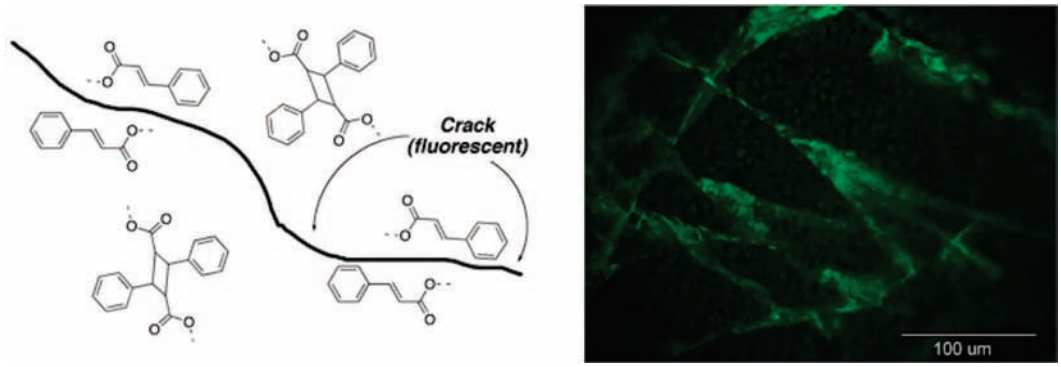

Figure 36. Fluorescent crack-sensing with cyclobutane-containing polymers of tricinnamates.[236]

tensile deformation initially caused a small red shift in the PL spectra and larger deformations or higher concentrations showed slight blue shifts.[56] Treatment of TPU/OPV blends to aid in excimer formation resulted in polymers that were minimally mechanochromic (marked by a change in color or luminescent properties due to mechanical deformation). This was likely due either to insufficient transfer of force or to the formation of aggregates that were too large to be dispersed, as dye sweating was observed. To overcome these problems, the OPVs were covalently incorporated into the TPU backbone to allow for more effective force transfer (Scheme 6). These new materials exhibited reversible, stress-dependent mechanoluminescent effects.[247] Investigations into the effect of the nucleation rate of the OPVs and polyethylene crystallinity showed that OPVs that aggregate faster gave rise to smaller, more easily dissipated aggregates.[248] Higher polymer crystallinities gave rise to increased dispersion of aggregates, with the lowest crystallinity polymer (9%) having no significant mechanoluminescence.

Other molecular architectures have been used to impart mechanoresponsiveness in polymers. Perylene bis-imides with linear (ES-PTCDI) or branched (EE-PTCDI) alkyl chains were incorporated into LLDPE.[35] ES-PTCDI aggregated at lower concentrations due to its more effective packing, but the fluorescence was rapidly quenched at high concentrations. Mechanical deformation led to an increase in overall fluorescence from the isolated dye, indicating aggregate breakup, but at higher concentrations this was attenuated due to greater aggregate stability. EE-PTCDI required higher concentrations to induce aggregation, but fluorescence was not quenched, resulting in the observation of aggregate emission. Presumably, due to the weaker aggregation, the EE-PTCDI polymers were significantly more mechanoresponsive, showing a change in emission color

from red to yellow-green upon deformation. In the deformed sections, the long axes of the isolated perylenes were found to be oriented parallel to the direction of drawing.

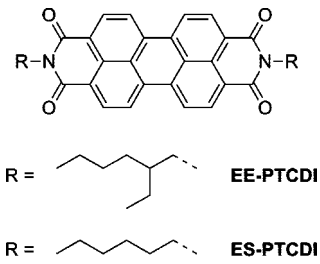

In some cases, the inability to break up aggregates leads to interesting anisotropies in the final polymer. When poly[(*m*-phenylene ethynylene)-alt-(*p*-phenylene ethynylene)] was blended with LLDPE at progressively higher concentrations, the formation of aggregates was detected by the red-shift in the emission spectra.[249] Under tensile deformation, no change in emission characteristics was noted. However, upon examination using a linear polarizer, significant dichroism was observed due to the resultant parallel orientation of the aggregates to the deformation direction.

Degradation by ultrasound (vide supra) of noncovalently linked supramolecular materials has also been studied and used to better understand the behavior of various biological materials such as amyloid fibers, DNA, and actin fibers. These biological fibers are complicated by large polydispersities, spontaneous breakage, and unwanted polymerization. In order to circumvent these difficulties, cylindrical micelles formed from polyferrocenyldimethylsilane block copolymers have been used as analogues. The ability to grow these micelles in a "living polymerization" results in narrow polydispersities.[250] When micelles suspended in solution are subjected to ultrasound, their length is decreased without affecting the integrity of the block copolymer.[251] The supramolecular scission of the micelles perpendicular to the main axis is similar to that of DNA, which cleaves without disturbing the double helix structure, although the scission rate of the micelles is more length dependent. Modeling of micelle scission as occurring randomly, in the center, or in a Gaussian distribution about the midpoint showed that the Gaussian distribution was the best approximation. The authors speculated that amyloid fibers also undergo this Gaussian fragmentation and should show similarly high length dependence.

3.1.2. Fluorescence Resonance Energy Transfer (FRET)

In fluorescence resonance energy transfer (FRET), an excited donor molecule nonradiatively transfers energy to an acceptor molecule located within its Förster radius (<10 nm), causing a decrease in donor molecule emission as well as a possible increase in acceptor emission. This method is commonly used to determine when labeled moieties are in close proximity to each other, i.e., binding and folding of proteins or membrane structure.[252,253] FRET has also been employed to create nanoscale force sensors which were used to measure forces in a small DNA loop as it was converted from single to double-stranded form[254] and in proteins such as collagen and α-actinin within living cells.[255]

More recently, FRET has been used to sense mechanical force in bulk polymers such as polyacrylamide[256] and thermoplastic polyetherureas.[257] In the polyacrylamide system, the donor−acceptor system of enhanced cyan fluorescent protein (eCFP) and enhanced yellow fluorescent protein (eYFP) was covalently bound within a spherical chaperonin (Figure 39).[256] The chaperonin was divided into two half spheres possessing large cavities with the connection between the halves being mechanically weak. Covalently bonding the donor−acceptor filled chaperonin to the polymer matrix and subjecting it to mechanical deformation was expected to modify the FRET in one of two ways. In the first scenario, separation of the two halves during deformation would lead to a reduction in FRET (Figure 39a). In the second case, internal stresses present in the polymer after polymerization would deform the chaperonin structure, reducing FRET overall. Upon deformation and subsequent crack formation, the area surrounding the cracks would relax, causing a localized increase in FRET (Figure 39b). Due to the low efficiency of FRET in the undeformed regions and the 1.5-fold increase in FRET in areas adjacent to cracks, this second mechanism is believed to be the mode of action.

Scheme 5. Formation of Cross-Linked Polymer 2MEP4F[237]

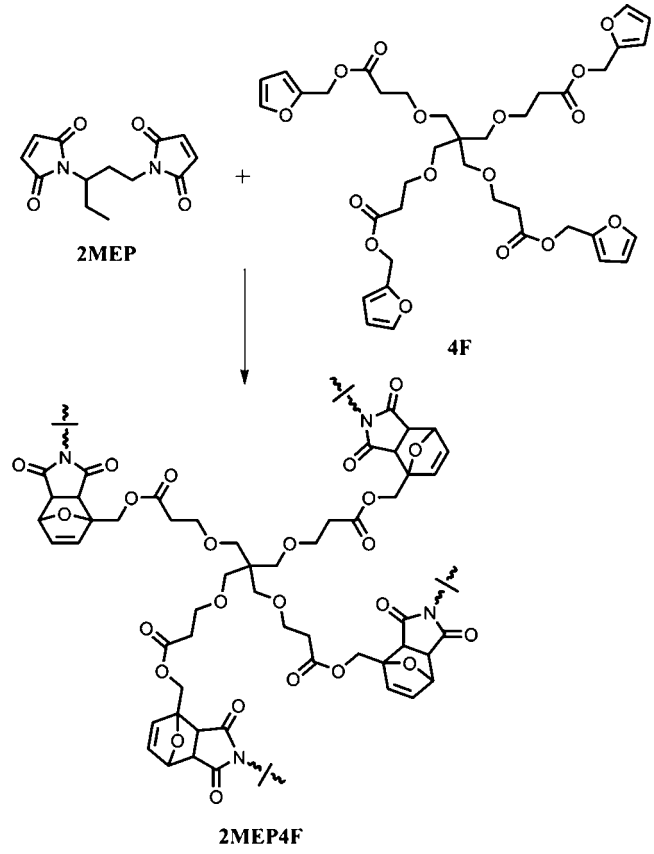

For the polyetherurea system,[257] two pairs were used. In one, the coumarin based donor molecules (Figure 40, **D1**) were noncovalently bound into the hard blocks using a bis-urea tail with the bis-polyether grafted naphthalimide acceptor molecules (**A1**) randomly dispersed in the soft blocks. The second system covalently linked the bis-urea donor molecules to the acceptor molecule using polyether linkages of two different lengths in a donor-linker-acceptor-linker-donor geometry (**DAD1** and **DAD2**). The FRET ratio (I_{507}/I_{376}) of the first system during elongation changed slightly up to 100% strain (0.57 vs 0.55) but decreased significantly when strained up to 500% (0.57 vs 0.33). After partial relaxation, the FRET ratio returned to a value consistent with the remaining plastic deformation. Use of the donor–acceptor–donor system gave significant changes in the FRET ratio at

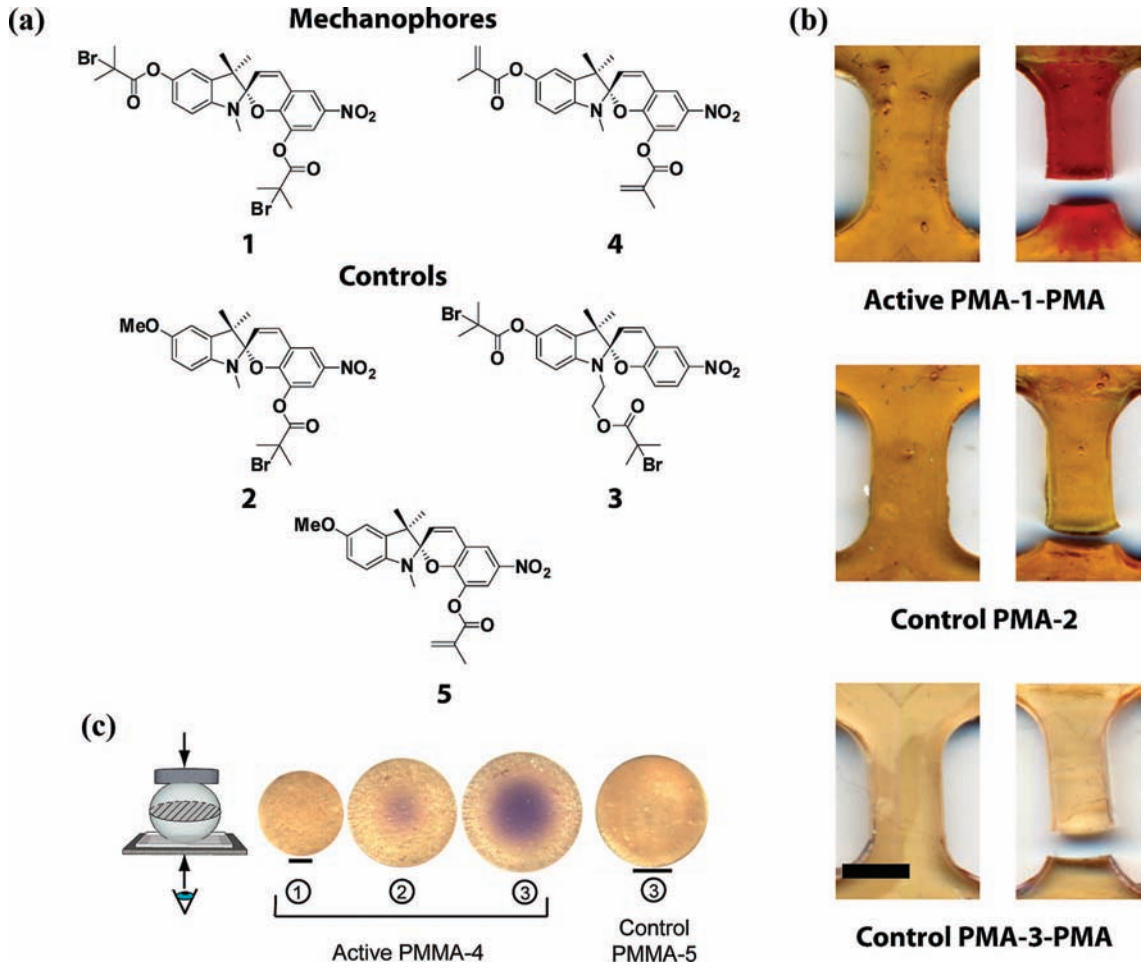

Figure 37. (a) Structures of the SP used as mechanophores in both linear PMA (1) and cross-linked PMMA (4) as well as the monofunctional (2, 5) and difunctional (3) controls. (b) Dog-bone samples of PMA-linked SP samples before (left) and after (right) stretching: active sample (top), monofunctional control (middle), difunctional control (bottom). (c) Cross-linked PMMA-SP beads before (1), during (2), and after compression (3). A monofunctional control bead compressed to the same degree as the final active bead is shown for comparison. Scale bars in (b) and (c) are 2 mm and 50 μm, respectively.[30] Reprinted with permission from ref 30. Copyright 2009 Nature Publishing Group.

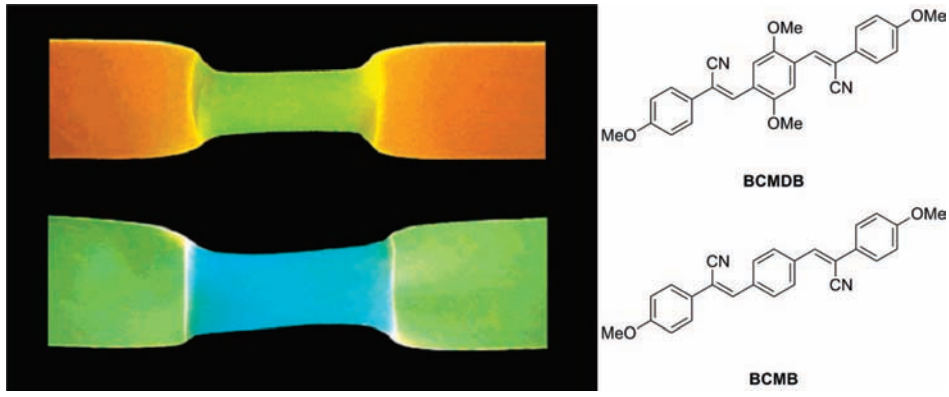

Figure 38. Melt processed LLDPE blends containing 1,4-bis(*R*-cyano-4-methoxystyryl)-2,5-dimethoxybenzene (BCMDB, top) or 1,4-bis(*R*-cyano-4-methoxystyryl)benzene (BCMB, bottom) elongated by 500% and illuminated by 365 nm light. Outer edges show excimer emission while thinner, center sections show the blue-shifted photoluminescence of the monomeric OPV species. Structures of the OPVs used in the deformed samples are shown on the right.[243] Reprinted with permission from ref 243. Copyright 2003 American Chemical Society.

strains <100%, 0.59−0.38 at 100% strain for **DAD1**, and 1.49−1.15 at 100% strain for **DAD2**.

3.1.3. Diacetylenes

The polymerization of diacetylene monomers by heat or UV radiation greatly shifts their UV−Visible absorption, giving rise to a deep blue color as the polymer becomes more highly conjugated. The absorption characteristics of the polymerized diacetylenes are sensitive to distortions of the backbone as well as to their environment. In 1986, Rubner incorporated diacetylenes into the hard segment of various polyurethanes.[54,55] The phase separation of the hard and soft

Scheme 6. Synthesis of Both Cross-Linked and Linear, Covalently-Bound OPV Polyurethanes

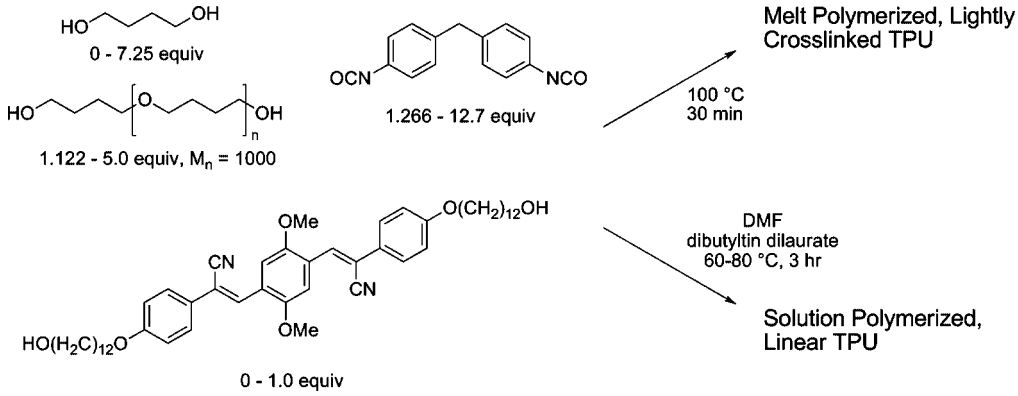

segments and aggregation of the diacetylene units within the hard segments allowed for polymerization of the diacetylenes to various degrees by UV light (Figure 41a). Highly phase-separated HDI-5,7-1000, formed from hexamethylene diisocyanate, 5,7-dodecadiyne-1,12-diol, and poly(tetramethylene oxide) (1 kDa), was partially cross-polymerized with UV light and used for mechanical testing (Figure 42).[54] Since the authors were interested in stress-induced disruptions of the hard domains of the polymer, the diacetylenes were only partially cross-polymerized to prevent significant modification of the modulus and rigidity of these domains. These polymers initially exhibited a large absorption peak at 615 nm (Figure 41b). As the polymer was stretched, this peak diminished in intensity and blue-shifted, and the polymer took on a red color. Once the strain reached 200%, a broad peak centered at 475 nm became apparent and grew more intense with increasing strain. This new peak was attributed to irreversible disorder introduced into the hard domains. This effect was corroborated by experiments in which the polymer was allowed to relax following strain. For strains up to 200%, the spectral changes were completely reversible; however, the broad peak at 475 nm remained at deformations greater than 200%. The changes in the spectra at 615 nm were attributed to reversible deformations of the backbone and changes in bond angle. HDI-2,4-1000 (made with 2,4-hexadiyne-l,6-diol, Figure 42) showed similar behavior, although the strain at which the domains were irreversibly deformed decreased to 110%. HDI-2,4-1000 was also cross-polymerized for twice as long as the previous two samples. The resulting polymer exhibited reversibility at higher strains than the original HDI-2,4-1000 polymer, and the hard domains of this polymer were less susceptible to disruption.

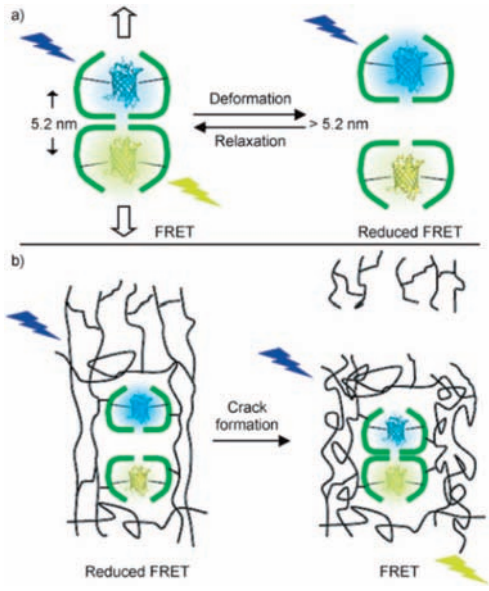

Figure 39. Overall structure and possible mechanisms for deformation-induced changes in FRET of donor−acceptor eCFP and eYFP pairs. (a) Reduction in FRET due to increased separation of the FRET complex. (b) Increase in FRET near cracks due to relaxation of internal stresses created during polymerization.[256] Reproduced with permission from ref 256. Copyright Wiley-VCH Verlag GmbH & Co. KGaA.

These polyurethane-based poly(diacetylenes) were then applied to the investigation of hard domain orientation in addition to domain disruption.[259] MDI-2,4-1000 (made with 4,4′-methylenebis(phenyl isocyanate)) was lightly cross-polymerized using E-beam radiation. Since the poly(diacetylenes) are highly anisotropic due to the one-dimensional nature of the polymer backbone, their behavior under polarized light can be utilized to gain information on orientation. At 0% strain, the visible spectra of the polymer films were identical using polarized light parallel and perpendicular to the drawing axis. As the strain was increased, the spectra obtained from the material parallel to the direction of drawing showed a similar response to that previously reported with a decrease in the band at 615 nm as a new broad peak at 500 nm appeared.[54] The spectra for the perpendicular direction showed an overall decrease in intensity to almost undetectable levels at 570% strain with no concurrent growth of a peak at 500 nm, indicating orientation of the long axis of the hard domains and poly(diacetylene) chains parallel to the drawing direction. Comparison of the dichroic ratios, obtained by dividing the area of the parallel curve by the area of the perpendicular curve ($A_{\parallel}/A_{\perp}$), during and after the release of strain, showed significant increasing anisotropic nature during deformation up to a ratio of 5.5 at 570% strain. In relaxed samples, the ratio returned values of 1 to 2.25, depending on the amount of strain incurred.

A closely related study investigated HDI-5,7-1000/2000 in a similar manner.[260] Deformation of HDI-5,7-1000 resulted in the formation of a new, well-defined peak at 495 nm, giving rise to a yellow color in the material, rather than only showing the appearance of a broad peak. This observation suggested a phase transition in which there was a shift from one molecular environment with a narrow distribution of effective conjugation lengths to a second molecular environment containing poly(diacetylenes) with shorter effective conjugation lengths, similar to those observed thermally.[54] HDI-5,7-2000, which has a longer soft segment, exhibited similar properties, although after allowing the sample to

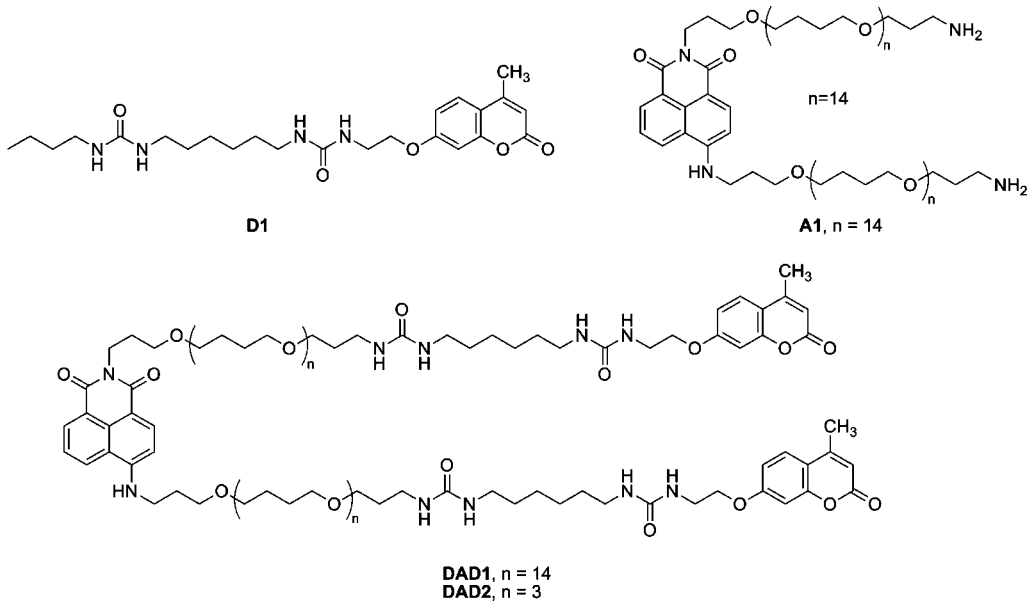

Figure 40. Structures of the noncovalently linked donor (D1) acceptor (A1) pair and the covalently linked donor−acceptor−donor molecules with different length polyether linkers, 1.1 kDa (DAD1) and 0.35 kDa (DAD2).[257]

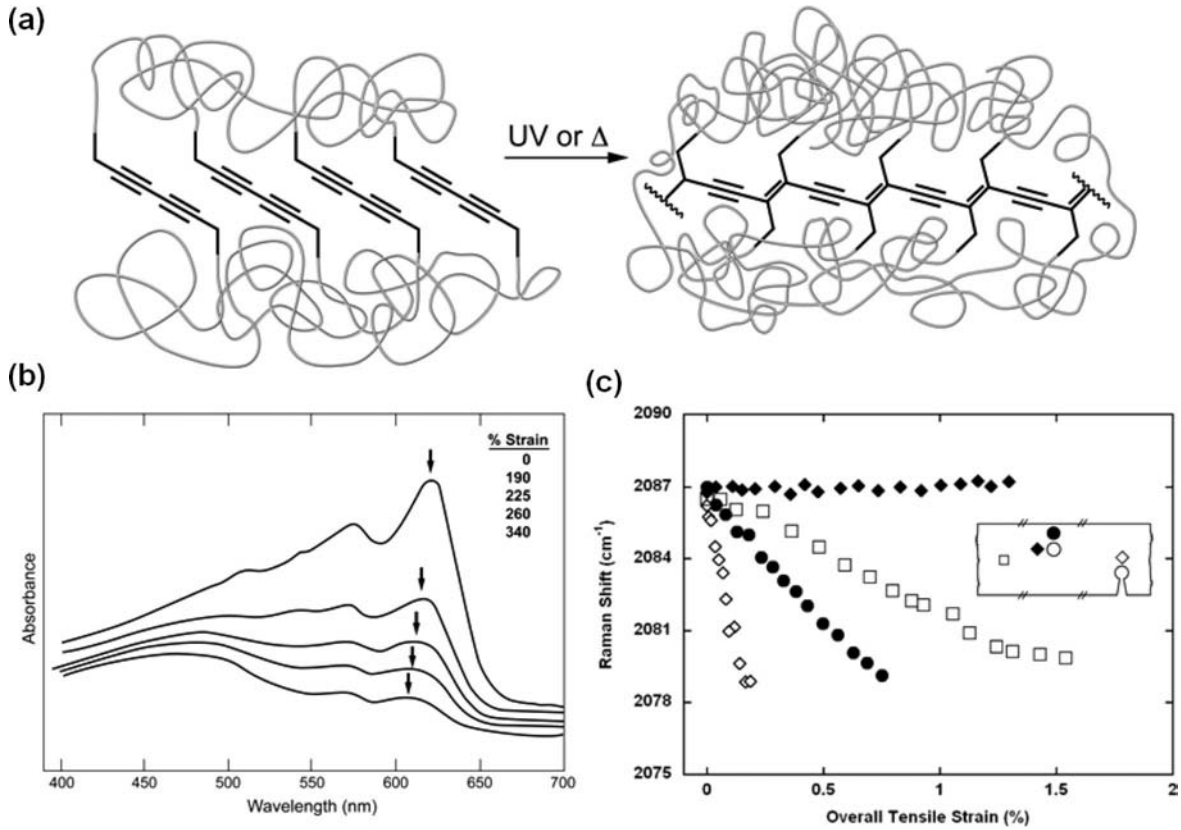

Figure 41. (a) Polymerization of diacetylene aggregates within the hard domains of polyurethanes gives rise to a highly conjugated polymer backbone. (b) The initial peak of the polydiacetylene at 615 nm decreases with increasing strain while a broad peak between 400 and 525 nm develops.[54] (c) Raman shifts of the C≡C peak (2080 cm^{-1}) at different points on a sample containing both a notch and a hole under uniaxial tensile strain.[258]

relax, it was possible to obtain samples possessing both of these well-defined molecular environments, unlike HDI-5,7-1000. With regard to the dichroic ratio, HDI-5,7-2000 was similar to MDI-2,4-1000, while HDI-5,7-1000 showed more residual orientation of the hard domains, which is likely due to the irreversible morphological changes that result from the increased interconnected nature of this material.

More recently, a lipidic diacetylene was self-assembled and cross-polymerized with UV light to produce robust, five bilayer nanotubes that were solvent resistant and thermally stable up to 140 °C.[261] The nanotubes were incorporated into an elastomeric polyurethane film by dissolving the polyurethane in 1,4-dioxane, adding powdered nanotubes, sonicating for 5 min, pouring into a mold, and allowing the solvent to evaporate. The resulting films showed mechanochromism upon 63% strain (4.3 MPa) with continued reversible color change after 100+ strain cycles. Other studies have focused on the mechanochromism of thin poly(diacetylene) films

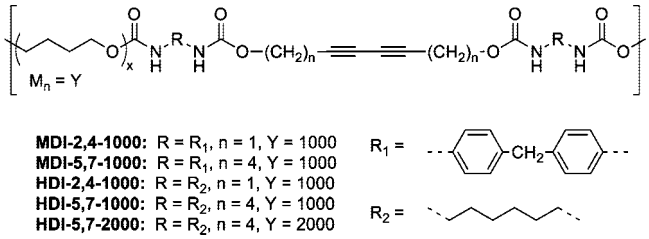

Figure 42. Structures of the investigated diacetylene polyurethanes. The diacetylenes were incorporated into the hard segments of the polymers, with poly(tetramethylene oxide) (M_n = 1 or 2 kDa) serving as the soft segment.

(1−3 molecular layers thick) at the nanoscale[262−264] or in silica nanocomposites.[265]

The stretching mode of C≡C bonds of poly(diacetylenes) possesses a characteristic Raman peak at 2080 cm^{-1}, which has been observed to shift to lower frequencies upon deformation in both glassy and elastomeric materials.[266] A series of papers used this effect to study stress/strain around holes and cracks in sheets and coatings of polyurethane containing poly(diacetylenes).[258,267−269] A variety of MDI based polyurethanes with polypropylene glycol (M_n = 0.4 kDa) as the soft segment and different hard/soft segment ratios were thermally cross-polymerized and tested. Under tensile deformation, polyurethane sheets showed a linear dependence of the Raman peak on strain up to ~1% strain. Above this level, plastic deformation and large deviations from linearity occurred.[258,267,269] Increasing hard segment content was found to correlate with increasingly larger shifts in the Raman peak for a given strain. Stress concentrations were mapped in the vicinity of either a hole or notch in a sheet of polyurethane under tensile stress, and the measurements correlated with those obtained by conventional methods (Figure 41c).[258,267−269] This same polymer was coated onto cross-linked polyurethane, a glass filament, and an aluminum sheet; the polymer displayed equivalent Raman shifts when deformed in the solid state.[267−269] Other tests reiterated the necessity of well-structured poly(diacetylene) domains for effective measurement of stresses, with polymers containing 27% hard segment still showing significant scatter in Raman peak shift under strain.[269]

Similar measurements have been performed in pure[270] and blended polyesters.[271−273] For pure polyesters, several molecular weights were synthesized (M_n = 0.3−4.1 kDa) from hexa-2,4-diyne-1,6-diol, terephthaloyl chloride, and benzoyl chloride.[270] One of these polymers (M_n = 1.3 kDa) was used in subsequent mechanical tests, since it melted before cross-polymerizing. This allowed the material to be compression molded and gave intense Raman signals (correlating with high crystallinity). Using this polymer, a linear relationship between Raman shift and strain (up to 0.20%) was established. The blends consisted of this same polyester blended with poly[ethylene-*co*-(vinyl acetate)] (EVA) in the following ratios (% polyester): 0, 20, 40, 60, 80, and 100. The pure polyester sample was used to calibrate the Raman shift with respect to stress. The Raman shifts of the blends were then used to determine the local stress of the polyester portions versus the overall strain of the material. Stress-transfer efficiency increased with increasing polyester content; that is, the lowest stresses were observed for a given overall strain in the 20% polyester sample.[271,272]

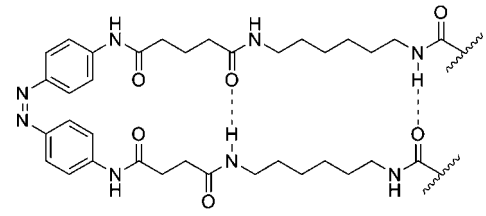

Figure 43. Hydrogen bonding of a copolyamide made from succinyl chloride, glutaryl chloride, and 1,6-hexanediamine was used to slow the thermal reversion of *cis*-azobenzene. Stretching of the polyurethane matrix, into which the polyamide was incorporated, broke the hydrogen bonds and allowed for an enhanced rate of conversion to the *trans* isomer.

3.1.4. Hydrogen Bonding

Azobenzenes undergo a well-known photoisomerization from the *trans* to the *cis* form. Generally, the *cis* form is less thermodynamically stable due to steric interactions and thermally reverts back to the *trans* form with time. This process is accelerated by visible light illumination. Conversion of *cis*-azobenzene to *trans* by mechanical force is a relatively straightforward concept; however, the instability of the *cis* form limits its usefulness as a mechanophore. Trapping of the *cis* isomer for use in mechanochromic materials was first suggested in 1992.[274] It was proposed that short oligomeric chains attached to either side of the azobenzene moiety could be bound together through the use of ionic or hydrogen bonds. These bound chains would prevent the *cis* isomer from opening at all or at least slow its rate.

In the final iteration of this polymer, an azobenzene mechanophore was incorporated into the center of a polyamide chain (M_n = 5 kDa).[31] The amide groups were hydrogen bonded and served as clasps for the *cis*-azobenzene (Figure 43). The polyamide oligomers were then incorporated into a polyurethane polymer at 0.1 wt % by reaction with tolylene diisocyanate (2,4 and 2,6 isomers), ethylene glycol, and PEG. Solvent cast films were irradiated with UV light while heating to 100 °C and were then rapidly cooled to allow the hydrogen bonds to form and trap the *cis* isomer. Films irradiated at lower temperatures (60 °C and room temperature) had higher rates of thermal isomerization, which the authors attributed to fewer intramolecular hydrogen bonds and unreleased matrix strain caused by the *cis*-azobenzene. The samples were stretched and relaxed three times to 2, 3, or 4 times their original length. Those polymers stretched to 2 times their original length showed a slight decrease in UV absorption, which was attributed to increased light scattering by the sample. Those stretched to 3 or 4 times their original length showed a significant increase in the 380 nm peak associated with the *trans*-azobenzene. Unfortunately, since the thermal lifetime of the *cis*-azobenzene is only ca. 6 h, its use as a strain sensing material is limited.

Supramolecular polymers held together by noncovalent forces,[275] including hydrogen bonds,[276,277] are well-known, and the reversibility of these noncovalent interactions has been exploited to make unique thermo-, solvato-, and photoresponsive materials. In 2008, Cordier et al. reported on a rubber-like, hydrogen-bonded supramolecular polymer that possessed self-healing properties at room temperature.[34] The polymer consisted of oligomers formed from polyfunctional carboxylic acids and diethylenetriamine, further functionalized with urea. The resulting material was a deformable solid with a T_g of 28 °C. Its oligomeric nature was confirmed

Scheme 7. Synthesis of UPy Hydrogen-Bonded Cross-Linker[a]

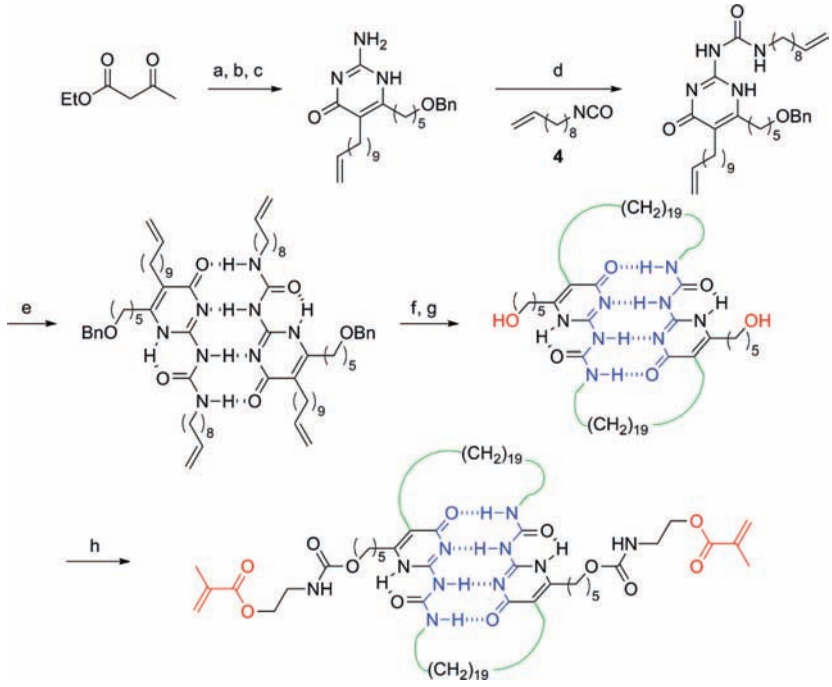

[a] Conditions: (a) NaH, *n*-BuLi, THF, $Br(CH_2)_4OBn$, 52%; (b) $Br(CH_2)_9CH{=}CH_2$, K_2CO_3, DMF, rt, 12 h, 47%; (c) guanidine carbonate, EtOH, reflux, 12 h, 72%; (d) 4, Py, reflux, 6 h, 83%; (e) DCM; (f) $(Cy_3P)_2RuCl_2{=}CHPh$, DCM, reflux, 1−2 h, 65%; (g) Pd(OH), 1 atm H_2, THF, 68%; (h) $CHCl_3$, 2-isocyanatoethyl methacrylate, DBTDL.[283]

by NMR, GPC, and intrinsic viscosity measurements; the latter measurement gave a molecular weight of 5.1 kDa when compared to the viscosity of polystyrene standards. Swelling with dodecane or water gave rise to rubber-like materials with lower T_g values of 8 and −15 °C, respectively. Upon breaking or cutting the material, immediate light pressure (6×10^4 Pa) was applied for 15 s followed by a period of rest, which allowed the samples to partially recover some of their original mechanical properties, such as elongation to break. Increased healing efficiencies were reported for samples experiencing longer rest times. If the samples were not immediately rejoined, a decrease in healing efficiency was observed. This was attributed to the reassociation of free H-bonding groups formed at breakage with neighboring groups, which prevented recombination upon rejoining the broken surfaces. The researchers did not rule out other possible mechanisms for healing besides the formation of new hydrogen bonds. Since materials above their T_g are susceptible to creep or viscous flow over long periods of time, the polymer chains could be re-entangling as observed in PMA (T_g = 10 °C) or materials swelled with solvent (see section 4.1.3).[278] The effect of the stoichiometry of the acid and amine, side reactions of the polyamide, and other preparation conditions on the polymer properties was investigated in more depth, although only the original material exhibited self-healing properties.[279] Later investigations used varying amounts of 2-aminoethylimidazolidone (UDETA) to cap the carboxylic acids before reaction with DETA and urea to give a range of supramolecular polymers from semicrystalline thermoplastics to rubbers.[280]

Inspired by muscle fibers, which exhibit both high strength and elasticity, and building on their previous work with linear polymers incorporating 4-ureido-2-pyrimidone (UPy)[281] or a quadruple H-bonding duplex,[282] Kushner et al. used the hydrogen bonding of UPy to create reversible cross-links in elastomeric poly(*n*-butyl acrylate).[283] UPy units were synthesized with two olefin terminated alkyl chains, which were allowed to form dimers; then ring-closing metathesis was used to cyclize the UPy dimers (Scheme 7). Further functionalization with two methacrylate units allowed the cyclized UPy dimer to be used as a cross-linker. PEG (M_n = 0.75 kDa) dimethacrylate with a similar unfolded length to the UPy dimer was used as a control cross-linker. At an equivalent cross-link density (2%), the UPy cross-linked polymer exhibited increases in the Young's modulus, tensile strength, and elongation at failure versus the control polymer. In poly(*n*-butyl acrylate) cross-linked with PEG, increasing amounts of cross-linker caused increases in the Young's modulus of the polymer but adversely affected the amount of elongation the polymer could sustain under constant tensile strength. In the UPy cross-linked polymer, increasing cross-linker density increased both the Young's modulus and tensile strength while the amount of elongation at failure was unaffected. No comment was made on the reassociation of UPy units after deformation.

Replacing the acrylate-terminated chains with slightly longer olefin-terminated chains and subsequent acyclic diene metathesis (ADMET) polymerization with Grubbs' second generation catalyst gave linear polymers with multiple UPy dimers per chain.[284] When compared to the brittle control polymer in which the hydrogen bonding was blocked by *ortho*-nitrobenzyl groups, this new polymer exhibited high modulus, increased toughness, and larger extensibility. Plastic strain accumulated over several loading cycles could be recovered to a significant degree by allowing the sample to rest for 18 h at room temperature or 30 s at 80 °C. The polymer also exhibited interesting shape memory effects when stretched at 80 °C and cooled to 5 °C to lock in the extended shape, and the stress was then released. Heating the polymer caused it to retract to its original length. This shape memory property was attributed to significant chain entanglement, which locked in the permanent shape and the

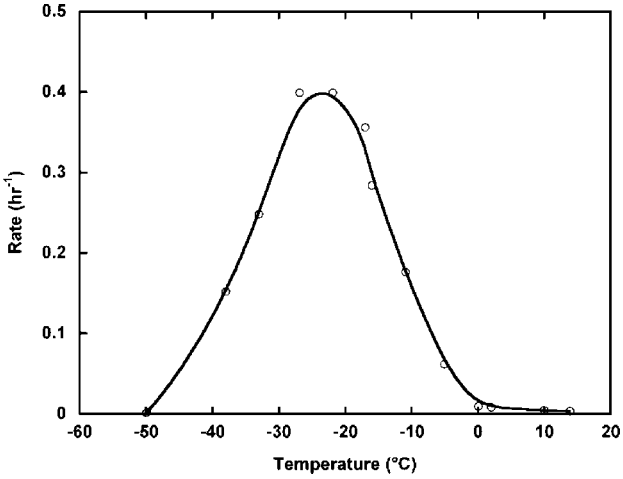

Figure 44. Crystallization rate of unvulcanized natural rubber with respect to temperature, showing a maximum between the glass transition temperature, −70 °C, and the melting temperature, 30 °C.[287]

reversibility of the hydrogen bonds, which served as temporary cross-links to fix the extended shape. Li et al. had previously used UPy dimers as such temporary cross-links to create shape memory effects in covalently cross-linked acrylate polymers.[285]

3.2. Induced Interactions

3.2.1. Strain-Induced Crystallization (SIC)

Depending on molecular structure, processing conditions, glass transition temperature (T_g), and melting temperature (T_m), a polymeric material may be completely amorphous or may possess significant crystallinity. Though not the same as the long-range order found in small molecule or inorganic crystals, chain segments in polymers locally exhibit periodic orientations and translations stabilized by noncovalent interactions. Quenching a sample below T_g kinetically suppresses crystallization due to the limited mobility of the segments. At temperatures between the T_g and the T_m, crystallization can occur.[286] A representative curve showing how crystallization rate depends on temperature for unvulcanized natural rubber is shown in Figure 44. The curve reflects the interplay between chain mobility, which increases, and the thermodynamic driving force for crystallization, which decreases as temperature rises.

In addition to the effects of temperature, the kinetic barrier to crystallization can be surmounted by mechanical activation (Figure 45). This is known as strain-induced crystallization (SIC) and has been studied extensively in a variety of polymers.[288] The most common example of SIC is found in natural rubber or its synthetic analogue, polyisoprene.[289,290] Other polymers known to exhibit this effect are polyethylene terephthalate,[291] *cis*-1,4-polybutadiene,[292] and polychloroprene.[293] The SIC of these polymers has the effect of increasing their tear or crack resistance as well as improving their tensile strength.[290]

Mechanical force affects the crystallization rate by modifying the entropy of activation. As a polymer is stretched, the chains align and the overall entropy of the region decreases. The change in entropy associated with crystallization decreases with respect to the undeformed polymer, thus increasing the rate of crystallization.[294] At the point that crystallization begins, the crystallization rate initially increases as more strain is applied.

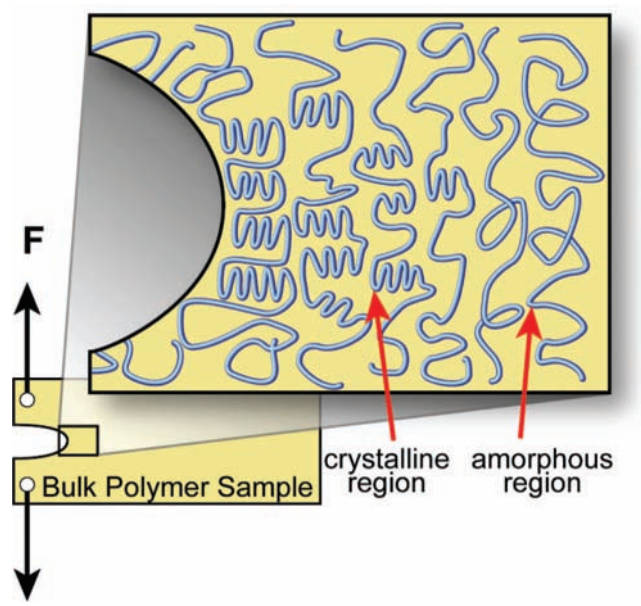

Figure 45. As a polymer is subjected to tension, a tear begins to propagate through the material. At the crack tip, deformation induces crystallization of the polymer chains, leading to slowing of crack growth.

The investigation of the effect of cross-link density and fillers on SIC has been advanced in recent years by the ability to measure crystallinity *in situ* with X-ray diffraction and local strains with deuterium NMR.[295,296] The amount of SIC is affected by the cross-link density. At high cross-link densities in natural rubber, the maximum crystallite size is limited. In contrast, at low cross-link densities, fewer crystal nucleation sites are present.[297] A maximum in crystallization rate was found between these two extremes in cross-link density, which closely matches the natural molecular weight between entanglements. Fillers such as carbon black or silica nanoparticles mimic covalent cross-links and improve mechanical properties.[298,299]

3.2.2. Excimer Formation

A counterexample to the dissociation of dye aggregates previously discussed is the formation of excimers. Ikawa et al. reported on the effect of tensile deformation on the overlap of carbazole units in poly(*N*-vinyl carbazole) dispersed in polystyrene.[36] The fluorescence emission of the carbazole units varies depending on the degree of overlap with the monomer (Figure 46a), with the partial overlap excimer and full overlap excimer possessing distinctive fluorescence bands. The stretching of the polystyrene (0.8% strain) caused an increase in the band associated with partial overlap (375 nm) and a corresponding decrease in the monomer band (345 nm) (Figure 46b). No change was observed in the bands associated with full overlap. Releasing the strain resulted in a reversion to the original monomer/partial overlap ratios. Under constant strain, the measured stress of the polymer decreased over time, but the monomer/partial overlap ratios remained the same. This observation suggested that the fluorescence change was a strain related phenomenon rather than a stress related one. A later study by Spanggaard et al. cast some doubt on this interpretation.[300] In this investigation, single or double *N*-carbazole small molecules were incorporated into the center of polystyrene−polyisoprene−polystyrene triblock polymers. The double carbazole polymers showed the expected change in excimer/monomer ratios, but

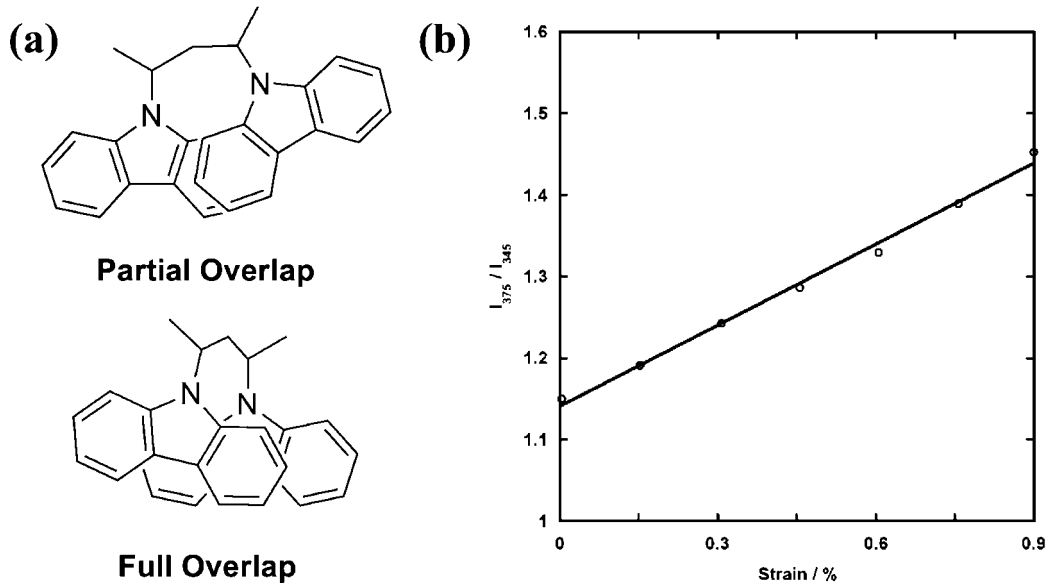

Figure 46. (a) Examples of partial and full overlap of carbazole units which give rise to distinct fluorescence bands. (b) The ratio of the fluorescence intensity of the partial overlap peak (375 nm) to the monomer peak (345 nm) versus strain shows a linear increase up to 0.8% strain. Release of the strain returns the ratio to its original value.[36]

surprisingly, the polymers containing only a single carbazole per chain also showed a change in ratio. The authors postulated that changes in the transition probabilities of the vibronic bands were responsible for this effect. However, the previously proposed mechanism was not ruled out.

Yang et al. demonstrated the formation of naphthalene excimers due to tensile deformation of acrylic copolymers.[38] Naphthalene units were introduced into the polymer by copolymerization of methyl methacrylate with 1-naphthylmethyl methacrylate at various concentrations. The lower concentrations showed no mechanoresponse, while the highest naphthyl concentration showed a reduction of the monomer peak (337 nm) and an increase of the excimer peak (390−420 nm) with increasing deformation. Excimers were present at zero strain and were likely dissociated during deformation. However, in order for an increase in excimer emission to occur, more excimers must form than are broken apart. It was postulated that elongation gave rise to denser packing, which promoted excimer formation.

3.2.3. Mechanically-Induced Optical Changes Due to Increased Conjugation

Increased conjugation along polymer chains can also lead to interesting optical changes. An interesting stress sensor was demonstrated using poly(3-octylthiophene) (P3OT, M_w = 47 kDa) dispersed in a PMMA matrix at low concentration (0.05−1.0%).[301] Stresses up to 1 MPa in the PMMA film were correlated with reversible changes in the fluorescence decay time on the picosecond time scale. As stress increased, there was a corresponding decrease in the decay time. It was shown that this was a stress (not strain) sensor by holding a sample at constant strain and allowing the polymer to stress relax. As the stress decreased over time, the decay time increased. The change in decay time was attributed to distortions of the conjugated backbone of the polymer. This system was used to detect residual stresses in a multilayer coated metal plate caused by the type of clear coat used and by exposure to heat and moisture,[302] but the system was limited to stresses ≤1 MPa.

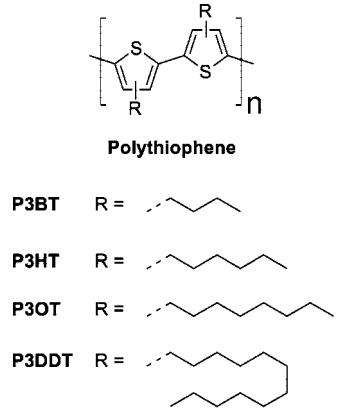

A more in-depth study was undertaken which looked at the effect of different poly(3-alkylthiophenes) (3-butyl, 3B; 3-hexyl, 3H; 3-octyl, 3O; 3-dodecyl, 3DD) and of different molecular weights of P3OT dispersed in PMMA.[303] All four polymers showed linear decreases in decay time with increasing stress up to an elastic strain of 0.053%, which was followed by an increase in decay time up to 0.2% elastic strain, at which point fluorescence lifetime no longer changed. Using P3HT, the crystallinity of the thiophene polymer was shown to have no effect on decay time. When comparing the effect of the length of the alkyl side chains, the longest side chains (P3DDT) had a 3-fold larger change in decay time compared to the shortest (P3BT). This behavior was attributed to increased interaction of the thiophene with the surrounding matrix. Five different molecular weights of P3OT (0.5−23 kDa) were tested, and the findings showed that the magnitude of the change in decay time was dependent on molecular weight. The shortest chains (0.5−1.6 kDa) showed no change under deformation while the magnitude of the change increased with increasing molecular weight for the remaining polymers. The decay time in undeformed samples was found to decrease with decreasing chain length. On the basis of these results, it was concluded that the observed changes in decay times were caused by changes in the conjugation length upon deformation.

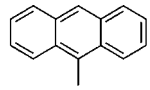

9-methylanthracene

In an effort to raise the limit of detectable stress above 1 MPa, new fluorophore−polymer blends were investigated.[303] 9-Methylanthracene (9-MeAn) had previously been shown to undergo changes in decay time when subjected to hydrostatic pressures up to 100 MPa in methylcyclohexane.[304] Several other highly fluorescent dyes were examined, including related anthracenes, coumarins, pyrene, benzothiophene, and Alq3, but upon testing, 9-MeAn was found to have the largest change in decay time (500 ps at 10 MPa) and was used in subsequent tests. Outdoor weathering of the coating followed by uniaxial deformation showed that the stress monitoring ability was not affected by one week of exposure while two weeks of exposure lead to deviations from the calibrated decay−stress curve. This degradation in stress monitoring ability was ascribed to the oxidation of 9-MeAn by light. Comparison to stresses obtained by the more traditional bimetallic method gave good agreement between the two methods. An extension of this system was utilized to measure residual stresses in injection molded PVC pieces mixed with carbon black.[305]

In diacetylenes, some of the color change can be attributed to a decrease in effective conjugation length as the polymer backbone is distorted. However, certain polymers exhibit enhanced conjugation through the use of pressure. The decreased interchain distances and changes in planarity as a result of this pressure can cause shifts in both the optical absorption and conductivity of the polymers. Moses et al. reported on pressure-induced changes in both conductivity[306] and optical absorption in polyacetylenes.[37] *trans*-Diacetylene showed a decrease in resistance as the pressure was increased to 8 kbar (0.8 GPa).[306] Both *cis*- and *trans*-diacetylenes showed a red shift in the energy gap and a broadening of the absorption peak when subjected to 13 kbar (1.3 GPa), as a result of increased interchain coupling.[37] Investigations of *trans*-diacetylene at even higher pressures showed that this red shift was reversible up to 5 GPa.[307] However, as the pressure was increased to 12 GPa, the absorption in the red region disappeared completely and irreversible changes occurred. The irreversibility is likely due to cross-links forming between chains at these increased pressures. Polyparaphenylene was tested under similar conditions and showed similar shifts but was not subjected to pressure-induced cross-linking.[308]

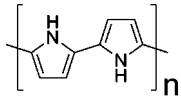

Polypyrrole

Polypyrroles are interesting for their high conductivity. This conductivity has been found to linearly increase with increasing pressure up to 200 MPa.[309] Further compression of the polymer to 1.1 GPa shows nonlinear changes and hysteresis upon unloading but eventually returns to its original value. Varying the amount of *p*-toluenesulphonate anion dopant affects the intrinsic conductivity as well as the polymers' response to pressure.[309,310] At lower dopant levels, the overall polymer conductivity decreases, but the relative change in conductivity increases. This dedoping is accomplished by reversing the current applied to the polymer during synthesis and leaves holes in the material. Collapse of these holes leads to greater changes in interchain distances and thus larger relative conductivity changes versus more highly doped polymers. Attempts have also been made to formulate a physical model of the effect of pressure on conductivity.[311] Fedorko examined the effect of reduced pressures (2 Pa) on BF_4^- doped polypyrroles, where the decrease in conductivity was attributed to a transition from an ordered, rodlike conformation to a disordered, coil-like one.[312]

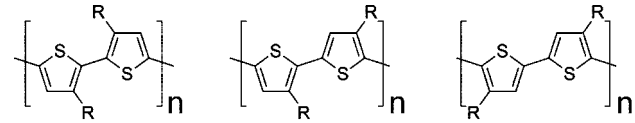

head to head head to tail tail to tail

Figure 47. The three possible ring conformations for thiophene polymers with respect to their alkyl side chains. In nonregioregular polythiophenes, significant amounts of head to head and tail to tail conformations are present. The steric interactions of the side chains within a subunit (head to head) or between subunits (tail to tail) cause significant deviations from planarity in the backbone.

Polythiophene exhibits the same changes in conductivity with pressure as polypyrrole,[313,314] but its optical and photoluminescent properties have been more extensively studied. Compression (0.8 GPa) of poly(3-alkylthiophenes) slightly red shifts the absorption peak.[313,315] Heating this polymer causes a blue shift, which can be reversed with pressure.[313] The shifts in absorption are attributed to changes in the torsional angles of the thiophene backbone and consequent changes in effective conjugation length. Due to the steric interaction of the alkyl side chains, the thiophene rings are not all planar but possess a slight twist. Increasing the temperature increases the disorder, and thus, the number of sites and degree of twisting increase. The resulting lower effective conjugation length results in higher absorption energy. Compression at normal and elevated temperatures increases the planarity of the chain, increasing the effective conjugation length and lowering the absorption energy.

Poly(3-hexylthiophene) (P3HT) shows a reversible decrease in photoluminescence intensity as well as a red shift in the absorption bands with increasing pressure.[316] This is again attributed to increased backbone planarity. However, at pressures over 3 GPa, the absorption peak of P3HT starts to move back to higher energies.[317] Unlike the polyacetylenes, this blue shift is not permanent and is thought to be caused by a bending of the main chains due to increased interchain sterics.

Up to this point, only randomly oriented poly(3-alkylthiophenes) have been considered. The ability to make regioregular poly(3-octylthiophene) (P3OT)—97% head-to-tail—allows for its properties to be compared to nonregioregular P3OT (Figure 47).[318] The regioregular P3OT experiences less steric interaction of its alkyl side chains and is therefore more planar with an average torsional angle of 25° vs 45°. This is evidenced by its slightly lower inherent absorption energy. Since the regioregular P3OT is initially more planar, compression causes smaller red shifts in the absorption than in the nonregioregular sample. The photoluminescence of head-to-tail P3HT also shows interesting effects. Unlike the nonregioregular P3HT, the head-to-tail P3HT shows a linear shift in PL up to 5 GPa with no blue shift.[319] Samuelsen's studies on P3OT suggested that the shifts in this regioregular polymer were due to increased interchain interaction,[320] and

the authors suggest this is responsible for some of the shift in regioregular P3HT. Head-to-head poly(3-C≡C-*n*-$C_{10}H_{21}$-thiophene), which is considered to be planar due to the lack of steric interactions between the alkyne and the thiophene ring, also shows these shifts in absorption.[321] The visible color of this polymer changes from red to blue upon application of 11 GPa of pressure.

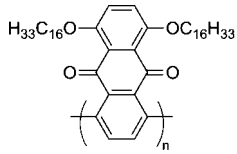

Poly(5,8-dihexadecyloxy-anthraquinone-1,4-diyl)

Anthraquinone polymers also exhibit piezochromism. In conjunction with their work on P3HT, Muramatsu et al. also investigated poly(5,8-dihexadecyloxyanthraquinone-1,4-diyl).[319] Under 11 GPa of pressure, the initial yellow color of the film changed to a dark red with a concurrent shift in the absorption peak from 428 to 640 nm. A later study by the same group reported that similar anthraquinones with shorter alkyl side chains did not show such significant piezochromism.[322]

Yang et al. investigated the reversible piezochromism of neat poly(2-methoxy-5-(2′-ethylhexoxy)-*p*-phenylenevinylene) (MEH-PPV) as well as blends in PMMA and PS.[323] On the basis of systematic investigations of the neat and blended polymers, it was suggested that the emission changes upon compression in neat MEH-PPV are due to increased chain interaction, which provides nonradiative pathways for relaxation. In the blends, increased chain interaction was also put forth as the reason for the initial decrease in both bands. The increase in the high energy bands present in the blends was ascribed to better Förster energy transfer from a poor emitter to a more efficient one. Further testing with various vinyl, styrene, or acrylate polymers showed similar behavior except for poly(4-vinylpyridine), which showed no increase at all.[324]

3.2.4. Mechanically-Induced Dichroism

Mechanically-induced dichroism has already been mentioned in the context of other mechanoresponses as a secondary effect, but further comment on this topic is needed. The reorientation of polymer chains parallel to the draw axis is well-known[325,326] and has been exploited to improve the mechanical properties of polymers, i.e., Kevlar and Spectra. Small molecules blended into polymers preferentially align with the direction of deformation, especially if the dopant molecules have high aspect ratios. Studies have addressed the mechanism by which the small molecules are oriented,[327,328] the anisotropic absorption and emission characteristics of the small molecule,[329] and the use of these materials as optical[330−334] and photoluminescent polarizers.[335−338] In this review, only dichroism, when the absorption or emission varies significantly with respect to the polarization of the light impinging upon it, that reflects on the overall or localized stress/strain of the material will be considered. Mechanically-induced dichroism could, in principle, be used as a stress/strain sensor, but this concept has not been demonstrated.[339,340]

Dirix et al. modeled the change in degree of dichroism at increasing levels of tensile deformation and also compared it to experiments conducted with Sudan Red in polyethylene.[341] Their model allowed them to make predictions on the effect of draw ratio, dye anisotropy and concentration, and film thickness on polarization; these predictions matched their experimental results. Triazo dye-doped polypropylene was used to further test their models.[342] Poly(2,5-dialkoxy-*p*-phenyleneethynylene) derivatives in polyethylene have also been used to make dichroic optical/photoluminescent films.[336,337] These films possessed large dichroic ratios in the drawn state and highlighted the importance of dispersing the chromophore throughout the matrix with little phase separation. Terthiophene based polarizers gave similarly high dichroic ratios.[334]

3.2.5. Ionic

Charged groups are capable of strong yet reversible noncovalent interactions, and their behavior in mechanical fields holds considerable promise for designing responsive polymers. For example, charged polymer brushes densely grafted onto a surface exhibit interesting mechanoacid behavior. Such chains naturally repel each other due to Coulombic forces, causing the chains to stretch from the surface when wet. These Coulombic forces can be overcome by the introduction of electrolytes which cause the collapse of the chains.[343] When the brushes are compressed by external force, an unfavorable environment of high ionic strength is created. If an easily ionizable molecule, such as a pH indicator, is present during this compression, ionization shields the Coulombic forces much like added electrolytes. Azzaroni et al. utilized poly[(2-methacroyloxy)ethyl]trimethylammonium chloride immobilized on a glass slide and bromothymol blue, a pH sensitive dye, to test this concept.[41] Infiltration of wet polymer brushes with pH 7 bromothymol blue solution initially led to equilibrium between the neutral (yellow) and anionic (blue) forms of the dye due to the charged environment and a slight decrease in film thickness. Compression of this dye/brush film led to a large increase in absorbance for the anionic form (625 nm) and an irreversible compression of the material (Figure 48). The irreversibility was ascribed to the strong ion pairing of the quaternary ammonium and sulfonate ions. Compression of neat polymer without dye resulted in no color change and no change in film thickness. Even in a more acidic environment, pH = 4, with more of the bromothymol blue molecules in their neutral state, compression still led to significant color changes and collapse of the film.

Ionic interactions have also been utilized in polymeric materials that exhibit self-healing functionality for use in ballistics applications.[344] Instead of external heat or alternative stimuli to promote polymer diffusion in a damaged area, Kalista and co-workers discovered that poly(ethylene-*co*-methacrylic acid) repaired itself after projectile puncture testing.[345,346] Self-healing was observed both at room temperature and under subambient conditions.[346] The healing mechanism is described in two stages: upon projectile impact, the ionomeric network is disrupted, but the heat generated by the projectile allows for elastic recovery. This disruption is followed by interdiffusion of the surfaces to fuse back together and seal the puncture. The most recent work reports that the ionic content of the polymer (neutralized or ionic) is not crucial for the ballistic healing process to occur, disproving a previously stated hypothesis for the observed healing.[346] Self-healing of polyethylene-*g*-poly(hexyl methacrylate) has also been reported in response to pinhole

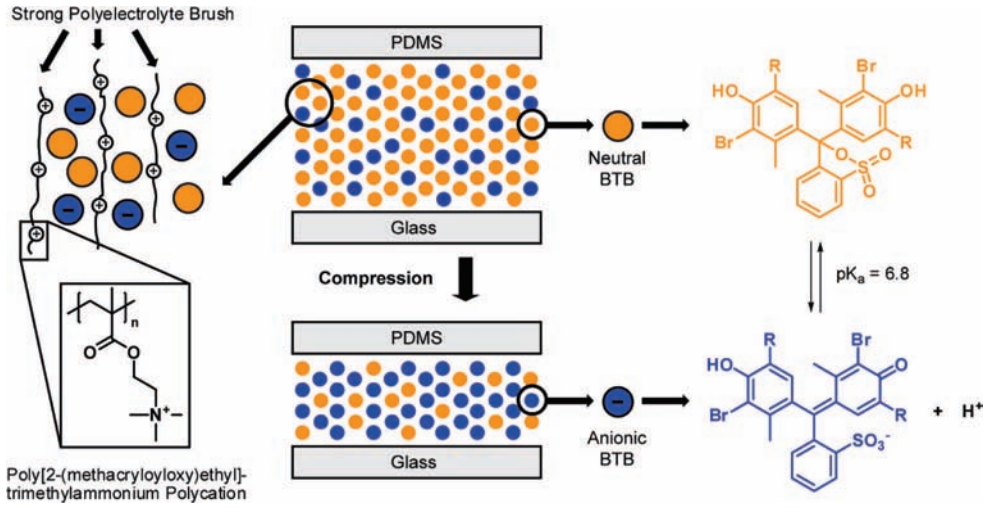

Figure 48. Bromothymol blue molecules in both neutral (orange) and anionic (blue) forms are interspersed throughout the positively charged polyelectrolyte brushes. Compression of the polymer brushes causes a shift in equilibrium to the anionic form and a change in color from yellow to blue.[41]

damage.[347] Residual stresses in the material formed from the damage event led to relaxation and molecular motion of the polymer chains. The healing response was found to be dependent on temperature, time, and grafting ratio.

4. Responses at the Microscopic and Macroscopic Levels

Depending on the degree of deformation in polymeric materials, the extent of damage and the response at the microscopic and macroscopic levels are varied and can include chain scission, slippage, crazing, or rupture/failure (refer to Figure 7).[9] In previous sections, we discussed deformations of polymeric materials on the atomic and molecular levels. The phenomenon of crazing in amorphous thermoplastic polymers is essential to understand because it is the link between microscopic deformation and macroscopic failure in certain polymers.[9] Crazing is a stress-induced cavitation process where small cracks appear on the surface and within the bulk thermoplastic polymer. Crazes range from the nanometer scale to a few micrometers in width and can be observed by the naked eye as white regions (due to the scattering of light).[130] Cross-linked polymers, such as epoxy thermosets, do not craze but experience crack damage upon deformation. When moving to macroscopic responses, however, the damage scale is much larger; one way to prevent catastrophic failure is by imparting self-healing functionality into the bulk polymer itself.

Macroscopic response to damage in terms of self-healing must fill the voids created by the damage and rebond damaged interfaces. This requires mechanisms triggered by mechanical damage to locally release healing agents that can be transported and polymerized at the site of damage. Although it seems counterintuitive to add liquid components to structural solid materials, it has been shown that liquid-filled compartments can improve the mechanical properties of the matrix.[348] This phenomenon of incorporating liquid-filled components into solid polymers that release upon damage marks a paradigm shift in designing polymeric materials. In this case, the transport of liquids to the site of damage spurs this nature-inspired process and offers self-healing benefits.[349] This section summarizes the behavior of polymers and composites on a micro- and macromolecular level with respect to their active responses (i.e., repair, function) to external mechanical stimuli.

4.1. Self-Healing Materials

Throughout their lifetimes, polymers used in common structural materials are susceptible to mechanical damage such as wear, degradation, and microcracking.[350] These and other forms of damage reduce the mechanical properties of the polymers, thus demanding frequent external repair and inspection over time. To overcome these limitations, an emerging field of research has resulted in the development of polymeric materials that can repair crack damage in an autonomic fashion without intervention through a repair mechanism described below.[349,351] Besides restoring mechanical properties, one can imagine the necessity to address other materials' needs at the site of damage. Such responses might include prevention of oxidation or corrosion, or restoration of electrical conductivity. In the following sections, the modes of repair and function will be further explored as macroscopic-level responses to mechanical stimuli.

The phenomenon of healing is defined as the recovery of a material's original mechanical properties after it incurs damage. Wool and co-workers discovered that thermoplastic materials could be healed after crack damage when fractured surfaces were rejoined to allow the polymer chains to re-entangle.[278] However, most of the early studies on crack healing involved the use of an external stimulus such as heat or solvents to promote chain entanglement across the damaged interface.[352] Dry and co-workers proposed a structural thermoset material that contained liquid healing components within hollow millimeter scale capillary tubes.[353] These hollow tubes were filled with liquid monomers that were released upon mechanical damage to the composite in order to heal the formed cracks. A variety of chemically distinct liquid healing agents (two-part epoxy, polyesters, vinyl monomers) and fibers were explored with limited success.[352] Hollow micrometer scale fibers were later incorporated into polymer composites as reinforcing agents and as carriers by which epoxy resin and hardener could be supplied to a damage site.[354] Upon mixing of these two components, a thermoset network was formed, and self-

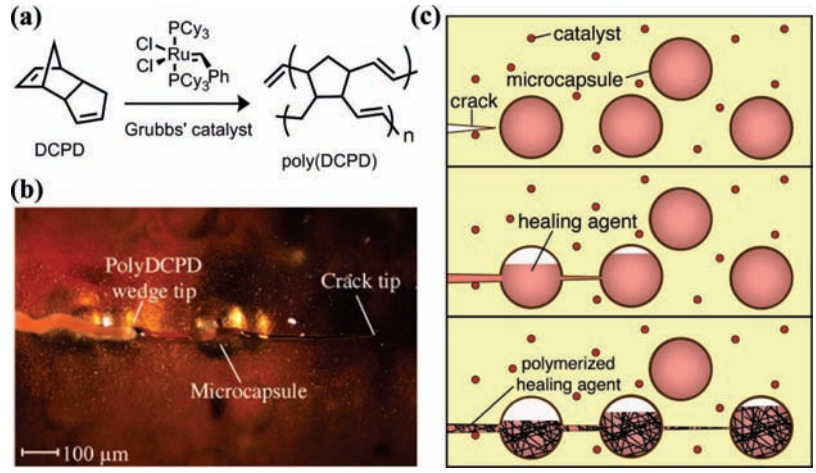

Figure 49. (a) Reaction scheme of the monomer DCPD undergoing ring-opening metathesis polymerization to form poly(DCPD). Reprinted with permission from ref 351. Copyright 2001 Nature Publishing Group. (b) Optical micrograph of an *in situ* fatigue specimen showing poly(DCPD) formed in the crack plane behind the crack tip. Reprinted with permission from ref 362. Copyright 2005 Elsevier. (c) The autonomic self-healing system showing crack initiation, rupture of microcapsules, and release of healing agent, and the resulting polymer formed in the crack plane. Reprinted with permission from ref 351. Copyright 2001 Nature Publishing Group.

healing ability was demonstrated.[355−358] The elegant approach of flowing a fluorescent dye through the fibers allowed for visual detection of crack damage in these composites.[355,356]

In 2001, it was discovered that the ring-opening metathesis polymerization (ROMP) of the olefin-based monomer dicyclopentadiene (DCPD) could be used as an effective chemical reaction to repair crack damage in an epoxy matrix using Grubbs' first generation catalyst (Figure 49a).[351] In the original paper on autonomic self-healing composites,[351] the components of this reaction—Grubbs' catalyst and polymer microcapsules containing the liquid DCPD as the core material—were both incorporated into an epoxy matrix. The microcapsules ruptured in response to mechanical damage in the form of a propagating crack through the epoxy composite (Figure 49c). Upon rupture, the liquid contents of the microcapsules wicked out into the crack plane of the epoxy through capillary action. When the DCPD and the embedded catalyst came into contact, the ROMP reaction occurred, resulting in polymer formation in the crack plane (Figure 49b). The fracture toughness of the epoxy composite was restored to up to 75−90% of the initial value.[351,359−361] Significant fracture toughness was recovered within an hour at room temperature, but up to 12 h were required for complete restoration.[361,362] Low temperature healing has been investigated with *exo*-DCPD, which remains liquid down to −78 °C and shows significantly faster polymerization kinetics compared to *endo*-DCPD.[363]

The healing efficiency in this microcapsule-based self-healing system is dependent on several factors including (1) monomer stability in the absence of catalyst, (2) polymerization kinetics, (3) adhesion of the new polymer to the surrounding matrix, and (4) chemical compatibility of the catalyst with the matrix. DCPD was selected as an appropriate monomer for the ROMP-based system because, unlike vinyl monomers, it has good stability in the absence of a metathesis catalyst. The poly(DCPD) formed in the crack plane is a hydrocarbon and incompatible with the epoxy matrix, thus limiting the adhesion through intermolecular interactions to the polar epoxy matrix system. In order to improve the adhesion of the newly formed polymer to the epoxy matrix, more polar healing agents and matrices have been considered.[364] The optimal catalyst is one that remains fully active when embedded in an epoxy matrix, but it rapidly dissolves and reacts upon contact with released monomer from microcapsules. One approach is the protection of the catalyst in wax microspheres, which has been found to enhance its stability with the matrix.[365] The following sections summarize the behavior of both required components—the monomer and catalyst—when contained in a polymeric system.

4.1.1. Microcapsule-Based Systems

Microcapsules are used in self-healing materials to compartmentalize the healing agents from the surrounding polymer matrix. Capsules are commonly prepared by an emulsification process whereby monomers polymerize to form a shell wall around suspended liquid droplets.[366] Various techniques have been used to prepare microcapsules and microspheres; different types are shown in Figure 50.[367] These microcapsules are incorporated into a polymer matrix, as shown in Figure 49c. The crack ruptures the embedded microcapsules, and the fluid is released through capillary action, covering the crack interface. The crack's trajectory is attracted to the microcapsules due to the difference in compliance between the matrix and microcapsules.[351]

In situ encapsulation techniques produce a robust, dense, and brittle shell wall, which is often ideal for compartmentalizing a hydrophobic core material in a polymer matrix (Figure 50a).[367,368] The reaction of urea and formaldehyde (shown in Scheme 8) was used to form the polymeric shell wall of DCPD-filled microcapsules.[368] Microcapsules provide additional benefits, such as improving the fracture toughness of a polymeric material.[348] The mechanical properties of the microcapsules *ex situ* were analyzed in terms of modulus and failure behavior by capsule compression testing.[369] For capsules to rupture in a reliable fashion, they must have an effective embedded modulus lower than that of the surrounding polymer matrix, which, as previously mentioned, is important for guiding cracks' trajectories to microcapsules.[351]

Conventional microencapsulation procedures have been modified to design more complex architectures with enhanced release capabilities. Microcapsules containing the monomer DCPD for use in self-healing materials were synthesized with urea−formaldehyde (UF) shell walls on the micro-[368] and nanoscale[370] for use in self-healing materials.

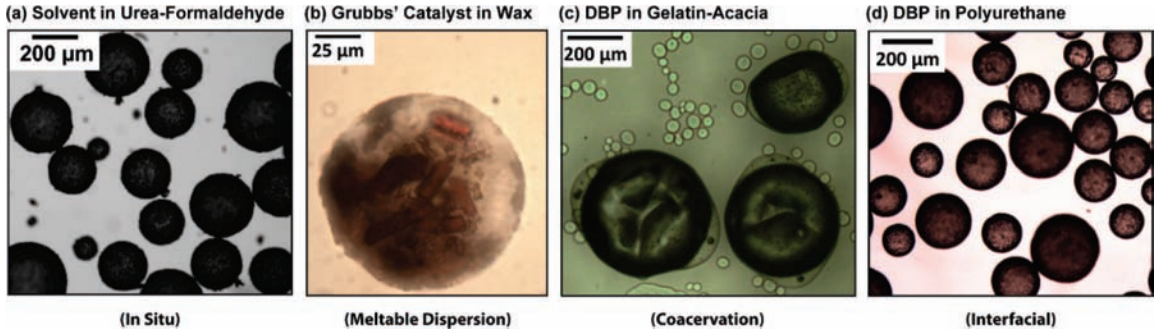

Figure 50. (a) Solvent-filled urea−formaldehyde (UF) capsules prepared by an in situ polymerization technique. (b) Grubbs' catalyst microspheres prepared by a meltable dispersion technique. (c) Dibutylphthalate (DBP)-containing gelatin−gum acacia microcapsules prepared by a coacervation technique. (d) DBP-containing polyurethane microcapsules produced using an interfacial polymerization technique.[367]

Scheme 8. Polymerization of Urea and Formaldehyde To Form Short Chain Oligomers That Make up the Shell Walls of Microcapsules (Reaction Conditions = 4 h at 55 °C, pH 3−5)[368]

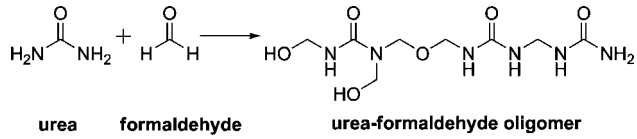

The UF capsule diameter size was controlled by the agitation rate of the emulsion, and nanocapsules were produced with the use of sonication and droplet stabilization techniques.[370] By using smaller capsules containing dibutylphthalate (secondary liquid) as Pickering stabilizers, binary microcapsules were prepared in which the main core material was DCPD.[371] This development allows for two liquids to be delivered from a single capsule architecture.

An extensive study was conducted to determine how microcapsules of various sizes affected the self-healing performance of the materials.[372] This work demonstrated that recovery of fracture toughness could be optimized by varying the amount of healing agent released, the size of the damage, and the volume fraction of microcapsules in the epoxy. The amount of healing agent released from the microcapsules scales with capsule diameter and with the percent loading of the microcapsules in the epoxy matrix. The total mass of fluid healing agent delivered to the crack plane ($M_{\text{healing agent}}$ in mg·cm^{-2}) is given by

$$M_{\text{healing agent}} = \rho_s \varphi D_c \qquad (4)$$

where ρ_s is the density of the matrix, φ is the mass fraction of microcapsules, and D_c is the mean diameter of the microcapsules.[372,373] To reduce the total crack volume in a self-healing specimen, shape memory alloy wires were embedded into the epoxy matrix and activated to apply crack closure forces. This ROMP-based system gave higher healing efficiencies than the original system.[374]

4.1.2. Fatigue Responses

In the previous sections, the self-repairing polymer systems respond to monotonic fracture as the mechanical stimulus. However, fatigue response is even more critical for extending the lifetime of structural materials. Fatigue-resistant materials are needed in a variety of structural applications, such as bioimplants, where it is neither safe nor practical to replace the implant after damage from repeated, cyclic loading. In structural applications, crack damage to unmodified epoxy thermosets is a major drawback, limiting their widespread use in advanced composites.[375] Their inherently brittle behavior has been improved with the addition of fillers such as inorganic particles[376,377] and thermoplastics.[378] In contrast to these physical approaches, the fracture toughness[348] and fatigue life[379] of the epoxy matrix has been improved using a chemically based DCPD-filled microcapsule system.

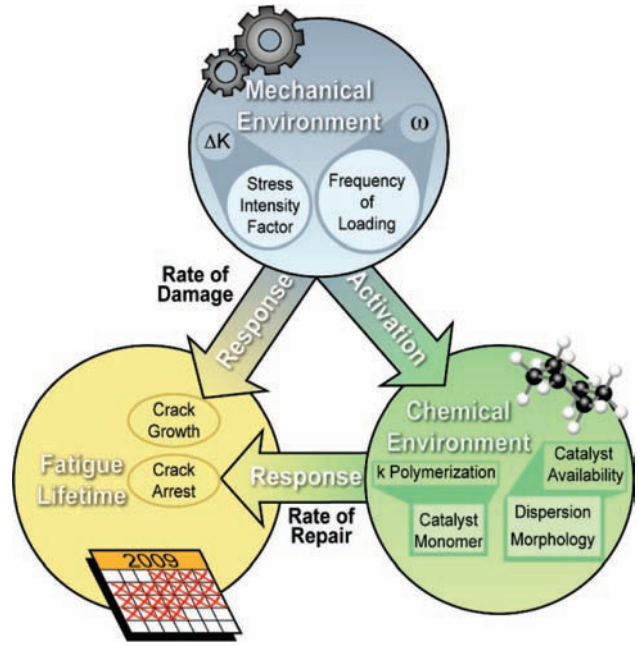

Figure 51. Diagram showing the interconnection between the mechanical and chemical environments of self-healing materials and their influence on fatigue lifetime.

Both the mechanical and chemical environments of a self-repairing system must be considered when analyzing the fatigue lifetime of a mechanically responsive self-healing material (Figure 51). The relative rates of mechanical damage and healing compete to govern the fatigue lifetime. For example, the loading frequency (ω) and stress intensity interval (ΔK_I) determine the rate at which damage occurs according to the Paris power law.[380] When damage leads to crack growth in a self-healing system, the chemical response is activated by microcapsules' rupture and release. The response or rate of repair is then determined by the chemical environment. For example, the rate at which healing occurs depends on the transport of monomer into the epoxy crack plane, dissolution of catalyst particles, and the rate of polymerization. Catalyst dissolution depends on the solid-state phase and catalyst particle size and shape.[381,382] The competition between the rate of damage and rate of repair

ultimately defines the stability of a dynamically loaded materials system.[349]

Using the tapered double-cantilever beam (TDCB) geometry for fracture testing,[359] Brown et al. studied the fatigue response of microcapsule-toughening epoxy by monitoring crack growth.[379,383] The fatigue testing protocol was initially examined at various stress intensity loading conditions.[383] Crack arrest was observed for self-healing samples containing DCPD microcapsules and embedded Grubbs' catalyst, provided that the rate of healing agent transport and DCPD polymerization was faster than the rate at which crack damage was imparted to the specimen. Conversely, when the rate of damage was greater than the rate of healing, the crack propagated quickly through the epoxy. Under these conditions, crack arrest was possible only when rest periods of 10 h were built into the fatigue cycle to allow for the DCPD polymerization to occur.[383] Catalyst availability also plays a critical role in the healing rate. For example, the fatigue behavior under higher stress intensities was explored in systems whereby Grubbs' catalyst was present in different morphologies and forms (recrystallized, freeze-dried, or protected in wax spheres).[381] When wax microspheres containing the catalyst were embedded in the matrix, the healing kinetics improved from the system using embedded catalyst particles in the matrix,[383] and the fatigue life dramatically increased. Kamphaus and co-workers also demonstrated crack arrest at lower frequencies in an alternative catalyst/monomer system, using tungsten hexachloride and ethylidene norbornene/DCPD monomer mixtures.[384] Efforts are currently underway to explore the fatigue response of other more economical self-healing systems.

4.1.3. Other Microencapsulated Self-Healing Chemistries

From a practical point of view, there are several drawbacks to the initial Grubbs'/DCPD self-healing system, including cost, toxicity, availability of Grubbs' catalyst, and the compatibility of the catalyst with sample manufacturing. For example, the amine curing agent present in the epoxy (DETA) reacts with and deactivates Grubbs' catalyst, which decreases potential healing efficiencies.[359] In order to overcome these problems, several modifications were studied: wax-protection of the catalyst,[365] different catalyst morphologies,[382] alternative metathesis catalysts,[364,384,385] and a change in matrix to an epoxy vinyl ester.[386,387] Ongoing research in this field continues to explore catalyst-free self-healing systems based on ring-opening reactions or solvent healing, with the goal of eliminating the dependence on the ROMP reaction of DCPD for recovery of damaged materials.[373,388,389]

Polydimethylsiloxane (PDMS) has also been exploited as a healing chemistry for self-healing materials. In one demonstration, the components PDMS and polydiethoxysiloxane (PDES) were phase-separated as droplets suspended in an epoxy vinyl ester matrix. This matrix also contained microcapsules of the catalyst, dibutyltin dilaurate (DBTL), dissolved in chlorobenzene (Figure 52).[386] Upon crack damage, the microcapsules ruptured, releasing the catalyst into the crack plane, thus initiating the formation of PDMS. Later studies involved a two-capsule PDMS system in which a platinum-based catalyst was encapsulated with the PDMS precursor in one capsule and the hydrosiloxane initiator encapsulated in another.[390] When the contents of both capsules were transported into the crack plane upon mechanical damage, hydrosilylation occurred, resulting in a cross-linked PDMS network. Healing efficiencies of 70−100%

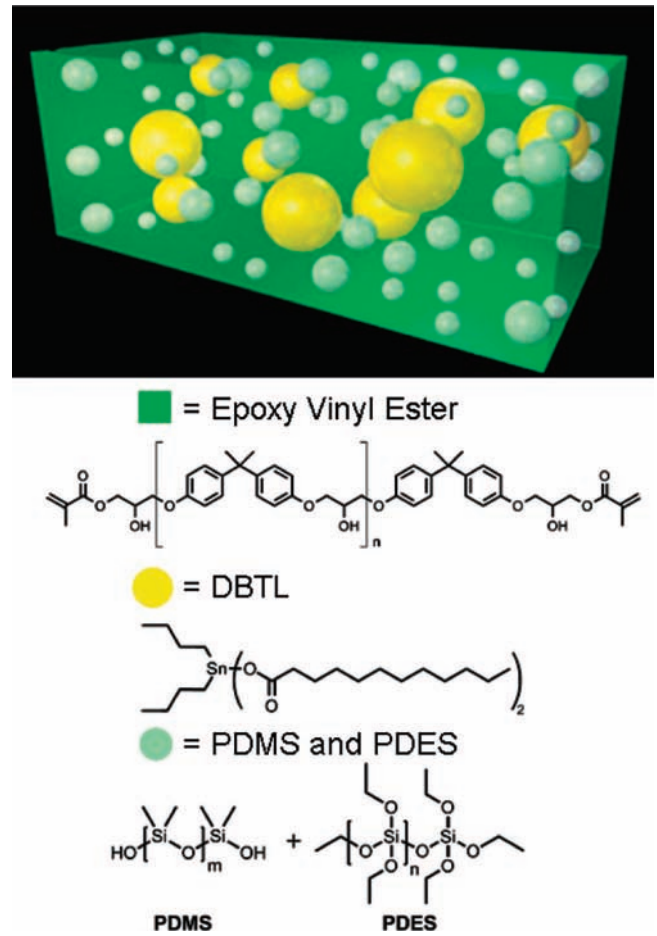

Figure 52. Schematic of the phase-separated PDMS self-healing system and chemical structures of each component.[386] Reproduced with permission from ref 386. Copyright 2006 Wiley-VCH Verlag GmbH & Co. KGaA.

were reported, based on tear strength recovery 48 h after the initial damage had occurred.[390] This chemistry was also used in a self-healing flexible laminate composite in which puncture holes were sealed upon the polymerization of the encapsulated PDMS and catalyst components.[391] The effectiveness of this self-healing elastomer was defined by the ability to prevent gas leakage through a punctured composite using a pressure test cell.

Other ring-opening reactions have been suggested for use in structural self-repairing materials. The reaction between epoxides and amines[375] to create a thermoset has been considered given the advantage that the healing chemistry produces the same material as the surrounding matrix. There are, however, challenges to making this system effective for self-repair. In this type of system, a self-healing thermoset composite has both epoxy- and amine-filled microcapsules.[392] The released epoxy is delivered to the damaged area and reacts with the released curing agent to produce a new cross-linked polymer. One challenge is to realize the acceptable stoichiometry between the two components. Another challenge is to efficiently mix the two components in the crack plane. Numerous examples of microcapsules containing epoxy monomer core solutions have been reported.[393−398] Due to the water solubility of aliphatic amine-based curing agents, *in situ* encapsulation techniques have proven difficult for use in preparing microcapsules with amine-functional core materials.[392] Alternative curing agents such as imidazole derivatives have been microencapsulated and used in combination

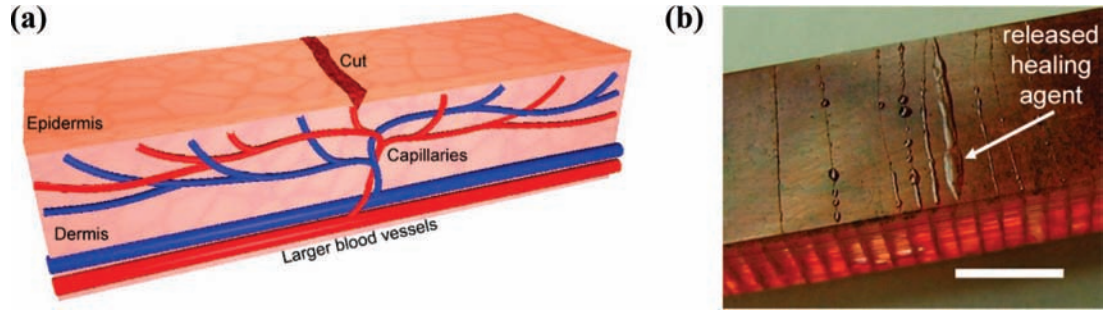

Figure 53. (a) Structural materials with fluid-containing microvascular channels have been designed to mimic the human body's circulatory system. (b) An epoxy sample with embedded microchannels showing released healing agent from the channels into the crack plane of the top coating (scale bar = 5 mm).[416] Reprinted with permission from ref 416. Copyright 2007 Nature Publishing Group.

with epoxy microcapsules to test for self-healing capability.[399−401] This system is nonautonomic, requiring external heat to promote the reaction of imidazole with epoxy, and the healing efficiencies over time (defined as the recovery rate of interlaminar fracture toughness in composites) initially decreased and then leveled off after storage times of up to 18 months.[402]

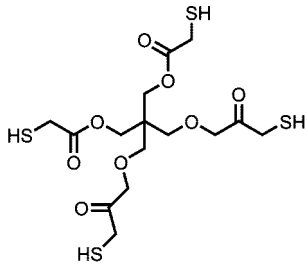

pentaerythritol tetrakis(3-mercaptopropionate)

To overcome these challenges, modifications have been made to the conventional two-part epoxy chemistry. In one case, a more robust, room temperature epoxy system was developed by encapsulating a polythiol curing agent, pentaerythritol tetrakis(3-mercaptopropionate).[403] Self-healing was demonstrated in a thermoset with these mercaptan and epoxy microcapsules embedded in the matrix.[404] High healing efficiencies were achieved at room temperature with low capsule loadings, and this system holds great promise for commercial products. More recently, Rong et al. prepared microcapsules[405] and sisal fibers[406] containing boron trifluoride diethyl etherate ($(C_2H_5)_2O\cdot BF_3$) as a curing agent to be used in place of the mercaptan-containing capsules. This cationic chain polymerization reaction between epoxy and $(C_2H_5)_2O\cdot BF_3$ is nonstoichiometric and provided a faster cure for use in self-healing systems.[406,407]

Solvent healing agents have also been explored for use in self-healing polymer composites. When an organic solvent is introduced into a polymer system, the mobility of polymer chains increases.[8,132] Early work in this field employed solvents such as ethanol and methanol to heal crack damage in thermoplastic polymers (i.e., PMMA) after heat treatment.[408−413] The healing mechanism proposed was the wetting of the polymer surface and resultant swelling of the bulk polymer material, which leads to reptation and interlocking of the chains across the crack plane to recover virgin mechanical properties. Recently, it was discovered that when microcapsules with solvent cores were incorporated into an epoxy thermoset, the release of solvents upon damage promoted the mobility of residual functional groups to entangle and react across the crack plane to render the material autonomically self-healing.[388] Solvent-promoted self-healing is only effective when residual, unreacted epoxy and amine segments remain in the matrix. Full recovery of fracture toughness (100% healing efficiencies) was achieved for a thermoset matrix that incorporates microcapsules containing unreacted epoxy monomer dissolved in the solvent healing agents.[373] Upon crack damage, the embedded capsules ruptured to release their components; the unreacted epoxy reacted with the residual amines in the matrix, healing the matrix with up to 100% efficiencies. More environmentally friendly solvents (ethyl phenylacetate and phenylacetate) were employed as healing agents in this work, showing promise for a commercial system.[373] This solvent-based healing system is under investigation for use in other advanced materials applications.

4.1.4. Microvascular Systems

One major shortcoming of microencapsulated healing agents in a polymeric system is that there is no means to replenish healing agents once they are consumed at the damage site.[414] For enhanced lifetime and extended usability in structural applications, multiple healing events are desirable. Materials systems with microvascular networks have been created that mimic the behavior of biological circulatory systems (Figure 53).[415] In these systems, the healing agent is continuously replenished to the site of damage.

Recently, the use of a microvascular network to deliver healing agent was expanded to the ROMP/DCPD system and demonstrated multiple healing events.[416,417] This system reported up to seven healing cycles for samples containing DCPD in the microchannels. By changing the healing chemistry of the networks to that of the well-known two-part epoxy reaction, the number of healing cycles was increased to 16 cycles. These samples contained multiple networks in order to provide a stoichoimetric amount of epoxy and curing agent to the site of damage. Hansen et al. recently reported the development of a three-dimensional interpenetrating microvascular network.[418] These networks were created based on two key advances in direct-write technologies:[419] dual ink deposition and vertical ink writing. Using low-viscosity, two-part epoxy healing agents flowing through the networks, damage to the structure underwent autonomic self-healing for over 30 healing cycles. This improved biomimetic architecture demonstrates the marked enhancement of repeated healing over earlier designs.[418]

Figure 54. Schematic of a microcapsule-containing self-healing coating and interfaces affected by mechanical damage.[435]

4.1.5. Alternative Damage Repair Systems

There have been a number of reviews on nonautonomic types of healing systems.[352,420,421] Most of these repair mechanisms depend on mobility and rearrangement of polymer segments with respect to external stimuli such as increasing temperatures,[422,423] reversible Diels−Alder reactions,[59,424−427] and noncovalent interactions[428] in response to mechanically-induced damage. Some of these responses have been covered in previous sections of this review, since the response is localized to an atomic or supramolecular level (see section 2.5.3).

Another system involving multiple hierarchical levels of polymeric responses to mechanical damage employs nanoparticles. When nanotubes or nanoparticle fillers are incorporated into a polymer network, they spontaneously migrate to cracks formed by damage.[429,430] For example, after surface modification of CdSe/ZnS nanoparticles, the enthalpic interactions of a multilayer composite were studied.[431] Upon crack damage, the nanoparticles segregated to the polymer−air interface (monitored by fluorescence of the particles). Entropic considerations drive the nanoparticles to the crack interface to release strain. This migration of nanoparticles upon crack damage has also been studied through modeling and computational experiments.[432] This group's most recent work involves simulating deformation of a network made up of nanoscopic gel particles.[433] Although there was no experimental proof of self-healing, the predictions will be used in detecting damage on the nanoscale and in developing novel advanced materials with self-repairing capabilities.

4.2. Self-Healing Coatings

Advanced coatings that sense a variety of stimuli such as change in pH, electrical current, radiation, and temperature have been developed.[434] Since this review concerns a materials' response to mechanical stimuli, discussion of these responsive coatings is outside the scope of this article. The other stimuli and their respective responses are discussed at length in a recent review.[434]

Coatings function to protect a substrate from external damage, such as abrasion/scratching, weathering, and corrosion.[435] The response to damage or stress in coatings usually does not require the repair of load bearing functionality. In comparison to structural polymers, coatings applications usually involve thin layers that limit the dimensions of fillers (such as microcapsules) or additional components. Mobility of matrix phases is also acceptable for coatings, which is not always feasible with structural plastics.

Self-healing coatings are either thermoplastic or thermoset polymers. Coating damage can result from stress developed at three different interfaces: coating−substrate, binder–filler, and coating−air (Figure 54).[435] Damage to the coating leads to capsule rupture and release of its contents. The polymeric components in the coating near the site of damage then respond with enhanced mobility of polymer chains.

The use of microcapsules in coatings applications has increased in recent years.[436] The commercial interest in self-healing coatings is growing, as evidenced by recent use in the automotive industry (i.e., Nissan and Toyota).[435] Microcapsules provide the advantage that protection agents can be compartmentalized in the system and released upon mechanical damage. The two most common ways of incorporating capsules into coatings is to spray a suspension on the top surface or mix the capsules in the coating formulation. For anticorrosion applications, the microcapsule content is released under mechanical stress by three possible mechanisms: shell wall breakage under pressure, shell wall degradation through chemical breakdown of shell components, or shell wall fracture upon swelling of the core material.[436]

This field has largely focused on the development of anticorrosion nanocontainers and their use in self-repairing coatings.[437] Defects are created on the exterior surface of coatings due to environmental weathering, leading to corrosion of the substrate (especially in marine applications). Thus, by designing coatings that can release antioxidants and anticorrosive agents, protection of the substrate can be realized.[437,438] Microcapsules containing photosensitive antioxidants have been prepared,[439] although their applications are more limited to the food and cosmetics industries. Corrosion inhibitors in nanocontainers[440,441] and halloysite (aluminosilicate clay) nanotubes[442] have also been embedded in layer-by-layer assemblies; release of these inhibitors is triggered by pH changes in the environment. Although the stimulus in this case is not mechanical, these materials serve as corrosion sensors, capable of giving feedback to indicate that the coating needs repair.

Recently, Kumar and co-workers developed coatings for steel substrates that respond to mechanical damage by introducing microcapsules into a commercial primer for paints.[443,444] The capsules contained tung oil, varnish, and camphor, which reduced/eliminated the occurrence of corrosion after these coatings were damaged. In a similar fashion, Suryanarayana et al. encapsulated linseed oil and observed the self-healing performance of these capsules in epoxy coatings.[445] The oil oxidized when released from the capsules to render the film anticorrosive.

4.2.1. PDMS-Based Systems

One specific chemical reaction that has been used for coatings repair is the metal-mediated reaction to synthesize the elastomer PDMS introduced in section 4.1.3 of this review. Encouraged by their initial success with the phase-separated PDMS-based self-healing system,[386] Braun and co-workers incorporated two types of microcapsules into a system for the repair of damaged coatings—one type contained an organotin catalyst, dimethyldineodecanoate tin (DMDNT), in chlorobenzene while the other type contained a combination of PDMS and PDES healing agents (Scheme 9).[446] The model system consisted of an epoxy vinyl ester matrix and only demonstrated healing at elevated temperatures (50 °C). The more impressive result from this study was the room temperature self-healing of a commercial epoxy coating by switching to the more effective hydrosilylation catalyst (tetrakis(acetoxydibutyltinoxy)silane, TKAS).[446] Although PDMS does not possess the load-bearing properties needed for use in structural materials, the self-healing variant

Scheme 9. Polycondensation Reaction Employed for PDMS-Based Self-Healing Coatings[446]

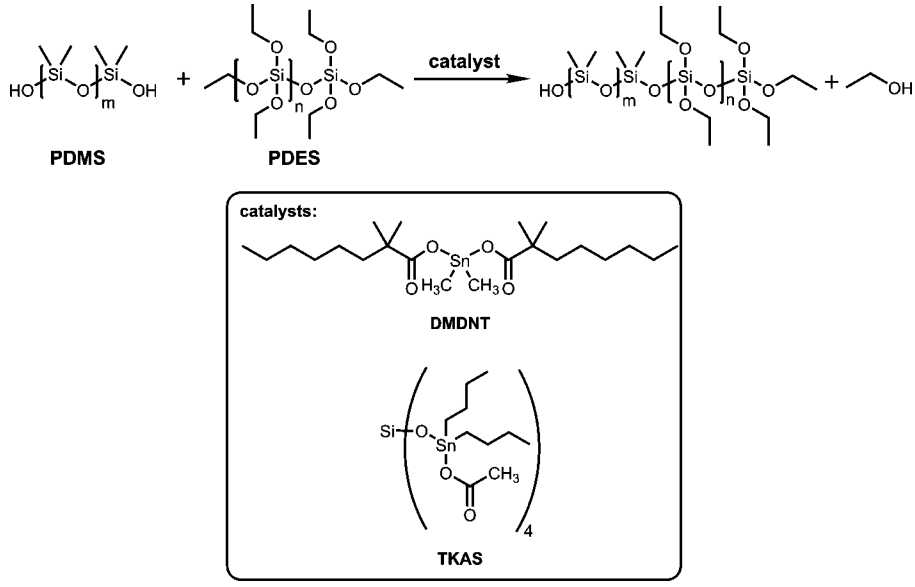

has potential use in coatings and low temperature applications such as cryogenic tanks, where repair of puncture damage is important to prevent gas leakage.[447] This simplistic, economical system shows great promise for commercialization in the upcoming years.

5. Conclusions and Outlook

Polymeric materials respond to mechanical forces on the molecular level by changing conformation, chain slippage, segmental alignment, disentanglement, and ultimately bond scission. These molecular scale events evolve to the macroscale, resulting in the formation of crazes and cracks, ending in catastrophic failure. As the research in this review has demonstrated, not all mechanochemical changes need be considered unproductive. Given suitably designed mechanoresponsive materials, the energy from applied mechanical fields is capable of inducing productive chemical changes that can restore functionality lost by damage. These changes may, for example, result in the autonomic repair of macroscopic damage for improved lifetime of structural materials made from polymeric components.

The societal impact of polymeric materials with enhanced lifetimes could be significant, especially with regard to safety and energy efficiency. Achieving greater longevity in device components that are inaccessible and therefore incapable of being replaced is of great importance. The combination of lightweight and high-strength has been a major advantage enjoyed by polymeric materials compared to other structural solids such as metals and ceramics. This characteristic feature makes polymeric materials—including composites—desirable for transportation vehicles or energy-harvesting structures, such as the rotor blades of wind turbines. Real-world engineered parts are often deliberately overdesigned to achieve a targeted lifetime. A consequence of overengineering is significantly added mass that reduces energy efficiency. The ability to achieve a greatly extended life from a self-healing, mechanoresponsive material will reduce the mass previously needed to achieve similar performance, thereby regaining the lightweight, high-strength advantage of organic polymers.

Nature provides fascinating examples of solids well-suited for load-bearing and structural applications that are also imparted with mechanoresponsive functionality. The development of mechanically responsive structural materials is in its infancy, but the existence of natural bone is evidence that these mechanoresponsive functions are indeed realizable. The remarkable ability of bone to repair fracture is a common example of self-healing that is known to everyone. The synthetic reproduction of this behavior has been realized during the past decade.[351] Adding compartmentalized liquids to structural solids may seem detrimental and counterintuitive, since liquid phases might be expected to compromise a material's desirable mechanical properties. However, liquid phases are the right choice for macroscopic damage repair because liquids exhibit rapid mass transport and molecular diffusion that allow for the possibility of postprocessing chemistry at precisely the time and location of need. Work to date has shown that microcapsules are not, in fact, detrimental to mechanical properties but instead favorably toughen epoxy materials. Moreover, the microcapsule and microvascular systems studied to date are capable of restoring mechanical properties at or near the level of the virgin material. Moving these demonstrated concepts into real-world applications will require more practical chemistries that are robust and environmentally compatible. Aging experiments of epoxy networks[448] to project long-term stability of self-healing composites are very preliminary, and these considerations are essential in producing robust systems. On the engineering side, a remaining challenge is to incorporate self-healing components into polymeric and composite materials using conventional processing and fabrication methods. The most extravagant self-healing systems have microvascular structures, and it remains a challenge on the chemistry side to develop a system that can spontaneously evolve into the desired 3D network of interconnected microchannels by a self-assembly process.

Another mechanoresponsive characteristic of bone is that its strength and toughness are locally modulated by use, a behavior that is not yet well-mimicked in synthetic polymeric materials. Should such a behavior become available, it might enable the autonomic postprocessing of materials in a time and spatial dependent manner dictated by the material's complex stress and strain distributions. Increasing our fundamental understanding of mechanochemical transduction

at the atomistic and supramoleclar levels may lead to mechanophores with enhanced mechanosensitivity having the ability to undergo selective mechanochemical reactions. Mechanophores that undergo cross-linking reactions triggered by a mechanical field could provide a mechanism for modulating material properties in response to an external force field. New mechanophore concepts such as mechanocatalysts and mechanoacids might cause local transformations to be performed by chemical catalysts or proton sources, which in turn are activated by external force fields. These possibilities are exciting for future development in the field of mechanochemistry, and their existence will greatly expand the mechanochemial toolbox.

To date, mechanoresponsive materials have largely focused on restoring functions such as mechanical properties of structural composites and barrier properties of protective coatings. Reference to Figure 1b shows that there are numerous areas of underdeveloped mechanoresponsive materials. The self-healing concept based on the release of liquid content from microcapsules is a general one that may potentially apply to other functionalities such as restoration of electrical or optical properties in damaged devices. Expanding the list of liquid agents that can be transformed to achieve desired functionality when released from microcapsules is an area ripe for further discovery.

The unrealized mechanoresponsive properties listed in this section and other mechanoresponsive properties that have yet to be conceived are sure to motivate fundamental and technological studies in the field of polymer mechanochemistry for years to come. These properties hold promise for bringing new functionality to polymeric materials in ways that will improve safety, increase longevity, and lighten the burden on the world's environment.

6. Abbreviations

ε	strain
σ	stress
9-MeAn	9-methylanthracene
ADMET	acyclic diene metathesis
Alq3	tris(8-hydroxyquinolinato)aluminum
BCB	benzocyclobutene
BBS	4,4′-bis(2-benzoxazolyl)stilbene
BCMDB	1,4-bis-(*R*-cyano-4-methoxystyryl)-2,5-dimethoxybenzene
COGEF	COnstrained Geometries simulate External Force
DCPD	dicyclopentadiene
DETA	diethylenetriamine
DFT	density functional theory
DMA	dynamic mechanical analysis
DPPH	2,2-diphenyl-1-picrylhydrazyl
eCFP	enhanced cyan fluorescent protein
eYFP	enhanced yellow fluorescent protein
ESR	electron spin resonance
EVA	poly[ethylene-*co*-(vinyl acetate)]
FRET	fluorescence resonance energy transfer
HDI	hexamethylene diisocyanate
LLDPE	linear low-density polyethylene
M_{lim}	limiting molecular weight
M_n	number average molecular weight
M_w	weight average molecular weight
MD	molecular dynamics
MDI	methylene diphenyl diisocyanate
MEH-PPV	poly(2-methoxy-5-(2′-ethylhexoxy)-*p*-phenylenevinylene)
OPV	oligo(*p*-phenylene vinylene)
P3BT	poly(3-*n*-butylthiophene)
P3DDT	poly(3-*n*-dodecylthiophene)
P3HT	poly(3-*n*-hexylthiophene)
P3OT	poly(3-*n*-octylthiophene)
PDMS	poly(dimethylsiloxane)
PE	polyethylene
PEG	poly(ethylene glycol)
PET	poly(ethylene terephthalate)
PETG	poly(ethylene terephthalate glycol)
PL	photoluminescence/photoluminescent
PMMA	poly(methyl methacrylate)
PMA	poly(methyl acrylate)
PMNB	pentamethyl nitrosobenzene
PS	poly(styrene)
PTCDI	perylene tetracarboxylic diimide
ROMP	ring-opening metathesis polymerization
SET-LRP	single-electron transfer living radical polymerization
SP	spiropyran
TABS	thermally activated barrier to scission
T_g	glass transition temperature
TPU	thermoplastic polyurethanes
UDETA	2-aminoethylimidazolidone
UF	urea-formaldehyde
UPy	4-ureido-2-pyrimidone

7. Acknowledgments

The authors gratefully acknowledge Dorothy Loudermilk and Mitchell Ong for graphics design, and helpful discussions with Ben J. Blaiszik and Aaron D. Finke. Financial support was provided by the Air Force Office of Scientific Research MURI (FA9550-05-1-0346), the Army Research Office MURI (W911NF-07-1-0409), and the Department of Defense (National Defense Science and Engineering Graduate Fellowship).

8. References

(1) Young, R. J. *Introduction to Polymers*; Chapman and Hall: London, 1981.
(2) Urry, D. W. *Angew. Chem., Int. Ed.* **1993**, *32*, 819.
(3) Stevens, M. P. *Polymer Chemistry: An Introduction*, 3rd ed.; Oxford University Press: New York, 1999.
(4) Shaw, M. T. *Introduction to Polymer Viscoelasticity*, 3rd ed.; Wiley & Sons: Hoboken, NJ, 2005.
(5) Ward, I. M. *Mechanical Properties of Solid Polymers*; Wiley-Interscience: New York, 1971.
(6) Launey, M. E.; Ritchie, R. O. *Adv. Mater.* **2009**, *21*, 2103.
(7) Porter, R. S.; Johnson, J. F. *Chem. Rev.* **1966**, *66*, 1.
(8) Wool, R. P. *Polymer Interfaces: Structure and Strength*; Hanser: Munich, 1994.
(9) Kausch, H. H.; Plummer, C. J. G. *Polymer* **1994**, *35*, 3848.
(10) Svaneborg, C.; Everaers, R.; Grest, G. S.; Curro, J. G. *Macromolecules* **2008**, *41*, 4920.
(11) French, A. S. *Annu. Rev. Physiol.* **1992**, *54*, 135.
(12) Comrie, J. E.; Huck, W. T. S. *Macromol. Rapid Commun.* **2008**, *29*, 539.
(13) Goodman, M. B.; Lumpkin, E. A.; Ricci, A.; Tracey, W. D.; Kernan, M.; Nicolson, T. *J. Neurosci.* **2004**, *24*, 9220.
(14) Gillespie, P. G.; Walker, R. G. *Nature* **2001**, *413*, 194.
(15) Menger, F. M. *Biochemistry* **1992**, *31*, 5368.
(16) Kallies, B.; Mitzner, R. *J. Mol. Model.* **1996**, *2*, 149.
(17) Klibanov, A. M.; Samokhin, G. P.; Martinek, K.; Berezin, I. V. *Biochim. Biophys. Acta* **1976**, *438*, 1.
(18) Staudinger, H.; Bondy, H. F. *Ber. Dtsch. Chem. Ges.* **1930**, *63*, 734.
(19) Staudinger, H.; Heuer, W. *Ber. Dtsch. Chem. Ges.* **1934**, *67*, 1159.
(20) Staudinger, H.; Leupold, E. O. *Ber. Dtsch. Chem. Ges.* **1930**, *63*, 730.
(21) Kauzmann, W.; Eyring, H. *J. Am. Chem. Soc.* **1940**, *62*, 3113.
(22) Sohma, J. *Prog. Polym. Sci.* **1989**, *14*, 451.
(23) Ayrey, G.; Moore, C. G.; Watson, W. F. *J. Polym. Sci.* **1956**, *19*, 1.
(24) Basedow, A. M.; Ebert, K. H. *Adv. Polym. Sci.* **1977**, *22*, 83.
(25) Porter, R. S.; Johnson, J. F. *J. Phys. Chem.* **1959**, *63*, 202.
(26) Keller, A.; Odell, J. A. *Colloid Polym. Sci.* **1985**, *263*, 181.
(27) Odell, J. A.; Keller, A. *J. Polym. Sci. Polym. Phys.* **1986**, *24*, 1889.

(28) Encina, M. V.; Lissi, E.; Sarasúa, M.; Gargallo, L.; Radic, D. *J. Polym. Sci. Polym. Lett. Ed.* **1980**, *18*, 757.
(29) Hickenboth, C. R.; Moore, J. S.; White, S. R.; Sottos, N. R.; Baudry, J.; Wilson, S. R. *Nature* **2007**, *446*, 423.
(30) Davis, D. A.; Hamilton, A.; Yang, J.; Cremar, L. D.; Van Gough, D.; Potisek, S. L.; Ong, M. T.; Braun, P. V.; Martinez, T. J.; White, S. R.; Moore, J. S.; Sottos, N. R. *Nature* **2009**, *459*, 68.
(31) Kim, S.-J.; Reneker, D. H. *Polym. Bull.* **1993**, *31*, 367.
(32) Berkowski, K. L.; Potisek, S. L.; Hickenboth, C. R.; Moore, J. S. *Macromolecules* **2005**, *38*, 8975.
(33) Potisek, S. L.; Davis, D. A.; Sottos, N. R.; White, S. R.; Moore, J. S. *J. Am. Chem. Soc.* **2007**, *129*, 13808.
(34) Cordier, P.; Tournilhac, F.; Soulie-Ziakovic, C.; Leibler, L. *Nature* **2008**, *451*, 977.
(35) Donati, F.; Pucci, A.; Cappelli, C.; Mennucci, B.; Ruggeri, G. *J. Phys. Chem. B* **2008**, *112*, 3668.
(36) Ikawa, T.; Shiga, T.; Okada, A. *J. Appl. Polym. Sci.* **1997**, *66*, 1569.
(37) Moses, D.; Feldblum, A.; Ehrenfreund, E.; Heeger, A. J.; Chung, T.-C.; MacDiarmid, A. G. *Phys. Rev. B* **1982**, *26*, 3361.
(38) Yang, J.; Li, H.; Wang, G.; He, B. *J. Appl. Polym. Sci.* **2001**, *82*, 2347.
(39) Pucci, A.; Bertoldo, M.; Bronco, S. *Macromol. Rapid Commun.* **2005**, *26*, 1043.
(40) Paulusse, J. M. J.; Sijbesma, R. P. *Angew. Chem., Int. Ed.* **2004**, *43*, 4460.
(41) Azzaroni, O.; Trappmann, B.; van Rijn, P.; Zhou, F.; Kong, B.; Huck, W. T. S. *Angew. Chem., Int. Ed.* **2006**, *45*, 7440.
(42) Pike, M.; Watson, W. F. *J. Polym. Sci.* **1952**, *9*, 229.
(43) Angier, D. J.; Chambers, W. T.; Watson, W. F. *J. Polym. Sci.* **1957**, *25*, 129.
(44) Harmon, D. J.; Jacobs, H. L. *Appl. Polym. Sci.* **1966**, *10*, 253.
(45) Porter, R. S.; Casale, A. *Polym. Eng. Sci.* **1985**, *25*, 129.
(46) Frendel, A.; Schmidt-Naake, G. *Chem. Eng. Technol.* **2001**, *24*, 798.
(47) Schmidt-Naake, G.; Frendel, A.; Drache, M.; Janke, G. *Chem. Eng. Technol.* **2001**, *24*, 889.
(48) Batchelor, A. W.; Stachowiak, G. W. *J. Orthop. Rheumatol.* **1996**, *9*, 3.
(49) Turssi, C. P.; Purquerio, B. D. M.; Serra, M. C. *J. Biomed. Mater. Res. B* **2003**, *65*, 280.
(50) van den Einde, R. M.; Akkermans, C.; van der Goot, A. J.; Boom, R. M. *Carbohydr. Polym.* **2004**, *56*, 415.
(51) van den Einde, R. M.; van der Goot, A. J.; Boom, R. M. *J. Food Sci.* **2003**, *68*, 2396.
(52) van den Einde, R. M.; Bolsius, A.; van Soest, J. J. G.; Janssen, L. P. B. M.; van der Goot, A. J.; Boom, R. M. *Carbohydr. Polym.* **2004**, *55*, 57.
(53) Wu, T.; Zivanovic, S.; Hayes, D. G.; Weiss, J. *J. Agric. Food Chem.* **2008**, *56*, 5112.
(54) Rubner, M. F. *Macromolecules* **1986**, *19*, 2129.
(55) Rubner, M. F. *Macromolecules* **1986**, *19*, 2114.
(56) Anuchai, K.; Weder, C.; Magaraphan, R. *Plast. Rubber Compos.* **2008**, *37*, 281.
(57) Chen, X.; Dam, M. A.; Ono, K.; Mal, A.; Shen, H.; Nutt, S. R.; Sheran, K.; Wudl, F. *Science* **2002**, *295*, 1698.
(58) Cordier, P.; Tournilhac, F.; Soulie-Ziakovic, C.; Leibler, L. *Nature* **2008**, *451*, 977.
(59) Reutenauer, P.; Buhler, E.; Boul, P. J.; Candau, S. J.; Lehn, J.-M. *Chem.—Eur. J.* **2009**, *15*, 1893.
(60) Boldyrev, W. *J. Chim. Phys.* **1986**, *83*, 821.
(61) Granick, S.; Bae, S. C. *Nature* **2006**, *440*, 160.
(62) Armstrong, R. W.; Corffey, C. S.; Elban, W. L. In *Advances in Chemical Reaction Dynamics*; Rentzepis, P., Capellos, C., Eds.; Reidel: Dordrecht, Netherlands, 1986; p 486.
(63) Evans, E.; Ritchie, K. *Biophys. J.* **1997**, *72*, 1541.
(64) Dudko, O. K. *Proc. Natl. Acad. Sci. U.S.A.* **2009**, *106*, 8795.
(65) Dudko, O. K.; Hummer, G.; Szabo, A. *Phys. Rev. Lett.* **2006**, *96*, 108101.
(66) Dudko, O. K.; Hummer, G.; Szabo, A. *Proc. Natl. Acad. Sci. U.S.A.* **2008**, *105*, 15755.
(67) Hummer, G.; Szabo, A. *Biophys. J.* **2003**, *85*, 5.
(68) Freund, L. B. *Proc. Natl. Acad. Sci. U.S.A.* **2009**, *106*, 8818.
(69) Beyer, M. K. *J. Chem. Phys.* **2000**, *112*, 7307.
(70) Aktah, D.; Frank, I. *J. Am. Chem. Soc.* **2002**, *124*, 3402.
(71) Beyer, M. K. *Angew. Chem., Int. Ed.* **2003**, *42*, 4913.
(72) Beyer, M. K.; Clausen-Schaumann, H. *Chem. Rev.* **2005**, *105*, 2921.
(73) Hickenboth, C. R.; Rule, J. D.; Moore, J. S. *Tetrahedron* **2008**, *64*, 8435.
(74) Ribas-Arino, J.; Shiga, M.; Marx, D. *Angew. Chem., Int. Ed.* **2009**, *48*, 4190.
(75) Saitta, A. M.; Soper, P. D.; Wasserman, E.; Klein, M. L. *Nature* **1999**, *399*, 46.
(76) Wool, R. P. *J. Polym. Sci., Polym. Phys. Ed.* **1975**, *13*, 1795.
(77) Wool, R. P. *Polym. Eng. Sci.* **1980**, *20*, 805.
(78) Wool, R. P.; Boyd, R. H. *J. Appl. Phys.* **1980**, *51*, 5116.
(79) Wool, R. P.; Statton, W. O. *J. Polym. Sci., Polym. Phys. Ed.* **1974**, *12*, 1575.
(80) Zhang, W.; Zhang, X. *Prog. Polym. Sci.* **2003**, *28*, 1271.
(81) Binnig, G.; Quate, C. F.; Gerber, C. *Phys. Rev. Lett.* **1986**, *56*, 930.
(82) Kishino, A.; Yanagida, T. *Nature* **1988**, *334*, 74.
(83) Bensimon, D.; Simon, A. J.; Croquette, V.; Bensimon, A. *Phys. Rev. Lett.* **1995**, *74*, 4754.
(84) Clausen-Schaumann, H.; Rief, M.; Tolksdorf, C.; Gaub, H. E. *Biophys. J.* **2000**, *78*, 1997.
(85) Grandbois, M.; Beyer, M.; Rief, M.; Clausen-Schaumann, H.; Gaub, H. E. *Science* **1999**, *283*, 1727.
(86) Zou, S.; Schönherr, H.; Vancso, G. J. *Angew. Chem., Int. Ed.* **2005**, *44*, 956.
(87) Serpe, M. J.; Kersey, F. R.; Whitehead, J. R.; Wilson, S. M.; Clark, R. L.; Craig, S. L. *J. Phys. Chem. C* **2008**, *112*, 19163.
(88) Frank, I.; Hofbauer, F. *Nat. Chem.* **2009**, *1*, 180.
(89) Liang, J.; Fernández, J. M. *ACS Nano* **2009**, *3*, 1628.
(90) Flosdorf, E. W.; Chambers, L. A. *J. Am. Chem. Soc.* **1933**, *55*, 3051.
(91) Sato, T.; Nalepa, D. E. *J. Coat. Technol.* **1977**, *49*, 45.
(92) Czechowska-Biskupa, R.; Rokita, B.; Lotfy, S.; Ulanski, P.; Rosiak, J. M. *Cabohydr. Polym.* **2005**, *60*, 175.
(93) Lorimer, J. P.; Mason, T. J.; Cuthbert, T. C.; Brookfield, E. A. *Ultrason. Sonochem.* **1995**, *2*, S55.
(94) Bradbury, J. H.; O'Shea, J. *Aust. J. Biol. Sci.* **1973**, *26*, 583.
(95) Freifelder, D.; Davison, P. F. *Biophys. J.* **1962**, *2*, 235.
(96) Karthikeyan, S.; Potisek, S. L.; Piermattei, A.; Sijbesma, R. P. *J. Am. Chem. Soc.* **2008**, *130*, 14968.
(97) Paulusse, J. M. J.; Sijbesma, R. P. *Chem. Commun.* **2008**, *37*, 4416.
(98) Price, G. J. In *Advances in Sonochemistry*; Mason, T. J., Ed.; JAI: Cambridge, 1990; Vol. 1.
(99) Suslick, K. S.; Price, G. J. *Annu. Rev. Mater. Sci.* **1999**, *29*, 295.
(100) Nguyen, T. Q.; Liang, Q. Z.; Kausch, H.-H. *Polymer* **1997**, *38*, 3783.
(101) Nguyen, T. Q. *Polym. Degrad. Stab.* **1994**, *46*, 99.
(102) Nguyen, T. Q.; Kausch, H.-H. *Int. J. Polym. Anal. Charact.* **1998**, *4*, 447.
(103) Vijayalakshmi, S. P.; Madras, G. *Polym. Degrad. Stab.* **2005**, *90*, 116.
(104) Doulah, M. S. *J. Appl. Polym. Sci.* **1978**, *22*, 1735.
(105) García-Alvarez, M.; López-Carrasquero, F.; Morillo, M.; Muñoz-Guerra, S. *J. Polym. Sci., Polym. Phys.* **1997**, *35*, 2379.
(106) Lueb, H. A.; Schoon, T. G. F. *J. Polym. Sci.: Polym. Symp.* **1976**, *57*, 147.
(107) Malhotra, S. L. *J. Macromol. Sci.* **1986**, *A23*, 729.
(108) Schoon, T. G.; Rieber, G. *Angew. Makromol. Chem.* **1972**, *23*, 43.
(109) Thomas, J. R.; deVries, L. *J. Phys. Chem.* **1959**, *63*, 254.
(110) van der Hoff, B. M. E.; Gall, C. E. *J. Macromol. Sci.* **1977**, *A11*, 1739.
(111) Mark, H. F. *Encyclopedia of Science and Technology*; Wiley Interscience: New York, 2005.
(112) Smith, W. B.; Temple, H. W. *J. Phys. Chem.* **1968**, *72*, 4613.
(113) Staudinger, H.; Schweitzer, O. *Ber. Dtsch. Chem. Ges.* **1930**, *63*, 3132.
(114) Keller, A.; Odell, J. A. *Colloid Polym. Sci.* **1985**, *263*, 181.
(115) Müller, A. J.; Odell, J. A.; Keller, A. *J. Non-Newtonian Fluid Mech.* **1988**, *30*, 99.
(116) Odell, J. A.; Keller, A.; Miles, M. *Polym. Commun.* **1983**, *24*, 7.
(117) Odell, J. A.; Keller, A.; Müller, A. J. *Colloid Polym. Sci.* **1992**, *270*, 307.
(118) Smith, D. E.; Chu, S. *Science* **1998**, *281*, 1335.
(119) Fuller, G. G.; Leal, L. G. *Rheol. Acta* **1980**, *19*, 580.
(120) Horn, A. F.; Merrill, E. W. *Nature* **1984**, *312*, 140.
(121) Merrill, E. W.; Leopairat, P. *Polym. Eng. Sci.* **1980**, *20*, 505.
(122) Nguyen, T. Q.; Kausch, H.-H. *J. Non-Newtonian Fluid Mech.* **1988**, *30*, 125.
(123) Nguyen, T. Q.; Kausch, H.-H. *Macromolecules* **1990**, *23*, 5137.
(124) Sheiko, S. S.; Sun, F. C.; Randall, A.; Shirvanyants, D.; Rubinstein, M.; Lee, H.; Matyjeszewski, K. *Nature* **2006**, *440*, 191.
(125) Park, I.; Sheiko, S. S.; Nese, A.; Matyjaszewski, K. *Macromolecules* **2009**, *42*, 1805.
(126) Lebedeva, N. V.; Sun, F. C.; Lee, H.; Matyjaszewski; Sheiko, S. S. *J. Am. Chem. Soc.* **2008**, *130*, 4228.
(127) Zysman, V.; Nguyen, T. Q.; Kausch, H.-H. *J. Polym. Sci., Part B: Polym. Phys.* **1994**, *32*, 1257.
(128) Wool, R. P.; Rockhill, A. T. *J. Macromol. Sci., Part B* **1981**, *B20*, 85.
(129) De Kee, D.; Wissbrun, K. F. *Phys. Today* **1998**, *51*, 24.
(130) Fried, J. R. *Polymer Science and Technology*, 2nd ed.; Prentice Hall: Upper Saddle River, NJ, 2003.
(131) Allcock, H. R.; Lampe, F. W.; Mark, J. E. *Contemporary Polymer Chemistry*, 3rd ed.; Pearson: New Jersey, 2003.
(132) Wool, R. P. *C. R. Chimie* **2006**, *9*, 25.

(133) Irie, M.; Kungwatchakun, D. *Makromol. Rapid Commun.* **1984**, *5*, 829.
(134) Irie, M.; Kobatake, S.; Horichi, M. *Science* **2001**, *291*, 1769.
(135) Anthanassiou, A.; Kalyva, M.; Lakiotaki, K.; Georgiou, S.; Fotakis, C. *Adv. Mater.* **2005**, *17*, 988.
(136) Koshima, H.; Ojima, N.; Uchimoto, H. *J. Am. Chem. Soc.* **2009**, *131*, 6890.
(137) Carrion-Vazquez, M.; Overhauser, A. F.; Fisher, T. E.; Marszalek, P. E.; Li, H.; Fernandez, J. M. *Prog. Biophys. Mol. Biol.* **2000**, *74*, 63.
(138) Merkel, R. *Phys. Rep.* **2001**, *346*, 343.
(139) Rief, M.; Grubmüller, H. *ChemPhysChem* **2002**, *3*, 255.
(140) Zhuang, X.; Rief, M. *Curr. Opin. Struct. Biol.* **2003**, *13*, 88.
(141) Kersey, F. R.; Loveless, D. M.; Craig, S. L. *J. R. Soc. Interface* **2007**, *4*, 373.
(142) Heinz, W. F.; Hoh, J. H. *Trends Biotechnol.* **1999**, *17*, 143.
(143) Nguyen, T. Q. *Chimia* **2001**, *55*, 147.
(144) Buchholz, B. A.; Zahn, J. M.; Kenward, M.; Slater, G. W.; Barron, A. E. *Polymer* **2004**, *45*, 1223.
(145) Toms, B. A. *Proc. 1st Int. Congress on Rhelogy*; North Holland: 1948; pp 135−141.
(146) Lumley, J. L. *Annual Review of Fluid Mechanics*; Annual Reviews Inc.: Palo Alto, CA, 1969.
(147) Casale, A.; Porter, R. S. *Polymer Stress Reactions*; Academic Press: New York, 1978.
(148) Ryskin, G. *J. Fluid Mech.* **1987**, *178*, 423.
(149) Rabin, Y. *J. Chem. Phys.* **1987**, *86*, 5215.
(150) Carrington, S. P.; Odell, J. A. *J. Non-Newtonian Fluid Mech.* **1996**, *67*, 269.
(151) Narh, K. A.; Odell, J. A.; Keller, A. *J. Polym. Sci., Polym. Phys.* **1992**, *30*, 335.
(152) Odell, J. A.; Keller, A.; Rabin, Y. *J. Chem. Phys.* **1988**, *88*, 4022.
(153) Nguyen, T. Q.; Kausch, H.-H. *Colloid Polym. Sci.* **1986**, *264*, 764.
(154) Nguyen, T. Q.; Kausch, H.-H. *Colloid Polym. Sci.* **1991**, *269*, 1099.
(155) Nguyen, T. Q.; Kausch, H.-H. *Adv. Polym. Sci.* **1992**, *100*, 73; DOI: 10.1007/BFb0051636.
(156) Yasuda, H.; Yamamoto, H.; Yamashita, M.; Yokota, K.; Nakamura, A.; Miyake, S.; Kai, Y.; Kanehisa, N. *Macromolecules* **1993**, *26*, 7134.
(157) Arita, T.; Buback, M.; Janssen, O.; Vana, P. *Macromol. Rapid Commun.* **2004**, *25*, 1376.
(158) Kayahara, E.; Yamago, S. *J. Am. Chem. Soc.* **2009**, *131*, 2508.
(159) Mao, B. W.; Gan, L. H.; Gan, Y. Y. *Polymer* **2006**, *47*, 3017.
(160) Percec, V.; Guliashvili, T.; Ladislaw, J. S.; Wistrand, A.; Stjerndahl, A.; Sienkowska, M. J.; Monteiro, M. J.; Sahoo, S. *J. Am. Chem. Soc.* **2006**, *128*, 14156.
(161) Simms, R. W.; Cunningham, M. F. *Macromolecules* **2007**, *40*, 860.
(162) Boffa, L. S.; Novak, B. M. *Macromolecules* **1997**, *30*, 3494.
(163) Nguyen, N. H.; Rosen, B. M.; Lligadas, G.; Percec, V. *Macromolecules* **2009**, *42*, 2379.
(164) Paulusse, J. M. J.; Sijbesma, R. P. *J. Polym. Sci., Part A: Polym. Chem.* **2006**, *44*, 5445.
(165) Mason, T. J.; Lorimer, J. P. *Applied Sonochemistry: Uses of Power Ultrasound in Chemistry and Processing*; Wiley-VCH Verlag: Weinheim, 2002.
(166) Jellinek, H. H. G.; White, G. *J. Polym. Sci.* **1951**, *7*, 21.
(167) Gooberman, G. *J. Polym. Sci.* **1960**, *42*, 25.
(168) Jellinek, H. H. G. *J. Polym. Sci.* **1959**, *37*, 485.
(169) Okkuama, M.; Hirose, T. *J. Appl. Polym. Sci.* **1963**, *7*, 591.
(170) Thomas, J. R. *J. Phys. Chem.* **1959**, *63*, 1725.
(171) Cravotto, G.; Cintas, P. *Angew. Chem., Int. Ed.* **2007**, *46*, 5476.
(172) Ballauff, M.; Wolf, B. A. *Macromolecules* **1981**, *14*, 654.
(173) Glynn, P. A. R.; Van der Hoff, B. M. E.; Reilly, P. M. *J. Macromol. Sci., Part A* **1972**, *A6*, 1653.
(174) Glynn, P. A. R.; Van der Hoff, B. M. E. *J. Macromol. Sci., Part A* **1973**, *A7*, 1695.
(175) Koda, S.; Mori, H.; Matsumoto, K.; Nomura, H. *Polymer* **1994**, *35*, 30.
(176) Henglein, V. A. *Makromol. Chem.* **1954**, *14*, 15.
(177) Henglein, V. A. *Makromol. Chem.* **1955**, *15*, 188.
(178) Tabata, M.; Miyazawa, T.; Kobayashi, O.; Sohma, J. *Chem. Phys. Lett.* **1980**, *73*, 178.
(179) Mason, T. J. *Advances in Sonochemistry*; Alden Press: Oxford, 1990.
(180) Melville, H. W.; Murray, A. J. R. *Trans. Faraday Soc.* **1950**, *46*, 996.
(181) Bestul, A. B. *J. Chem. Phys.* **1956**, *24*, 1196.
(182) Odell, J. A.; Muller, A. J.; Narh, K. A.; Keller, A. *Macromolecules* **1990**, *23*, 3092.
(183) Zhurkov, S. N.; Korsukov, V. E. *J. Polym. Sci., Polym. Phys. Ed.* **1974**, *12*, 385.
(184) Roth, W. R.; Rekowski, V.; Börner, S.; Quast, M. *Liebigs Ann. Chem.* **1996**, *1996*, 409.
(185) Price, G. J.; Smith, P. F. *Polymer* **1993**, *34*, 4111.
(186) Mostafa, M. A. K. *J. Polym. Sci.* **1958**, *28*, 519.
(187) Noltingk, B. E.; Neppiras, E. A. *Proc. Phys. Soc., Sect. B* **1950**, *63B*, 674.
(188) Thomas, B. B.; Alexander, W. J. *J. Polym. Sci.* **1957**, *25*, 285.
(189) Neppiras, E. A.; Noltingk, B. E. *Proc. Phys. Soc., Sect. B* **1951**, *64B*, 1032.
(190) Basedow, A. M.; Ebert, K. H. *Makromol. Chem.* **1975**, *176*, 745.
(191) Basedow, A. M.; Ebert, K. H.; Fosshag, E. *Makromol. Chem.* **1978**, *179*, 2565.
(192) El'tsefon, V. S.; Berlin, A. A. *Polym. Sci. U. S. S. R.* **1964**, *5*, 668.
(193) Golubev, S. V.; Tikhonova, Z. A.; Semchikov, Y. D.; Trubina, I. V. *Vyskomol. Soedin. Ser. A* **1987**, *29*, 2393.
(194) Madras, G.; Chattopadhyay, S. *Polym. Degrad. Stab.* **2001**, *71*, 273.
(195) Malhotra, S. L. *J. Macromol. Sci. Part A* **1982**, *17*, 601.
(196) Price, G. J.; Smith, P. F. *Eur. Polym. J.* **1993**, *29*, 419.
(197) Schmid, G.; Beutenmuller, E. *Z. Elektrochem.* **1943**, *49*, 325.
(198) Thomas, B. B.; Alexander, W. J. *J. Polym. Sci.* **1955**, *15*, 361.
(199) Schittenhelm, N.; Kulicke, W.-M. *Macromol. Chem. Phys.* **2000**, *201*, 1976.
(200) Daraboina, N.; Madras, G. *Ultrason. Sonochem.* **2009**, *16*, 273.
(201) Sivalingam, G.; Agarwal, N.; Madras, G. *AIChE. J.* **2004**, *50*, 2258.
(202) Desai, V.; Shenoy, M. A.; Gogate, P. R. *Chem. Eng. J.* **2008**, *140*, 483.
(203) Grönroos, A.; Pentti, P.; Hanna, K. *Ultrason. Sonochem.* **2008**, *15*, 644.
(204) Casale, A. *J. Appl. Polym. Sci.* **1975**, *19*, 1461.
(205) Chakraborty, J.; Sarkar, J.; Kumar, R.; Madras, G. *Polym. Degrad. Stab.* **2004**, *85*, 555.
(206) Mauler, R. S.; Guaragna, F. M.; Gobbi, D. L.; Samios, D. *Eur. Polym. J.* **1997**, *33*, 399.
(207) Vijayalakshmi, S. P.; Madras, G. *Polym. Degrad. Stab.* **2004**, *84*, 341.
(208) Chattopadhyay, S.; Madras, G. *J. Appl. Polym. Sci.* **2003**, *88*, 2818.
(209) Yen, H.-Y.; Yang, M.-H. *Polym. Test.* **2003**, *22*, 129.
(210) Desai, V.; Shenoy, M. A.; Gogate, P. R. *Chem. Eng. Proc.* **2008**, *47*, 1451.
(211) Gooberman, G. *J. Polym. Sci.* **1960**, *47*, 229.
(212) Jellinek, H. H. G.; White, G. *J. Polym. Sci.* **1951**, *7*, 33.
(213) Brett, H. W. W.; Jellinek, H. H. G. *J. Polym. Sci.* **1954**, *13*, 441.
(214) Kanwal, F.; Liggat, J. J.; Pethrick, R. A. *Polym. Degrad. Stab.* **2000**, *68*, 445.
(215) Porter, R. S.; Cantow, M. J. R.; Johnson, J. F. *J. Appl. Phys.* **1964**, *35*, 15.
(216) Taghizadeh, M. T.; Mehrdad, A. *Ultrason. Sonochem.* **2003**, *10*, 309.
(217) Florea, M. *J. Appl. Polym. Sci.* **1993**, *50*, 2039.
(218) Mason, T. J.; Lorimer, J. P. *Sonochemistry: Theory, Applications and Uses of Ultrasound in Chemistry*; Ellis Horwood: New York, 1989.
(219) Taghizadeh, M. T.; Asadpour, T. *Ultrason. Sonochem.* **2009**, *16*, 280.
(220) Frank, I.; Friedrichs, J. *Nat. Chem.* **2009**, *1*, 264.
(221) Ong, M. T.; Leiding, J.; Tao, H.; Virshup, A. M.; Martínez, T. J. *J. Am. Chem. Soc.* **2009**, *131*, 6377.
(222) Lenhardt, J. M.; Black, A. L.; Craig, S. L. *J. Am. Chem. Soc.* **2009**, *131*, 10818.
(223) Huang, Z.; Yang, Q.-Z.; Khvostichenko, D.; Kucharski, T. J.; Chen, J.; Boulatov, R. *J. Am. Chem. Soc.* **2009**, *131*, 1407.
(224) Yang, Q.-Z.; Huang, Z.; Kucharski, T. J.; Khvostichenko, D.; Chen, J.; Boulatov, R. *Nat. Nanotechnol.* **2009**, *4*, 302.
(225) Piermattei, A.; Karthikeyan, S.; Sijbesma, R. P. *Nat. Chem.* **2009**, *1*, 133.
(226) Rathore, J. S.; Nelson, A. *Nat. Chem.* **2009**, *1*, 102.
(227) Åbbas, K. B.; Kirschner, T.; Porter, R. S. *Eur. Polym. J.* **1978**, *14*, 361.
(228) Åbbas, K. B.; Porter, R. S. *J. Polym. Sci., Polym. Chem. Ed.* **1976**, *14*, 553.
(229) Berlin, A. A.; Penskaya, E. A.; Volkova, G. I. *J. Polym. Sci.* **1962**, *56*, 477.
(230) Jellinek, H. H. G.; Fok, S. Y. *Makromol. Chem.* **1967**, *104*, 18.
(231) Lozinsky, V. I.; Domotenko, L. V.; Vainerman, E. S.; Mamtsis, A. M.; Rogozhin, S. V. *Polym. Bull.* **1986**, *15*, 333.
(232) Patat, V. F.; Hogner, W. *Makromol. Chem.* **1964**, *75*, 85.
(233) Rand, W. G.; Mukherji, A. K. *J. Polym. Sci., Polym. Lett. Ed.* **1982**, *20*, 501.
(234) Wang, S.; Yan, X.; Ding, J.; Liu, M.; Cheng, R.; Wu, C.; Qian, R. *J. Macromol. Sci., B: Phys.* **1997**, *B36*, 187.
(235) Chung, C.-M.; Roh, Y.-S.; Cho, S.-Y.; Kim, J.-G. *Chem. Mater.* **2004**, *16*, 3982.
(236) Cho, S.-Y.; Kim, J.-G.; Chung, C.-M. *Sens. Actuators, B* **2008**, *134*, 822.
(237) Chen, X.; Wudl, F.; Mal, A. K.; Shen, H.; Nutt, S. R. *Macromolecules* **2003**, *36*, 1802.
(238) Plaisted, T. A.; Nemat-Nasser, S. *Acta Mater.* **2007**, *55*, 5684.

(239) Liu, Y.-L.; Hsieh, C.-Y. *J. Polym. Sci., Part A: Polym. Chem.* **2006**, *44*, 905.
(240) Szalai, M. L.; McGrath, D. V.; Wheeler, D. R.; Zifer, T.; McElhanon, J. R. *Macromolecules* **2007**, *40*, 818.
(241) Trabesinger, W.; Renn, A.; Hecht, B.; Wild, U. P.; Montali, A.; Smith, P.; Weder, C. *J. Phys. Chem. B* **2000**, *104*, 5221.
(242) Löwe, C.; Weder, C. *Adv. Mater.* **2002**, *14*, 1625.
(243) Crenshaw, B. R.; Weder, C. *Chem. Mater.* **2003**, *15*, 4717.
(244) Kinami, M.; Crenshaw, B. R.; Weder, C. *Chem. Mater.* **2006**, *18*, 946.
(245) Kunzelman, J.; Crenshaw, B. R.; Kinami, M.; Weder, C. *Macromol. Rapid Commun.* **2006**, *27*, 1981.
(246) Pucci, A.; Cuia, F.; Signori, F.; Ruggeri, G. *J. Mater. Chem.* **2007**, *17*, 783.
(247) Crenshaw, B. R.; Weder, C. *Macromolecules* **2006**, *39*, 9581.
(248) Crenshaw, B. R.; Burnworth, M.; Khariwala, D.; Hiltner, A.; Mather, P. T.; Simha, R.; Weder, C. *Macromolecules* **2007**, *40*, 2400.
(249) Pucci, A.; Biver, T.; Ruggeri, G.; Meza, L. I.; Pang, Y. *Polymer* **2005**, *46*, 11198.
(250) Wang, X.; Guérin, G.; Wang, H.; Wang, Y.; Manners, I.; Winnik, M. A. *Science* **2007**, *317*, 644.
(251) Guérin, G.; Wang, H.; Manners, I.; Winnik, M. A. *J. Am. Chem. Soc.* **2008**, *130*, 14763.
(252) Sapsford, K. E.; Berti, L.; Medintz, I. L. *Angew. Chem., Int. Ed.* **2006**, *45*, 4562.
(253) Silvius, J. R.; Nabi, I. R. *Mol. Membr. Biol.* **2006**, *23*, 5.
(254) Shroff, H.; Reinhard, B. M.; Siu, M.; Agarwal, H.; Spakowitz, A.; Liphardt, J. *Nano Lett.* **2005**, *5*, 1509.
(255) Meng, F.; Suchyna, T. M.; Sachs, F. *FEBS J.* **2008**, *275*, 3072.
(256) Bruns, N.; Pustelny, K.; Bergeron, L. M.; Whitehead, T. A.; Clark, D. S. *Angew. Chem., Int. Ed.* **2009**, *48*, 5666.
(257) Karthikeyan, S.; Sijbesma, R. P. *Macromolecules* **2009**, *42*, 5175.
(258) Day, R. J.; Hu, X.; Stanford, J. L.; Young, R. J. *Polym. Bull.* **1991**, *27*, 353.
(259) Hammond, P. T.; Nallicheri, R. A.; Rubner, M. F. *Mater. Sci. Eng., A* **1990**, *126*, 281.
(260) Nallicheri, R. A.; Rubner, M. F. *Macromolecules* **1991**, *24*, 517.
(261) Lee, S. B.; Koepsel, R. R.; Russell, A. J. *Nano Lett.* **2005**, *5*, 2202.
(262) Burns, A. R.; Carpick, R. W.; Sasaki, D. Y.; Shelnutt, J. A.; Haddad, R. *Tribol. Lett.* **2001**, *10*, 89.
(263) Carpick, R. W.; Sasaki, D. Y.; Marcus, M. S.; Eriksson, M. A.; Burns, A. R. *J. Phys.: Condens. Matter* **2004**, *16*, R679.
(264) Carpick, R. W.; Sasaki, D. Y.; Burns, A. R. *Langmuir* **2000**, *16*, 1270.
(265) Yang, Y.; Lu, Y.; Lu, M.; Huang, J.; Haddad, R.; Xomeritakis, G.; Liu, N.; Malanoski, A. P.; Sturmayr, D.; Fan, H.; Sasaki, D. Y.; Assink, R. A.; Shelnutt, J. A.; van Swol, F.; Lopez, G. P.; Burns, A. R.; Brinker, C. J. *J. Am. Chem. Soc.* **2003**, *125*, 1269.
(266) Stanford, J. L.; Young, R. J.; Day, R. J. *Polymer* **1991**, *32*, 1713.
(267) Hu, X.; Day, R. J.; Stanford, J. L.; Young, R. J. *J. Mater. Sci.* **1992**, *27*, 5958.
(268) Hu, X.; Stanford, J. L.; Day, R. J.; Young, R. J. *Macromolecules* **1992**, *25*, 684.
(269) Stanford, J. L.; Day, R. J.; Hu, X.; Young, R. J. *Prog. Org. Coat.* **1992**, *20*, 425.
(270) Lovell, P. A.; Stanford, J. L.; Wang, Y.-F.; Young, R. J. *Polym. Int.* **1994**, *34*, 23.
(271) Lovell, P. A.; Stanford, J. L.; Wang, Y.-F.; Young, R. J. *Polym. Bull.* **1993**, *30*, 347.
(272) Lovell, P. A.; Stanford, J. L.; Wang, Y.-F.; Young, R. J. *Macromolecules* **1998**, *31*, 834.
(273) Lovell, P. A.; Stanford, J. L.; Wang, Y.-F.; Young, R. J. *Macromolecules* **1998**, *31*, 842.
(274) Reneker, D. H.; Mattice, W. L.; Quirk, R. P.; Kim, S. J. *Smart Mater. Struct.* **1992**, *1*, 84.
(275) Brunsveld, L.; Folmer, B. J. B.; Meijer, E. W.; Sijbesma, R. P. *Chem. Rev.* **2001**, *101*, 4071.
(276) ten Cate, A. T.; Sijbesma, R. P. *Macromol. Rapid Commun.* **2003**, *23*, 1094.
(277) Binder, W.; Zirbs, R. In *Hydrogen Bonded Polymers*; Springer: New York, 2007.
(278) Wool, R. P. In *Adhesion and Absorption of Polymers, Part A*; Lee, L.-H., Ed.; Plenum Publishing Corp.: New York, 1979; Vol. 12A.
(279) Montarnal, D.; Cordier, P.; Soulié-Ziakovic, C.; Tournilhac, F.; Leibler, L. *J. Polym. Sci., Part A: Polym. Chem.* **2008**, *46*, 7925.
(280) Montarnal, D.; Tournilhac, F.; Hidalgo, M.; Couturier, J.-L.; Leibler, L. *J. Am. Chem. Soc.* **2009**, *131*, 7966.
(281) Guan, Z.; Roland, J. T.; Bai, J. Z.; Ma, S. X.; McIntire, T. M.; Nguyen, M. *J. Am. Chem. Soc.* **2004**, *126*, 2058.
(282) Roland, J. T.; Guan, Z. *J. Am. Chem. Soc.* **2004**, *126*, 14328.
(283) Kushner, A. M.; Gabuchian, V.; Johnson, E. G.; Guan, Z. *J. Am. Chem. Soc.* **2007**, *129*, 14110.
(284) Kushner, A. M.; Vossler, J. D.; Williams, G. A.; Guan, Z. *J. Am. Chem. Soc.* **2009**, *131*, 8766.
(285) Li, J.; Viveros, J. A.; Wrue, M. H.; Anthamatten, M. *Adv. Mater.* **2007**, *19*, 2851.
(286) Mandelkern, L. *Crystallization of Polymers: Kinetics and Mechanisms*; Cambridge University Press: Cambridge, U.K., 2002.
(287) Wood, L. A.; Bekkedahl, N. *J. Appl. Phys.* **1946**, *17*, 362.
(288) Seguela, R. *J. Macromol. Sci., Polym. Rev.* **2005**, *45*, 263.
(289) Tosaka, M. *Polym. J.* **2007**, *39*, 1207.
(290) Gent, A. N.; Kawahara, S.; Zhao, J. *Rubber Chem. Technol.* **1998**, *71*, 668.
(291) Martins, C. I.; Cakmak, M. *Polymer* **2007**, *48*, 2109.
(292) Gent, A. N.; Zhang, L.-Q. *J. Polym. Sci., Part B: Polym. Phys.* **2001**, *39*, 811.
(293) Krigbaum, W. R.; Roe, R.-J. *J. Polym. Sci., Part A* **1964**, *2*, 4391.
(294) Flory, P. J. *J. Chem. Phys.* **1947**, *15*, 397.
(295) Dupres, S.; Long, D. R.; Albouy, P.-A.; Sotta, P. *Macromolecules* **2009**, *42*, 2634.
(296) Rault, J.; Marchal, J.; Judeinstein, P.; Albouy, P.-A. *Euro. Phys. J. E: Soft Matter Biological Phys.* **2006**, *21*, 243.
(297) Chenal, J.-M.; Chazeau, L.; Guy, L.; Bomal, Y.; Gauthier, C. *Polymer* **2007**, *48*, 1042.
(298) Chenal, J.-M.; Gauthier, C.; Chazeau, L.; Guy, L.; Bomal, Y. *Polymer* **2007**, *48*, 6893.
(299) Rault, J.; Marchal, J.; Judeinstein, P.; Albouy, P.-A. *Macromolecules* **2006**, *39*, 8356.
(300) Spanggaard, H.; Jørgensen, M.; Almdal, K. *Macromolecules* **2003**, *36*, 1701.
(301) Shiga, T.; Okada, A.; Takahashi, H.; Kurauchi, T. *J. Mater. Sci. Lett.* **1995**, *14*, 1754.
(302) Shiga, T.; Narita, T.; Tachi, K.; Okada, A.; Takahashi, H.; Kurauchi, T. *Polym. Eng. Sci.* **1997**, *37*, 24.
(303) Shiga, T.; Ikawa, T.; Okada, A. *J. Appl. Polym. Sci.* **1998**, *67*, 259.
(304) Tanaka, F.; Okamoto, M.; Hirayama, S. *J. Phys. Chem.* **1995**, *99*, 525.
(305) Ikawa, T.; Shiga, T.; Okada, A. *J. Appl. Polym. Sci.* **2002**, *83*, 2600.
(306) Moses, D.; Chen, J.; Denenstein, A.; Kaveh, M.; Chung, T. C.; Heeger, A. J.; MacDiarmid, A. G.; Park, Y. W. *Solid State Commun.* **1981**, *40*, 1007.
(307) Brillante, A.; Hanfland, M.; Syassen, K.; Hocker, J. *Physica B+C* **1986**, *139−140*, 533.
(308) Hanfland, M.; Brillante, A.; Syassen, K.; Stamm, M.; Fink, J. *J. Chem. Phys.* **1989**, *90*, 1930.
(309) Maddison, D. S.; Unsworth, J.; Lusk, J. *Synth. Met.* **1988**, *22*, 257.
(310) Maddison, D. S.; Lusk, J.; Unsworth, J. *Synth. Met.* **1989**, *32*, 219.
(311) Lundin, A.; Lundberg, B.; Sauerer, W.; Nandery, P.; Naegele, D. *Synth. Met.* **1990**, *39*, 233.
(312) Fedorko, P.; Skákalová, V. *Synth. Met.* **1998**, *94*, 279.
(313) Yoshino, K.; Nakao, K.; Onoda, M.; Sugimoto, R. *Solid State Commun.* **1988**, *68*, 513.
(314) Isotalo, H.; Ahlskog, M.; Stubb, H. *Synth. Met.* **1992**, *48*, 313.
(315) Yoshino, K.; Nakao, K.; Onoda, M.; Sugimoto, R. *J. Phys.: Condens. Matter* **1989**, 1009.
(316) Hess, B. C.; Kanner, G. S.; Vardeny, Z. *Phys. Rev. B* **1993**, *47*, 1407.
(317) Iwasaki, K.-i.; Fujimoto, H.; Matsuzaki, S. *Synth. Met.* **1994**, *63*, 101.
(318) Kaniowski, T.; Niziol, S.; Sanetra, J.; Trznadel, M.; Pron, A. *Synth. Met.* **1998**, *94*, 111.
(319) Muramatsu, Y.; Yamamoto, T.; Hasegawa, M.; Yagi, T.; Koinuma, H. *Polymer* **2001**, *42*, 6673.
(320) Samuelsen, E. J.; Mårdalen, J.; Konestabo, O. R.; Hanfland, M.; Lorenzen, M. *Synth. Met.* **1999**, *101*, 98.
(321) Sato, T.; Yagi, T.; Tajima, H.; Fukuda, T.; Yamamoto, T. *React. Funct. Polym.* **2008**, *68*, 369.
(322) Yamamoto, T.; Muramatsu, Y.; Lee, B.-L.; Kokubo, H.; Sasaki, S.; Hasegawa, M.; Yagi, T.; Kubota, K. *Chem. Mater.* **2003**, *15*, 4384.
(323) Yang, G.; Li, Y.; White, J. O.; Drickamer, H. G. *J. Phys. Chem. B* **1999**, *103*, 5181.
(324) Yang, G.; Li, Y.; White, J. O.; Drickamer, H. G. *J. Phys. Chem. B* **1999**, *103*, 7853.
(325) Peterlin, A. *J. Mater. Sci.* **1971**, *6*, 490.
(326) Peterlin, A. *Colloid Polym. Sci.* **1987**, *265*, 357.
(327) Jang, Y. T.; Phillips, P. J.; Thulstrup, E. W. *Chem. Phys. Lett.* **1982**, *93*, 66.
(328) Phillips, P. J. *Chem. Rev.* **1990**, *90*, 425.
(329) Michl, J.; Thulstrup, E. W. *Acc. Chem. Res.* **1987**, *20*, 192.
(330) Bastiaansen, C.; Schmidt, H. W.; Nishino, T.; Smith, P. *Polymer* **1993**, *34*, 3951.
(331) Ciardelli, F.; Cellai, C.; Pucci, A.; Regoli, L.; Ruggeri, G.; Tirelli, N.; Cardelli, C. *Polym. Adv. Technol.* **2001**, *12*, 223.
(332) Pucci, A.; Cappelli, C.; Bronco, S.; Ruggeri, G. *J. Phys. Chem. B* **2006**, *110*, 3127.

(333) Pucci, A.; Ruggeri, G.; Moretto, L.; Bronco, S. *Polym. Adv. Technol.* **2002**, *13*, 737.
(334) Tirelli, N.; Amabile, S.; Cellai, C.; Pucci, A.; Regoli, L.; Ruggeri, G.; Ciardelli, F. *Macromolecules* **2001**, *34*, 2129.
(335) Carson, T. D.; Seo, W.; Tam-Chang, S.-W.; Casey, S. M. *Chem. Mater.* **2003**, *15*, 2292.
(336) Eglin, M.; Montali, A.; Palmans, A. R. A.; Tervoort, T.; Smith, P.; Weder, C. *J. Mater. Chem.* **1999**, *9*, 2221.
(337) Montali, A.; Palmans, A. R. A.; Eglin, M.; Weder, C.; Smith, P.; Trabesinger, W.; Renn, A.; Hecht, B.; Wild, U. P. *Macromol. Symp.* **2000**, *154*, 105.
(338) Pucci, A.; Elvati, P.; Ruggeri, G.; Liuzzo, V.; Tirelli, N.; Isola, M.; Ciardelli, F. *Macromol. Symp.* **2003**, *204*, 59.
(339) Bernabò, M.; Ciardelli, F.; Pucci, A.; Ruggeri, G. *Macromol. Symp.* **2008**, *270*, 177.
(340) Pucci, A.; Ruggeri, G.; Bronco, S.; Bertoldo, M.; Cappelli, C.; Ciardelli, F. *Prog. Org. Coat.* **2007**, *58*, 105.
(341) Dirix, Y.; Tervoort, T. A.; Bastiaansen, C. *Macromolecules* **1995**, *28*, 486.
(342) Dirix, Y.; Tervoort, T. A.; Bastiaansen, C. *Macromolecules* **1997**, *30*, 2175.
(343) Ruhe, J.; Ballauff, M.; Biesalski, M.; Dziezok, P.; Grohn, F.; Johannsmann, D.; Houbenov, N.; Hugenberg, N.; Konradi, R.; Minko, S.; Motornov, M.; Netz, R. R.; Schmidt, M.; Seidel, C.; Stamm, M.; Stephan, T.; Usov, D.; Zhang, H. N. In *Polyelectrolytes with Defined Molecular Architecture I*; Springer-Verlag: Berlin, 2004; Vol. 165, pp 1−41.
(344) Varley, R. Ionomers as Self Healing Polymers. In *Self Healing Materials. An Alternative Approach to 20 Centuries of Materials Science*; van der Zwaag, S., Ed.; Springer: New York, 2007; pp 95−114.
(345) Kalista, S.; Ward, T. *J. R. Soc. Interface* **2007**, *4*, 405.
(346) Kalista, S. J.; Ward, T. C.; Oyetunji, Z. *Mech. Adv. Mater. Struct.* **2007**, *14*, 391.
(347) Shimada, S.; Takahasi, Y.; Sugino, Y.; Hara, S.; Yamamoto, K. *J. Polym. Sci., Part B: Polym. Phys.* **2004**, *42*, 1705.
(348) Brown, E. N.; White, S. R.; Sottos, N. R. *J. Mater. Sci.* **2004**, *39*, 1703.
(349) White, S. R.; Caruso, M. M.; Moore, J. S. *MRS Bull.* **2008**, *33*, 766.
(350) Youngblood, J. P.; Sottos, N. R. *MRS Bull.* **2008**, *33*, 732.
(351) White, S. R.; Sottos, N. R.; Geubelle, P. H.; Moore, J. S.; Kessler, M. R.; Sriram, S. R.; Brown, E. N.; Viswanathan, S. *Nature* **2001**, *409*, 794.
(352) Wool, R. P. *Soft Matter* **2008**, *4*, 400.
(353) Dry, C. *Comp. Struct.* **1996**, *35*, 263.
(354) Bleay, S. M.; Loader, C. B.; Hawyes, V. J.; Humberstone, L.; Curtis, P. T. *Composites Part A* **2001**, *32*, 1767.
(355) Pang, J. W. C.; Bond, I. P. *Composites, Part A* **2005**, *36*, 183.
(356) Pang, J. W. C.; Bond, I. P. *Compos. Sci. Technol.* **2005**, *65*, 1791.
(357) Trask, R. S.; Bond, I. P. *Smart Mater. Struct.* **2006**, *15*, 704.
(358) Trask, R. S.; Williams, G. J.; Bond, I. P. J. R. *Soc. Interface* **2007**, *4*, 363.
(359) Brown, E. N.; Sottos, N. R.; White, S. R. *Exp. Mech.* **2002**, *42*, 372.
(360) Kessler, M. R.; Sottos, N. R.; White, S. R. *Composites, Part A* **2003**, *34*, 743.
(361) Kessler, M. R.; White, S. R. *J. Polym. Sci., Part A: Polym. Chem.* **2002**, *40*, 2373.
(362) Brown, E. N.; White, S. R.; Sottos, N. R. *Compos. Sci. Technol.* **2005**, *65*, 2474.
(363) Mauldin, T. C.; Rule, J. D.; Sottos, N. R.; White, S. R.; Moore, J. S. *J. R. Soc. Interface* **2007**, *4*, 389.
(364) Wilson, G. O.; Caruso, M. M.; Reimer, N. T.; White, S. R.; Sottos, N. R.; Moore, J. S. *Chem. Mater.* **2008**, *20*, 3288.
(365) Rule, J. D.; Brown, E. N.; Sottos, N. R.; White, S. R.; Moore, J. S. *Adv. Mater.* **2005**, *17*, 205.
(366) Benita, S., Ed. *Microencapsulation: Methods and Industrial Applications*, 2nd ed.; Informa Healthcare: 2005.
(367) Blaiszik, B. J. Ph.D. Thesis, University of Illinois at Urbana-Champaign, 2009.
(368) Brown, E. N.; Kessler, M. R.; Sottos, N. R.; White, S. R. *J. Microencapsulation* **2003**, *20*, 719.
(369) Keller, M. W.; Sottos, N. R. *Exp. Mech.* **2006**, *46*, 725.
(370) Blaiszik, B. J.; Sottos, N. R.; White, S. R. *Compos. Sci. Technol.* **2008**, *68*, 978.
(371) Mookhoek, S. D.; Blaiszik, B. J.; Fischer, H. R.; Sottos, N. R.; White, S. R.; van der Zwaag, S. *J. Mater. Chem.* **2008**, *18*, 5390.
(372) Rule, J. D.; Sottos, N. R.; White, S. R. *Polymer* **2007**, *48*, 3520.
(373) Caruso, M. M.; Blaiszik, B. J.; White, S. R.; Sottos, N. R.; Moore, J. S. *Adv. Funct. Mater.* **2008**, *18*, 1898.
(374) Kirkby, E. L.; Rule, J. D.; Michaud, V. J.; Sottos, N. R.; White, S. R.; Månson, J.-A. E. *Adv. Funct. Mater.* **2008**, *18*, 2253.
(375) May, C. A., Ed. *Epoxy Resins: Chemistry and Technology*; Dekker: New York, 1976.
(376) Chen, C.; Justice, R.; Schaefer, D.; Baur, J. *Polymer* **2008**, *49*, 3805.
(377) Wetzel, B.; Rosso, P.; Haupert, F.; Friedrich, K. *Eng. Fract. Mech.* **2006**, *73*, 2375.
(378) Hodgkin, J. H.; Simon, G. P.; Varley, R. J. *Polym. Adv. Technol.* **1998**, *9*, 3.
(379) Brown, E. N.; White, S. R.; Sottos, N. R. *J. Mater. Sci.* **2006**, *41*, 6266.
(380) Paris, P. C.; Gomez, M. P.; Anderson, W. E. *Trends Eng. Univ. Wash.* **1961**, *13*, 9.
(381) Jones, A. S.; Rule, J. D.; Moore, J. S.; Sottos, N. R.; White, S. R. *J. R. Soc. Interface* **2007**, *4*, 395.
(382) Jones, A. S.; Rule, J. D.; Moore, J. S.; White, S. R.; Sottos, N. R. *Chem. Mater.* **2006**, *18*, 1312.
(383) Brown, E. N.; White, S. R.; Sottos, N. R. *Compos. Sci. Technol.* **2005**, *65*, 2466.
(384) Kamphaus, J. M. Ph.D. Thesis, University of Illinois at Urbana-Champaign, 2007.
(385) Kamphaus, J. M.; Rule, J. D.; Moore, J. S.; Sottos, N. R.; White, S. R. *J. R. Soc. Interface* **2008**, *5*, 95.
(386) Cho, S. H.; Andersson, H. M.; White, S. R.; Sottos, N. R.; Braun, P. V. *Adv. Mater.* **2006**, *18*, 997.
(387) Wilson, G. O.; Moore, J. S.; White, S. R.; Sottos, N. R.; Andersson, H. M. *Adv. Funct. Mater.* **2008**, *18*, 44.
(388) Caruso, M. M.; Delafuente, D. A.; Ho, V.; Sottos, N. R.; Moore, J. S.; White, S. R. *Macromolecules* **2007**, *40*, 8830.
(389) Yang, J.; Keller, M. W.; Moore, J. S.; White, S. R.; Sottos, N. R. *Macromolecules* **2008**, *41*, 9650.
(390) Keller, M. W.; White, S. R.; Sottos, N. R. *Adv. Funct. Mater.* **2007**, *17*, 2399.
(391) Beiermann, B. A.; Keller, M. W.; Sottos, N. R. *Smart Mater. Struct.* **2009**, *18*, 085001.
(392) McIlroy, D. A.; Blaiszik, B. J.; Braun, P. V.; White, S. R.; Sottos, N. R. 235th ACS National Meeting, New Orleans, 2008.
(393) Blaiszik, B. J.; Caruso, M. M.; McIlroy, D. A.; Moore, J. S.; White, S. R.; Sottos, N. R. *Polymer* **2009**, *50*, 990.
(394) Cosco, S.; Ambrogi, V.; Musto, P.; Carfagna, C. *Macromol. Symp.* **2006**, *234*, 184.
(395) Cosco, S.; Ambrogi, V.; Musto, P.; Carfagna, C. *J. Appl. Polym. Sci.* **2007**, *105*, 1400.
(396) Yuan, L.; Gu, A.; Liang, G.-Z. *Mater. Chem. Phys.* **2008**, *110*, 417.
(397) Yuan, L.; Liang, G.-Z.; Xie, J. Q.; Li, L.; Guo, J. *Polymer* **2006**, *47*, 5338.
(398) Yuan, L.; Liang, G.-Z.; Xie, J. Q.; Li, L.; Guo, J. *J. Mater. Sci.* **2007**, *42*, 4390.
(399) Cao, M.; Xie, P.; Jin, Z.; Zhang, Y.; Zhang, R.; Chung, T.-S.; He, C. *J. Appl. Polym. Sci.* **2002**, *85*, 873.
(400) Xu, H.; Fang, Z.; Tong, L. *J. Appl. Polym. Sci.* **2008**, *107*, 1661.
(401) Yin, T.; Rong, M. Z.; Zhang, M. Q.; Yang, G. C. *Compos. Sci. Technol.* **2007**, *67*, 201.
(402) Yin, T.; Rong, M. Z.; Zhang, M. Q.; Zhao, J. Q. *Smart Mater. Struct.* **2009**, *18*, 074001.
(403) Yuan, Y. C.; Rong, M. Z.; Zhang, M. Q. *Polymer* **2008**, *49*, 2531.
(404) Yuan, Y. C.; Rong, M. Z.; Zhang, M. Q.; Chen, J.; Yang, G. C.; Li, X. M. *Macromolecules* **2008**, *41*, 5197.
(405) Xiao, D. S.; Yuan, Y. C.; Rong, M. Z.; Zhang, M. Q. *Polymer* **2009**, *50*, 560.
(406) Xiao, D. S.; Yuan, Y. C.; Rong, M. Z.; Zhang, M. Q. *Adv. Funct. Mater.* **2009**, *19*, 2289.
(407) Xiao, D. S.; Yuan, Y. C.; Rong, M. Z.; Zhang, M. Q. *Polymer* **2009**, *50*, 2967.
(408) Hsieh, H.-C.; Yang, T.-J.; Lee, S. *Polymer* **2001**, *42*, 1227.
(409) Jud, K.; Kausch, H. H.; Williams, J. G. *J. Mater. Sci.* **1981**, *16*, 204.
(410) Lin, C. B.; Lee, S.; Liu, K. S. *Polym. Eng. Sci.* **1990**, *30*, 1399.
(411) Shen, J.-S.; Harmon, J. P.; Lee, S. *J. Mater. Res.* **2002**, *17*, 1335.
(412) Wang, P. P.; Lee, S.; Harmon, J. P. *J. Polym. Sci., Part B: Polym. Phys.* **1994**, *32*, 1217.
(413) Wu, T.; Lee, S. *J. Polym. Sci., Part B: Polym. Phys.* **1994**, *32*, 2055.
(414) Trask, R. S.; Williams, H. R.; Bond, I. P. *Bioinspirational Biomimetics* **2007**, *2*, 1.
(415) Bond, I. P.; Trask, R. S.; Williams, H. R. *MRS Bull.* **2008**, *33*, 770.
(416) Toohey, K. S.; Sottos, N. R.; Lewis, J. A.; Moore, J. S.; White, S. R. *Nat. Mater.* **2007**, *6*, 581.
(417) Toohey, K. S.; Sottos, N. R.; White, S. R. *Exp. Mech.* **2009**, *49*, 707.
(418) Hansen, C. J.; Wu, W.; Toohey, K. S.; Sottos, N. R.; White, S. R.; Lewis, J. A. *Adv. Mater.* **2009**, *21*, DOI: 10.1002/adma.200900588.
(419) Therriault, D.; Shepherd, R. F.; White, S. R.; Lewis, J. A. *Adv. Mater.* **2005**, *17*, 395.
(420) Bergman, S. D.; Wudl, F. *J. Mater. Chem.* **2008**, *18*, 41.
(421) Wu, D. Y.; Meure, S.; Solomon, D. *Prog. Polym. Sci.* **2008**, *33*, 479.
(422) Jones, F. R.; Zhang, W.; Hayes, S. A. Thermally Induced Self Healing of Thermosetting Resins and Matrices in Smart Composites. In *Self Healing Materials. An Alternative Approach to 20 Centuries of*

Materials Science; van der Zwaag, S., Ed.; Springer: New York, 2007; pp 69−93.
(423) Yufa, N. A.; Li, J.; Sibener, S. J. *Polymer* **2009**, *50*, 2630.
(424) Park, J. S.; Takahashi, K.; Guo, Z.; Wang, Y.; Bolanos, E.; Hamann-Schaffner, C.; Murphy, E.; Wudl, F.; Hahn, H. T. *J. Compos. Mater* **2008**, *42*, 2869.
(425) Tian, Q.; Yuan, Y. C.; Rong, M. Z.; Zhang, M. Q. *J. Mater. Chem.* **2009**, *19*, 1289.
(426) Zhang, Y.; Broekhuis, A. A.; Picchioni, F. *Macromolecules* **2009**, *42*, 1906.
(427) Park, J. S.; Kim, H. S.; Hahn, H. T. *Compos. Sci. Technol.* **2009**, *69*, 1082.
(428) Wisse, E.; Spiering, A. J. H.; Pfeifer, F.; Portale, G.; Siesler, H. W.; Meijer, E. W. *Macromolecules* **2008**, *42*, 524.
(429) Balazs, A. C.; Emrick, T.; Russell, T. P. *Science* **2006**, *314*, 1107.
(430) Lin, Y.; Böker, A.; He, J.; Sill, K.; Xiang, H.; Abetz, C.; Li, X.; Wang, J.; Emrick, T.; Long, S.; Wang, Q.; Balazs, A. C.; Russell, T. P. *Nature* **2005**, *434*, 55.
(431) Gupta, S.; Zhang, Q.; Emrick, T.; Balazs, A.; Russell, T. *Nat. Mater.* **2006**, *5*, 229.
(432) Balazs, A. C. *Mater. Today* **2007**, *10*, 18.
(433) Kolmakov, G. V.; Matyjaszewski, K.; Balazs, A. C. *ACS Nano* **2009**, *3*, 885.
(434) Feng, W.; Patel, S. H.; Young, M. Y.; Iii, Z.; Xanthos, M. *Adv. Polym. Technol.* **2007**, *26*, 1.
(435) van Benthem, R. A. T. M.; Ming, W.; de With, G. Self-Healing Coatings. In *Self Healing Materials. An Alternative Approach to 20 Centuries of Materials Science*; van der Zwaag, S., Ed.; Springer: New York, 2007; pp 139−159.
(436) Ghosh, S. K. *Functional Coatings*; Wiley-VCH: Weinheim, 2006.
(437) Shchukin, D. G.; Möhwald, H. *Small* **2007**, *3*, 926.
(438) Shchukin, D. G.; Zheludkevich, M.; Yasakau, K.; Lamaka, S.; Ferreira, M. G. S.; Möhwald, H. *Adv. Mater.* **2006**, *18*, 1672.
(439) Koo, B.-M.; Jung, J.-E.; Han, J.-H.; Kim, J.-W.; Han, S.-H.; Chung, D. J.; Suh, K.-D. *Macromol. Rapid Commun.* **2008**, *29*, 498.
(440) Andreeva, D.; Fix, D.; Möhwald, H.; Shchukin, D. *Adv. Mater.* **2008**, *20*, 2789.
(441) Zheludkevich, M. L.; Shchukin, D. G.; Yasakau, K. A.; Möhwald, H.; Ferreira, M. G. S. *Chem. Mater.* **2007**, *19*, 402.
(442) Lvov, Y. M.; Shchukin, D. G.; Möhwald, H.; Price, R. R. *ACS Nano* **2008**, *2*, 814.
(443) Kumar, A.; Stephenson, L. D.; Murray, J. N. *Prog. Org. Coat.* **2006**, *55*, 244.
(444) Stephenson, L. D. *Mater. Perform.* **2008**, *47*, 21.
(445) Suryanarayana, C.; Rao, K. C.; Kumar, D. *Prog. Org. Coat.* **2008**, *63*, 72.
(446) Cho, S. H.; White, S. R.; Braun, P. V. *Adv. Mater.* **2009**, *21*, 645.
(447) Moll, J. L. Master's Thesis, University of Illinois at Urbana-Champaign, 2008.
(448) Brinson, L. C.; Gates, T. S. *Int. J. Solids Struct.* **1995**, *32*, 827.

CR9001353